Analytical Modeling of Self-Healing and Super Healing in Cementitious Materials

DISSERTATION

Zur Erlangung des akademischen Grades
Doktor-Ingenieur (Dr.-Ing.)
an der Fakultät Bauingenieurwesen der Bauhaus-Universität Weimar

vorgelegt von
Chahmi Oucif
aus Oran, Algerien
(interner Doktorand)

Gutachter:

Prof. Dr.-Ing. Timon Rabczuk, Bauhaus-Universität Wiemar

Prof. Dr.-Ing. habil. Carsten Könke, Bauhaus-Universität Weimar

Prof. Dr. Esteban Samaniego, University of Cuenca

Tag der Öffentlichen Disputation: 27.07.2020

This work is dedicated to:
My beloved mother and father, for all their sacrifices, their love, their tenderness, their support and their prayers throughout my studies.
My dear wife for her patience and encouragement throughout this work.
My sweet daughter.
The memory of my grandfather Chahmi (bouya) and my former teacher at USTO Prof. Mohammed Bénali Benmansour.
My brothers, my sisters and their children.
My big family.
My friends.

Acknowledgements

I would like to express my sincerest gratitude to my supervisor, Prof. Dr.-Ing. Timon Rabczuk, for his guidance and support during the course of my research work. His valuable suggestions and comments enabled me to overcome many difficulties. It has been an honor and pleasure working under his supervision. My acknowledgement also goes to Prof. George Z. Voyiadjis from Louisiana State University for his collaboration and valuable comments in this research. I am particularly grateful to him for hosting me to spend a research stay at his department.

I would also appreciate the Deutscher Akademischer Austauschdienst (DAAD) for their generous sponsorship during my PhD studies.

I would like to thank my colleagues at Institute of Structural Mechanics, particularly Luthfi Muhammad Mauludin who shared with me the office during the last four years, for his friendly support.

This journey would not have been possible without the support of my family. I would particularly like to thank my mother, father, brothers and sisters for encouraging me in all of my pursuits and inspiring me to follow my dreams. Special thanks must go to my beloved parents for their prayers and support.

My thanks also go to my dear wife for her patience and support during this journey, and to my sweet daughter who is the joy of my life.

Weimar, July 2019 Chahmi Oucif

Abstract

Self-healing materials have recently become more popular due to their capability to autonomously and autogenously repair the damage in cementitious materials. The concept of self-healing gives the damaged material the ability to recover its stiffness. This gives a difference in comparing with a material that is not subjected to healing. Once this material is damaged, it cannot sustain loading due to the stiffness degradation. Numerical modeling of self-healing materials is still in its infancy. Multiple experimental researches were conducted in literature to describe the behavior of self-healing of cementitious materials. However, few numerical investigations were undertaken.

The thesis presents an analytical framework of self-healing and super healing materials based on continuum damage-healing mechanics. Through this framework, we aim to describe the recovery and strengthening of material stiffness and strength. A simple damage healing law is proposed and applied on concrete material. The proposed damage-healing law is based on a new time-dependent healing variable. The damage-healing model is applied on isotropic concrete material at the macroscale under tensile load. Both autonomous and autogenous self-healing mechanisms are simulated under different loading conditions. These two mechanisms are denoted in the present work by coupled and uncoupled self-healing mechanisms, respectively. We assume in the coupled self-healing that the healing occurs at the same time with damage evolution, while we assume in the uncoupled self-healing that the healing occurs when the material is deformed and subjected to a rest period (damage is constant). In order to describe both coupled and uncoupled healing mechanisms, a one-dimensional element is subjected to different types of loading history.

In the same context, derivation of nonlinear self-healing theory is given, and comparison of linear and nonlinear damage-healing models is carried out using both coupled and uncoupled self-healing mechanisms. The nonlinear healing theory includes generalized nonlinear and quadratic healing models. The healing efficiency is studied by varying the values of the healing rest period and the parameter describing the material characteristics. In addition, theoretical formulation of different self-healing variables is presented for both isotropic and anisotropic maerials. The healing variables are defined based on the recovery in elastic modulus, shear modulus, Poisson's ratio, and bulk modulus. The evolution of the healing variable calculated based on cross-section as function of the healing variable calculated based on elastic stiffness is presented in both hypotheses of elastic strain equivalence and elastic energy equivalence. The components of the fourth-rank healing tensor are also obtained in the case of isotropic elasticity, plane stress and plane strain.

Recent research revealed that self-healing presents a crucial solution also for the strengthening of the materials. This new concept has been termed "Super Healing". Once the stiffness of the material is recovered, further healing can result as a strengthening material. In the present thesis, new theory of super healing materials is defined in isotropic and anisotropic cases using sound mathematical and mechanical principles which are applied in linear and nonlinear super healing theories. Additionally, the link of the proposed theory with the theory of undamageable materials is outlined. In order to describe the super healing efficiency in linear and nonlinear theories, the ratio of effective stress to nominal stress is calculated as function of the super healing variable. In addition, the hypotheses of elastic strain and elastic energy equivalence are applied. In the same context, new super healing matrix in plane strain is proposed based on continuum damage-healing mechanics.

In the present work, we also focus on numerical modeling of impact behavior of reinforced concrete slabs using the commercial finite element package Abaqus/Explicit. Plain and reinforced concrete slabs of un-

confined compressive strength 41 MPa are simulated under impact of ogive-nosed hard projectile. The constitutive material modeling of the concrete and steel reinforcement bars is performed using the Johnson-Holmquist-2 damage and the Johnson-Cook plasticity material models, respectively. Damage diameters and residual velocities obtained by the numerical model are compared with the experimental results and effect of steel reinforcement and projectile diameter is studied.

Contents

List of Figures

List of Tables

Chapter 1

Introduction

This chapter introduces the background and motivation of the present research work. General overview of the self-healing process with the emphasis on numerical modeling of self-healing in cementitious materials is given. The research objectives are set out alongside the list of publications and the outline of the thesis.

1.1 Background and motivation

In materials science, one of the objectives of research is to develop a stronger material that possesses high performance in terms of material behavior. Therefore, composite materials that exhibit advanced material properties comparing to the conventional materials have received much attention by scientific researchers. Nevertheless, cracking of these materials represents a serious issue that can expose them to failure. Damage of materials affects the integrity and service life of infrastructures due to the reduction in the mechanical properties of materials and crack formation under continuous loading. Final macroscopic fracture of the material is reached due to crack initiation and propagation.

Cementitious materials such as concrete are strong and the most used construction material worldwide. However, this kind of material is subjected to natural and artificial degradation due to environmental and mechanical conditions. Reparation of these materials and amelioration of their lifetime is indispensable when damage occurs. Huge amount of energy and funding are employed in the construction in-

dustry. It was estimated in Europe that the cost of maintenance is taking the half of the total construction budget [12, 13]. The American Society of Civil Engineers estimated that the cost of rehabilitation of bridges and dams in the US are over 76 and 57 billion dollars, respectively [14].

Engineers are well aware of the importance of maintenance and repair of damaged infrastructures. Manual methods are usually used to repair the damaged zones of the materials. However, in some infrastructures the cracks are difficult to detect and the damaged zones are inaccessible. For this objective, researchers have proposed new methods which are capable of repairing materials and their functionality. Among them, smart materials such as self-healing materials that has attracted the attention of material scientists.

The concept of self-healing materials has recently become more popular due to its capability of self-repairing of the cracks and also due to its low cost for reparation of structures. It is based on embedding repairing mechanisms into the materials in order to heal the damaged zones and to recover the original stiffness of the material after it has been damaged. The inspiration of the self-healing mechanism and its embedding into the civil engineering practice has come from the process of healing in biological materials such as clotting of blood in human body and repairing fracture in the bones. Self-healing can be either autogenous [15, 16] or autonomous [17, 18]. The first mechanism is due to the ongoing hydration of clinker minerals or carbonation of calcium hydroxide, while the second one is based on embedding a healing agent inside capsules or hollow fibres into the material mixture. Another concept aims at strengthening of materials called “Super Healing“ which comes into play after the material is repaired. Using this concept, the material is able not only to automatically heal itself, but also to automatically strengthen itself without human intervention.

Numerical and analytical simulations are a widely applied techniques used in the analysis of complex problems. They reduce cost and time consumed to conduct experimental tests and contribute to the design of physical mechanisms efficiently. Comparing to the experimental investigations of self-healing materials that have received much attention, few investigations on numerical modeling of self-healing materials were carried out. This effort needs to be completed with performing mechanical and analytical models to describe the behavior of self-healing materials.

1.1 Background and Motivation

In recent years, numerical modeling of self-healing materials has been concerned by many researchers, and some interesting investigations and outcomes have been presented. Several numerical models of self-healing materials developed in literature are based on fracture mechanics and continuum damage-healing mechanics (CDHM). CDHM is the extension of the continuum damage mechanics (CDM) with the introduction of the healing variable into the constitutive equations. The healing variable represents the variable that describes the material state; if damaged or healed. If the healing variable is equal to 0 it means the material is not healed (damaged), while if it equals to 1 it means the material is totally healed. Comparing to the numerical investigations that focus on fracture behavior of self-healing materials, there is still a lack in the focus on CDHM. The most common self-healing models based on fracture mechanics are the models of Schapery (1989) [19], Little et al. (2007) [20] and Bhasin et al. (2008) [21]. In addition, further researchers have contributed additional insights into damage-healing mechanics such as Abu Al-Rub et al. (2010) [5], Voyiadjis et al. (2011) [22] and Darabi et al. (2012) [23]. Nevertheless, these investigations are formulated using many material parameters that are difficult to be experimentally identified, and are limited to linear self-healing theory. In addition, no detailed formulation of super healing theory was given.

One of the prime objectives of materials research in to develop and design effective materials with desired properties in order to predict their behaviors under specific conditions. Over the past few decades some progress has been made for the understanding of the behavior of self-healing materials but the development of new materials such as super healing is often relied upon empirical equations. In our work, we employ the CDHM to predict the behavior of autonomous and autogenous self-healing concrete under different conditions using both classical (linear) and nonlinear self-healing theories along with the application of plane stress and plane strain cases. The investigation of super healing materials elaborated in the present thesis aims to open an area of new research in materials science and pave the way for new technologies that can be exploited for rehabilitation of structures.

Concrete is the most advantageous material used in the construction of structures due to its resistance of the effect of blast. It becomes ductile when is appropriately reinforced, especially under tensile loads, and is transformed into the most suitable material in the construction of nuclear and protective infrastructures due to

the improvement in its strength and performance. The study of impact behavior of reinforced concrete (RC) structures has received much attention over the last decades.

Many experimental studies have been conducted on the description of the impact behavior of RC structures, in which the results showed that the RC structures exhibit high resistance when high concrete strength is used. Besides the experimental investigations, the implementation of numerical models is indispensable to understand the impact behavior of RC structures. Few numerical investigations were performed to study the behavior of concrete slabs under impact loads and reinforced with different congurations of longitudinal steel reinforcements mixed with transverse steel reinforcements.

1.2 Objectives of the thesis

The objective of this work is to propose an analytical framework of self-healing and super healing materials based on continuum damage-healing mechanics in order to describe the recovery and strengthening of the material stiffness and strength. We also aim at describing the concrete behavior under impact loads. The following interrelated objectives are included:

1- Development of damage-healing model of concrete material and description of the behavior of different mechanisms of self-healing in different loading conditions.

2- Development of new strengthening theory based on the super healing materials and application to isotropic and anisotropic materials.

3- Application of the nonlinear self-healing and super healing theories and comparison to the linear self-healing and super healing theories.

4- Numerical modeling of ballistic behavior of plain and reinforced concrete slabs under high velocity impact.

1.3 Publications

The following papers have been published as part of the present thesis:

1- **Oucif C.**, Voyiadjis G. Z., Kattan P. I., Rabczuk T. Nonlinear Super Healing and Contribution to the Design of New Strengthening Theory. Journal of Engineering Mechanics, 144(7), 1-17, 2018.

2- **Oucif C.**, Voyiadjis G. Z., Rabczuk T. Modeling of damage-healing and nonlinear self healing concrete behaviour: Application to coupled and uncoupled self-healing mechanisms. Theoretical and Applied Fracture Mechanics, 96, 216-230, 2018.

3- **Oucif C.**, Voyiadjis G. Z., Kattan P. I., Rabczuk T. Investigation of the super healing theory in continuum damage and healing mechanics. International Journal of Damage Mechanics, 1-22, 2018.

4- **Oucif C.**, Mauludin L.M. Continuum Damage-Healing and Super Healing Mechanics in Brittle Materials: A State-of-the-Art Review. Applied Sciences, 8(12), 2350, 2018.

5- Voyiadjis G. Z. **Oucif C.**, Kattan P. I., Rabczuk T. "Damage and healing mechanics in plane stress, plane strain, and isotropic elasticity." International Journal of Damage Mechanics, 1-25, 2020.

6- **Oucif C.**, Mauludin L. M. Numerical modeling of high velocity impact applied on reinforced concrete panel. Underground Space, 4(1), 1-9, 2019.

7- **Oucif, C**., Mauludin, L. M., Abed, F. (2020). Ballistic behavior of plain and reinforced concrete slabs under high velocity impact. Frontiers of Structural and Civil Engineering, 14(2), 299-310.

The author is also named in the following papers as second author:

1- Mauludin L. M., **Oucif C.** Interaction between matrix crack and circular capsule under uniaxial tension. Underground Space, 3(3), 181-189, 2018.

2- Mauludin L. M., **Oucif C.** The effects of interfacial strength on fractured microcapsules. Frontier of Structural and Civil Engineering, 13(2). 353-363, 2019.

3- Mauludin L. M., **Oucif C.** Modeling of Self-Healing Concrete: A Review. Journal of Applied and Computational Mechanics, 4(3), 536-539, 2019.

1.4 Outline of the thesis

In the previous sections, an overview of the problematic and objectives addressed in the present dissertation were given along with an introduction of the research work. The following parts of the dissertation are arranged as follows:

Chapter 2 provides a literature review of self-healing materials and self-healing mechanisms. This chapter includes also various self-healing models that are developed based on damage-healing and fracture mechanics.

Chapter 3 presents the modeling of self-healing concrete using a new time-dependent healing law coupled to damage mechanics. The proposed model is applied on both autonomous and autogenous self-healing mechanisms in the case of both linear and nonlinear healing theories. In this chapter, comparison of linear and nonlinear healing behaviors is carried out and qualitative comparison of the numerical results to the experimental investigations is also considered.

Chapter 4 presents a theoretical formulation of self-healing variables calculated based on the recovery of elastic modulus, shear modulus, Poisson's ratio, and bulk modulus. The formulation is given for both isotropic and anisotropic materials. Consistency of the healing variables calculated based on elastic stiffness with the continuum damage-healing mechanics is demonstrated. The hypotheses of elastic strain equivalence and elastic energy equivalence are used to describe the evolution of the healing variable calculated based on cross-section. The components of the fourth-rank healing tensor are also obtained in the case of plane stress, plane strain and isotropic elasticity.

Chapter 5 introduces a contribution to the design of new theory of strengthening materials based on super healing. This theory is applied using both linear and nonlinear healing models. Two examples are solved to elucidate the mechanism of

the proposed theory of super healing. The first consists of the special cases of plane stress and plane strain, and the second consists of a one-dimensional damage-healing model.

In Chapter 6, an investigation of super healing theory defined based on the elastic stiffness variation is presented. Both hypothesis of elastic strain equivalence and elastic energy equivalence are used to describe the healing and super healing efficiencies.

Chapter 7 focuses on the numerical simulation of ballistic penetration and high velocity impact behavior of plain and reinforced concrete slabs using the commercial finite element package Abaqus/Explicit. Comparison of the performance of the plain and reinforced concrete slabs of unconfined compressive strength 41 MPa under ballistic impact is performed. Concrete material is simulated using the Johnson-Holmquist-2 damage model, while the steel reinforcement bars are simulated using the Johnson-Cook plasticity model. The effect of steel reinforcement and projectile diameter are studied along with the validation of the numerical modeling with experimental results.

Chapter 8 summarizes the dissertation and suggests some recommendations for future works.

Chapter 2

Literature review

2.1 Introduction

This chapter provides a review of literature of self-healing materials and self-healing mechanisms. This review includes also various damage-healing models, methodologies, hypotheses and advances in continuum damage and healing mechanics.

2.2 Self-healing materials

Self-healing materials can be defined as any kind of material that itself recovers and improves its performance after it has been damaged. The French Academy of Science presented the first report defining the self-healing theory in 1836 [24]. It was found that the calcium hydroxide exuded from the hydrated cement is conversed and converted to calcium carbonate on exposure to the atmosphere. Among the first investigations was carried out on autogenous self-healing concrete in 1913 [25] where it was concluded that the healing results from the hydration of unhydrated cement particles. Later on [26], Gilkey found that the healing is influenced by the age of concrete and it can be represented by hydration continued by the stresses. It was also found that the cracks can be healed by calcium carbonate. In another investigation, Lauer and Slate [27] found that the strength recovery from autogenous healing in relative humidity environment is greater than the strength recovery from healing in the water.

In 1973, the authors in [28] conducted experimental tests investigating the self-healing in mortars with different aggregates/cement ratios. The results revealed that all the samples exhibit healing behavior and strength recovery due to the higher content of cement comparing to other samples with higher water/cement ratio that showed slow healing in time. Further investigations showed the ability of self-healing of concrete due to the reduction in water permeability between the cracked and intact zones [29, 30, 31]. The authors in [32] showed that the cracks in brick masonry are filled up to 50-70 μm due to precipitation of high amount of $CaCO_3$. These self-healing investigations demonstrated that the healing process plays a role not only in cracks filling but also in the recovery of the original behavior of the material. The success of the healing process depends on the material mixture and the age of the material at the time of healing [33].

2.3 Self-healing mechanisms

Based on whether self-healing is a natural process in cementitious materials or an artificial process that requires external trigger to activate the healing mechanism, two classes of self-healing can be categorized, namely autogenous and autonemous self-healing mechanisms.

2.3.1 Autogenous healing mechanism

Autogenous healing in cementitious materials is associated to the healing process resulting from physical and chemical composition of the material mixture. Concrete contains 20 % to 30 % of unhydrated cement particles. Low water/cement ratio results in high percentage of unhydrated cement particles. After cracking of concrete, a part of cement particles becomes exhibited to moisture which leads to the start of new hydration of unhydrated cement particles that fill up the crack. Autogenous healing relies also on other mechanisms such as formation of calcium carbonate form calcium hydroxide, settlement of cement grains in the presence of water and swelling of hydrated cementitious matrix (Figure 2.1) [1]. Healing due to the hydration of unhydrated cement particle was found to be the main healing mechanism of concrete at early age [33], while the formation of calcium carbonate becomes dominant for

old concrete [31].

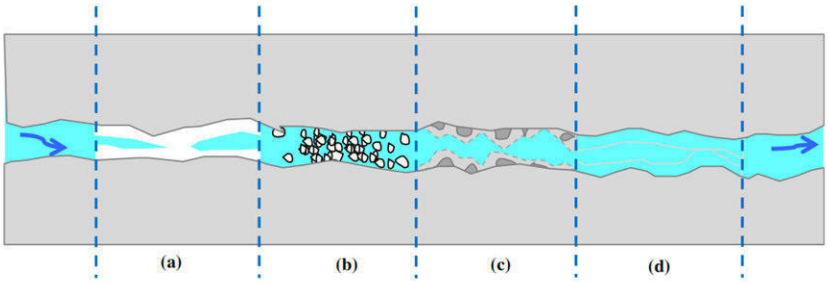

Figure 2.1: Autogenous healing mechanism: (a) formation of calcium carbonate; (b) settlement of the cement particles; (c) hydration of unhydrated cement particles; (d) swelling of unhydrated cementitious matrix [1].

Researchers have found out that autogenous healing is limited to small cracks and is only effective when water is available and is difficult to control [34]. The limit of healable crack width by autogenous healing was found to be 200 μm and 300 μm. Several researches were undertaken to investigate the autogenous healing in concrete. In order to resolve the problem of the limitation of healable crack widths, researchers proposed to apply compressive forces [35] or to include fiber reinforcements in the cementitious composites [36, 37]. Other alternatives were proposed to activate hydration through adding supplement water using superabsorbent polymers [38, 39, 40] and lightweight aggregates [41, 42], adding certain chemical components to the cementitious mixture [43, 44, 45], and through extension of healing period by introducing polymer modified concrete [46, 47, 48].

2.3.2 Autonomous healing mechanism

Autonomous self-healing represents the mechanism in which artificial components are embedded into the material mixture in the form of chemical or biological healing agents. In general, the autonomic healing concept is applied using two types of container shape. The first type based on using microcapsules with either spherical or cylindrical shapes. Many researches were carried out especially on microcapsules [49, 50, 51]. The concept of autonomous self-healing using microcapsules was originally proposed by White et al. [2]. Figure 2.2 represents the autonomous healing

mechanism using microcapsules [2]. Different healing materials can be embedded inside the capsules such as bacterial materials [52, 53], chemical materials [54] and water [55, 56]. In the second type, hollow tubes (named also vascular system) are used [53, 57]. When damage increases and reaches a certain critical level, the microcracks occur and break the microcapsule. Following that, the healing agent releases from the microcapsule, reacts with the catalyst, fills the microcracks and forms a solid material. Many studies on self-healing composite materials have been performed by White and their colleagues. In [58, 59], Brown et al. studied retardation and repair of fatigue cracks. They discovered that the introduction of the healing effect in the deformed state may leads to a high healing efficiency. The rest periods were used to prolong the fatigue life in loading case when the crack grows rapidly, while a complete arrest of crack growth was achieved at lower values of stress intensity factor. The rest period is the time taken to allow the material to be healed.

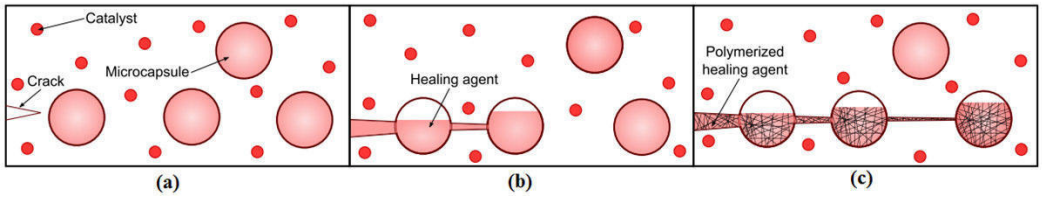

Figure 2.2: Autonomous self-healing mechanism using microcapsules [2].

The introduction of autonomous self-healing in concrete was first proposed by Dry [60]. In this work, the author addressed the concrete and cement permeability and brittleness by the incorporation of chemicals in fibers which repair and fill the cracks and voids in cementitious matrices. In [61], the same author developed a method to protect concrete reinforcing steel against corrosion. This system of protection is activated automatically where porous fibers are filled with calcium nitrite and coated with a salt-sensitive substance to control the response.

Researchers have found that large crack widths can be healed using the autonomous healing mechanism comparing to the autogenous healing. For instance, in [62] it was found that 500 μm of maximum crack width can be healed by autonomous healing in the form of bio-hydrogels. In addition, it was found in [52] that 970 μm of maximum crack width can be healed using microcapsuled bacteria-based

self-healing concrete. It should be noted that the performance of the autonomous healing mechanism is affected by several factors including the strength of the healing agent, size and percentage of microcapsules, shell thickness and encapsulation technique [13].

2.4 Continuum damage and healing mechanics

Most of the numerical models of self-healing materials developed in literature are based either on fracture mechanics or continuum damage-healing mechanics (CDHM). Comparing to the numerical investigations that focus on fracture modeling of self-healing materials, there is still a lack in the focus on CDHM. CDHM is the extension of the continuum damage mechanics (CDM) with the introduction of the healing variable into the constitutive equations.

The presentation of CDM was first given by Kachanov [62] who originally applied the continuum damage mechanics framework to handle the response of the creep failure of metal alloys. CDM framework was further extended by many researchers who aimed at describing the process of damage [63, 64] where it was assumed that the material starts to rupture once the damage variable reaches a critical level. At the beginning of the application of CDM, much attention was given to the analysis of damage due to creep [65, 66, 67, 68]. Later on, further developments were carried out using the principles of continuum damage mechanics [69, 70, 71, 72, 73]. In general, damage mechanics interests in the study of the material in different scales, namely, microscopic, mesoscopic, macroscopic, and mixed scale (statistical method), in which the damage models are applied to describe the variation of the material properties and material failure due to crack initiation and propagation. The basic issue of CDM is to quantify the damage in the material. Many researchers defined the damage variable as the ratio of the number of damaged and total cross-section [74, 75], while other researchers used the concept of the effective stress to define the damage variable [76, 77]. Another method used to calculate the damage variable which is based on the elastic stiffness reduction was also proposed by Lemaitre [78], and investigated further by many researchers [79, 80]. Damage can be isotropic presented by a scalar variable, and anisotropic presented by a tensor [81, 82].

Self-healing concept aims at automatically repairing the damages occurred in

the material. Inspired from this idea, Barbero et al. [83] developed the continuum damage-healing mechanics for composite materials. In their work, they extended the CDM with introduction of the healing variable and proposed a thermodynamic framework to describe the general behavior of self-healing composite materials. The healing variable can be calculated based either on cross-section or on elastic stiffness and it is defined as scalar for isotropic materials and as tensor for anisotropic materials [84].

Following the continuum damage-healing mechanics, many researchers have contributed additional insights into self-healing of materials. In [22, 85, 86, 87, 88], the authors studied theoretically many aspects of damage and healing of materials. In [22], the authors proposed based on a thermodynamic framework a coupled inelastic-damage-healing process. Two new yield surfaces for damage and healing were proposed that take into account the isotropic hardening effect. This theory was extended further in [85] to capture the damage and healing responses of self-healing polymers. Two anisotropic damage and healing variables were presented to describe the ability of the theory to capture the multi-axial case of anisotropic damage and healing. In [84], the mechanical behavior of self-healing materials with the introduction of two new healing variables based on cross-section and elastic stiffness was studied. Several investigations were conducted on anisotropic damage-healing mechanics. For instance, in [85], inelastic, damage and healing anisotropic thermodynamic framework was presented. The consistent formulation was applied to describe the anisoropic damage-healing behavior of glassy polymers. In [89], the healing variable and healing tensor were decomposed into healing due to cracks and healing due to voids. Two cases were considered, namely decomposition of healing without damage being decomposed and both damage and healing are decomposed. Several damage-healing models are proposed in literature based on either fracture mechanics or continuum damage-healing mechanics. In the next section, an overview of damage-healing models and some advances will be reviewed.

2.5 Self-healing modeling

In this section, review of proposed formulations of healing laws applied on brittle materials are discussed. Some of them are not based on CDHM, but they are

highlighted in this section in order to provide the reader an overall idea of mathematical, mechanical and phenomenological propositions of healing laws. In addition, the damage-healing models that have been developed since 2005 and applied on different materials based on CDHM and the anisotropic formulations are also reviewed. The main differences and limitations between these models are also discussed.

2.5.1 Healing model based on parameter recovery

A theory of crack healing of polymers was developed by Wool and OConnor [3] based on a recovery parameter R which is defined as a convolution product. According to this theory, the healing is defined in terms of five stages of healing; (a) surface rearrangement, (b) surface approach, (c) wetting, (d) diffusion and (e) randomization (Figure 2.3). Different mechanical properties of the material were considered in the intact state of the material such as fracture stress σ_∞, strain at failure ϵ_∞, tensile modulus Y_∞ and fracture energy $E_\infty$when the healing history is subjected. The healing history was measured such that the five stages of healing occur simultaneously and the mechanical properties of the material represent the sum of wetting and diffusion process initiated at different times. Based on this assumption, the healing variable was defined as follows:

$$R = \int_{\tau=\infty}^{\tau=t} R_h\left(t-\tau\right) \frac{d\phi\left(\tau, X\right)}{d\tau} d\tau \tag{2.1}$$

where $R_h(t)$ is the intrinsic healing function, $\phi(\tau, X)$ is the wetting diffusion function and τ is the nucleation time and represents the running variable of the time axis. The intrinsic healing function was related to the wetting and diffusion for the measure of recovery based on stress or energy consideration. The wetting is obtained when two free surfaces touch each other in which the time is controlled by self-diffusion of the overlapping free surfaces. The diffusion is controlled by the stage of surface rearrangement. When the material is damaged and the cracks appear, the molecular ends start to be able to move on the surface following the wetting stage. When two surfaces contact each other, their diffusion across the interface results in the healing and recovery of part of the initial strength. Two cases of wetting diffusion function are considered, namely instant wetting and constant rate wetting. In the case of instant wetting, the two surfaces wet instantaneously at time $t = 0$ and the wetting

diffusion function is expressed as follows:

$$\frac{d\phi}{dt} = \delta\left(t\right) \tag{2.2}$$

where $\delta(t)$ is the Dirac-delta function. Consequently, the healing variable in equation (2.1) and the intrinsic healing function become similar as follows:

$$R = R_h\left(t\right) = R_0 + Kt^{1/4}/\sigma_\infty \tag{2.3}$$

where K is a material constant and σ_∞ is the fracture strength of the intact material. R_0 is the wetting component ($R_0 = \sigma_0/\sigma_\infty$). On the other hand, in the case of constant rate wetting, the wetting diffusion function is written as:

$$\frac{d\phi\left(t\right)}{dt} = k_d U\left(t\right) \tag{2.4}$$

where k_d and U(t) are the wetting rate and the Heaviside step function, respectively. Thus, the healing variable is expressed as follows:

$$R = R_0 k_d t + 4k_d K t^{5/4}/5\sigma_\infty \tag{2.5}$$

According to equations (2.3) and (2.5), it is observed that the wetting components of the healing variable is time-independent in the case of instant wetting, while it is time-dependent in the case constant wetting rate. In addition, it is concluded that equations (2.3) and (2.5) are defined based on empirical assumption using large number of material parameters. Figure 2.4 shows the plot $R - R_0$ with respect to the crack healing.

2.5.2 Fracture-mechanics-based healing models

A crack closing model applied on linear and isotropic viscoelastic materials was developed by Schapery [19]. Time-dependent constitutive equations based on continuum mechanics were proposed in which the crack length and contact size are predicted, and the whole healing process is considered. The crack healing model was based on crack area reduction $\dot{a}_b$ which is related to the Poissons ratio, fracture process zone, effective bond energy and the tensile bond force. $\dot{a}_b$ is expressed as

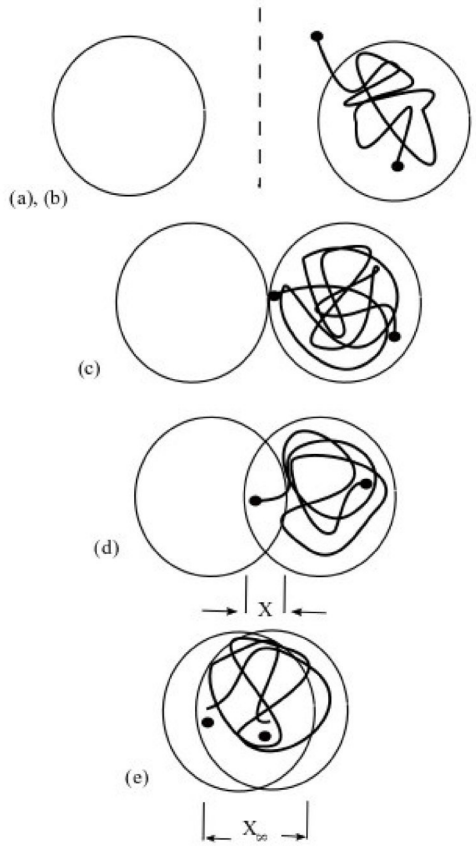

Figure 2.3: Five stages of healing of two random-coil chains on opposite crack surfaces [3].

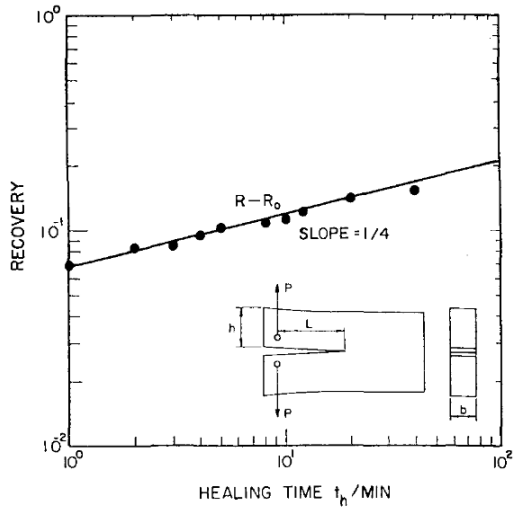

Figure 2.4: Log of recovery of the fracture load minus the wetting component [3].

follows:

$$\dot{a}_b = \pi[4\Gamma_b^{'}]^{(2+1)/m}[(1-\upsilon^2 D_1^+ \gamma_m / C_m)]^{1/m}[E_R^+/(1-\upsilon^2)K_I^R]^{2(1+1/m)}/8\sigma_b^2 C_m^2 \quad (2.6)$$

where $\Gamma_b^{'}$, E_R^+, σ_b, υ and K_I^R are the effective bond energy, elastic modulus, tensile bond force, Poissons ratio and mode I stress intensity factor, respectively. γ_m, C_m, D_1^+ and m are material constants. The crack closing model is known by the fact that there is no difference between the crack closing based on wetting and on diffusion. Moreover, the model is formulated based on different materials that make it difficult to be realized in the case of anisotropic material.

Based on the healing variable proposed in [3] and the crack area reduction in equation (2.6) [19], a new formulation was given in [20, 21] in which they used the variable R to simulate the healing effect in bituminous materials as follows:

$$\frac{d\phi\,(t,X)}{dt} = \dot{a}_b = \beta\left[\frac{1}{D_1 k_m}\left\{\frac{\pi W_c}{4\,(1-\upsilon^2)\,\sigma_b^2\beta}\right\}\right]^{-1/m} \quad (2.7)$$

where W_c, β and k_m are the work of cohesion, the healing process zone and material constant, respectively. The rest of the parameters are defined previously in equation

(2.6). It should be noted that the parameters related to the proposed equation (2.7) are difficult to be identified due to the lack of enough experimental data.

2.5.3 Creep damage-healing model for salt rock

Rock salt is generally subjected to creep damage and cracks that result in the increase of the permeability of the material. Based on the reason that damage results in inelastic flow in rock salt under hydrostatic compression an extension of continuum damage approach to the healing of creep damage was developed in [90]. It was assumed that the macroscopic strain rate is influenced by the healing mechanism along with damage and creep. Anisotropic healing was also considered such that the conjugate stress measure for healing can be expressed as

$$\sigma_{eq}^{h} = \frac{1}{3}\left(I_1 - x_{10}\sigma_1\right) \tag{2.8}$$

where I_1, x_{10} and σ_1 are the first invariant of the Cauchy stress, material constant and the maximum principal stress, respectively. It is considered that the healing is isotropic when $x_{10} = 0$ and anisotropic when $x_{10} \neq 0$. The kinetic equations of the healing were formulated based on an experimental observation that suggests two healing mechanisms can be activated in (Waste Isolation Pilot Plant) WIPP salt. The first mechanism assumes that the healing is present in a much smaller time period which results in unchanged damage variable, while the second mechanism assumes that the healing is present in a larger time period which reduces the damage variable. The healing variable proposed in [90] is considered to be the first-order kinetic equation expressed as

$$h = \frac{\omega \sigma_{eq}^{h_2} H\left(\sigma_{eq}^{h_2}\right)}{\tau_2 \mu} \tag{2.9}$$

where ω, H, τ_2, μ are the damage variable, Heaviside function, time characteristic constant and the shear modulus, respectively. h_2 describes the removal of damage. The healing variable defined in equation (2.9) is characterized by the fact that only individual healing mechanism can be simulated. This leads to the difficulty of finite element implementation of the healing model due to the challenging identification of the healing time involving non-relative loading histories. Thus, the starting time

and the period of the healing become ambiguous.

A simplified version of the healing model proposed in [90] was further developed in [91]. Instead of defining two separate healing mechanisms, a single healing mechanism based on damage, kinetic equation and equivalent stress was proposed. The simplified healing variable was defined with only one kinetic equation for one healing mechanism in contrast to the previous investigation in which one kinetic equation for each healing mechanism was defined. After modification of the kinetic equation, the following healing variable was obtained:

$$h = \frac{\omega \left(\sigma_{eq}^{h} - \sigma_b\right) H \left(\sigma_{eq}^{h} - \sigma_b\right)}{\tau \mu} \tag{2.10}$$

with

$$\sigma_b = x_7 \left| \frac{\sigma_1 - \sigma_3}{x_2 x_7} \right|^{1/x_6} \tag{2.11}$$

where σ_1, σ_3 and σ_{eq} are principal stresses and equivalent stress, respectively. x_2, x_6 and x_7 are materials constants. According to equation (2.10), healing can be activated only when $\sigma_{eq} > \sigma_b$. In addition, the healing reduces the volumetric strain to zero. The axial and lateral strains are also recovered under hydrostatic compression. In [92], a thermodynamic framework of CDHM was proposed in which the concept of healing surface and loading-unloading conditions were used. Rate-dependent and rate-independent formulations were also given and applied in the case of isotropic healing. The general thermodynamic framework was applied to study the healing crushed rock salt. The surface-based healing function takes the following expression:

$$F = s : s - c_B[(B^{sp})^2 + (B^d)^2] + c_S(\omega)^2 - F_0 \tag{2.12}$$

where s, B, ω and F_0 are the Cauchy stress tensor, constrained modulus, surface energy per unit area, and the material positive constant, respectively. c_B and c_S are positive material parameters related to the changes in material parameters and surface area. If the healing surface $F < 0$ the material is supposed unhealed, while the healing is occurring when $F = 0$. The simulation of the densification of crushed rock salt revealed that the healing model is able to describe the healing mechanism in

terms of Youngs modulus and inelastic strain recovery. Even though, the formulation was limited to isotropic material behavior.

Further investigations of damage-healing of salt rock were undertaken. Based on the formulation in [91], the authors in [93] proposed an anisotropic damage-healing formulation for the modeling of creep process in salt rock. The healing process was defined with respect to a viscoplastic scalar healing variable, and the healing strain component was used to account the reduction of the deformation. However, it was assumed that the healing compensate deformation only in the lateral directions. In addition, the crack healing was assumed to result in an instant reduction of deformation in which τ represents the characteristic time needed to close the cracks of the material subject to salt creep. The simplified healing variable that accounts only for diffusion subject to compressive mean stress was expresses as

$$\dot{h} = \frac{tr\,(A)\,pH\,(p)}{\tau G} \tag{2.13}$$

where A, p, H and G are the new damage variable, first stress invariant, Heaviside function, and the shear modulus, respectively. For more details of the formulation and application of equation (2.13), the reader can refer to [94, 95, 96, 97, 98]. Xu et al. [99] implemented an elastoplastic damage healing model of mudstone and defined the healing variable as function of the non-associated dissipation criterion. The healing variable was expressed as

$$h = \frac{A_h}{A_{ud}} \tag{2.14}$$

where A_h and A_{ud} are the healed and undamaged cross-section areas, respectively. It was assumed that the undamaged cross-section area of the healed cross-section area carry the loads. Following this assumption, the effective stress was expressed as follows:

$$\bar{\sigma} = \frac{\sigma}{(1-d)\,(1+h)} \tag{2.15}$$

According to this formulation, the cross-section area of the material is divided into three regions; undamaged A_{ud}, unhealed A_{uh} and healed A_h cross-section areas. The damage in mudstone cannot be fully healed which results that the unhealed

cross-section area is greater than zero. Therefore, it was assumed for simplicity that the healed cross-section area exhibits similar mechanical behavior to that of the original material. However, the boundary conditions of the healing and damage of equation (2.15) was unclear. For further self-healing investigations on geomaterials, the reader can refer to [100, 101, 102, 103, 104, 105, 106, 107, 108].

2.5.4 Micro-damage healing models for asphalt mixtures

In [4], an elastic-viscoelastic model with healing for asphalt concrete subjected to fatigue loading was proposed. The model was extended from the work presented in [109, 110] in which the pseudo-strain variables are given and adopted to eliminate the dependency of the stress-strain material behavior to time. The irreversible thermodynamic framework was used to simulate the healing of micro-damage. Growing damage was simulated using uniaxial viscoelastic constitutive equations that are extended to account for the micro-damage healing. Uniaxial tensile tests under cyclic loading were conducted under controlled-strain and controlled-stress models with rest periods. In order to induce damage in the specimens, two stress-strain levels were used in the tests. The rest periods introduced during each test vary from 0.5 to 32 min. The variation of the material stiffness before and after the rest period was studied as function of the number of cycles (Figure 2.5). The region I in Figure 5 depicts the reduction of the stiffness due to the damage evolution without rest period, while region II depicts the reduction of the stiffness due to the damage evolution after rest period. After the introduction of the rest period, it was shown that the stiffness increases from point B to point A due to micro-damage-healing and decreases after damage of the healed material. Based on the experimental results and stiffness variation in the regions I and II, the following healing function was proposed:

$$H = \left[S^R_{B,i} + C_2\left(S_{2,i}\right)\right] C_3\left(S_{3,i}\right) - C_1\left(S_{1n}\right) - \sum_{j=1}^{i-1}\left(S^R_{B,j} - S^R_{C,j}\right) \tag{2.16}$$

$$\text{when } S^R > S^R_{B,i} \text{ (region I)}$$

$$H = \sum_{j=1}^{i} \left(S_{B,j}^{R} - S_{C,j}^{R} \right) \tag{2.17}$$

$$\text{when } S^{R} < S_{B,i}^{R}$$

where $(S_{2,i})$ represents the healing evolution during the ith rest period and $(S_{3,i})$ represents the damage evolution after the ith rest period. $C_1(S_{1n})$ and (S_{1n}) are the material function and the normalized damage variable. Several experimental investigations were carried out for the study of the micro-damage healing of asphalt mixtures (e.g. [111, 112, 113, 114, 115, 116, 117]). Although the implemented micro-damage-healing model was able to describe the hysteretic behavior under controlled-strain and controlled-stress modes the identification of the experimental data to simulate the healing behavior is not an easy task.

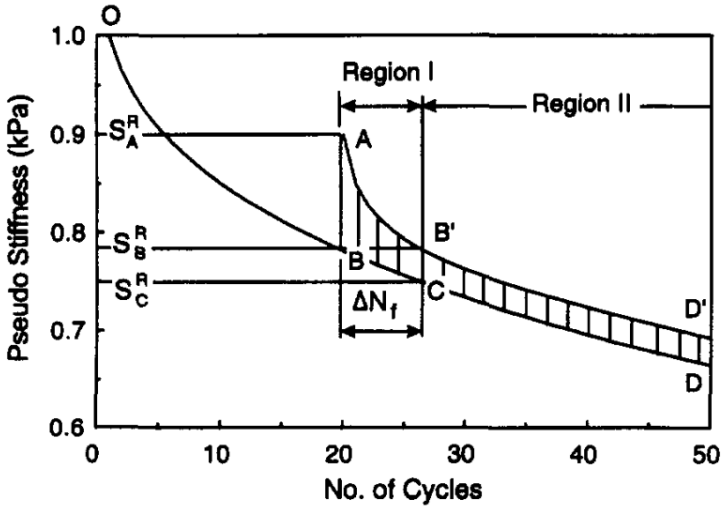

Figure 2.5: Variation of the stiffness before and after the rest period [4].

Another micro-damage-healing model applied to asphalt mixtures subjected to fatigue loads was proposed in [5].The damage healing model was extended from the viscoelastic, viscoplastic and viscodamage model. The authors defined a healing variable which is a function of the healing time and history, damage level and temperature. The proposed healing variable takes the following expression:

$$\dot{h} = \Gamma^h(T)\left(1-\bar{\phi}\right)^{b_1}(1-h)^{b_2} \tag{2.18}$$

where $\dot{h}$ is the rate of the healing variable, Γ^h is the healing viscosity parameter and b_1 and b_2 are material constants. $\Gamma^h(T)$ is a function of temperature and is the parameter that determines the speed of the healing. It is expressed as

$$\Gamma^h(T) = \Gamma_0^h exp\left[-\delta_3\left(1-\frac{T}{T_0}\right)\right] \tag{2.19}$$

where Γ_0^h and δ_3 are the healing viscosity parameter at temperature T_0 and the healing-temperature coupling parameter, respectively. According to equation (2.18), it was assumed that the healing starts to evolve once the temperature reaches a certain reference level (temperature threshold) and decreases when the temperature is less than the reference level. The model was applied to predict the behavior of creep-recovery tests in compression and in tension. An example of the results of the evolution of the creep strain and the effective damage density as function of time in compression is shown in Figure 2.6. From Figure 2.6(a), it is shown that the introduction of the healing improves the material behavior compared to the model without healing. On the other hand, one can see from Figure 2.6(b) that the effective damage increases during loading and decreases during rest period while it remains stable during unloading.

The micro-damage healing law proposed in [5] was further investigated in [23, 118, 119, 120]. In [23], a continuum damage mechanics framework was proposed to simulate the micro-damage-healing of materials subjected to cyclic loading. The hypotheses of elastic strain, elastic energy and power equivalence were used to relate the strain tensor and tangent stiffness in the damaged and healed configurations. The authors worked on the update of the current stress tensors in the damaged and healed configurations. Examples of the uniaxial constant strain and stress rates were applied. The results revealed that the hypotheses of strain equivalence and power equivalence overestimate the elastic strain energy in the healed configuration comparing to the one in the damaged configuration. On the other hand, the strain equivalence hypothesis overestimates the expanded power in the healing configuration comparing to the one in the damaged configuration, while the elastic energy equivalence hypothesis underestimates the expanded power in the healed configura-

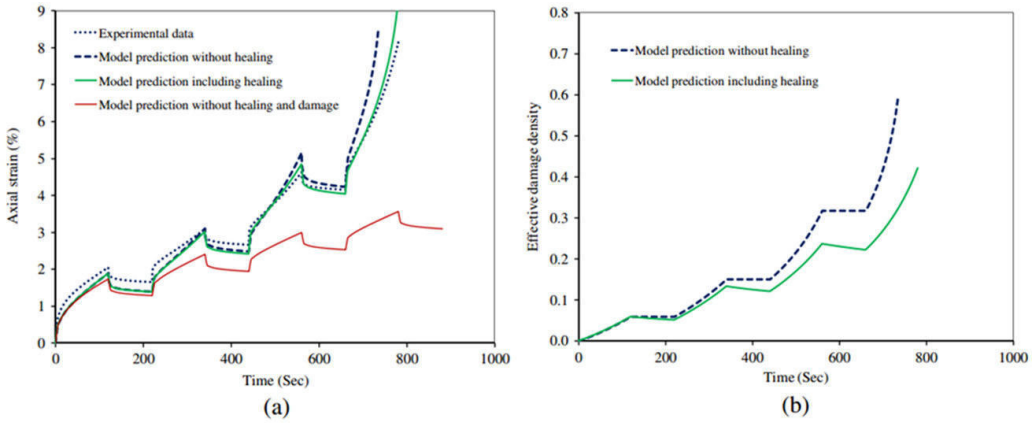

Figure 2.6: Results of repeated recovery test in compression with 120s loading time and 100s of rest period. (a) Compared creep strain, (b) evolution of the effective damage density [5].

tion comparing to the one in the damaged configuration. It should be noted that these results apply on both strain-controlled and stress-controlled uniaxial tests. The same authors used the micro-damage healing model to simulate fatigue damage of asphalt concrete [118]. They also studied the effect of compressive stresses on the crack closure which is called the "unilateral effect". Based on the formulation presented in [5], a theoretical framework of cohesive zone healing model was proposed in [119] and implemented into a finite element code in [120]. The effect of different parameters such as damage history, healing history and resting time were studies. For further investigations on the visco-damage-healing models, the reader can refer to [121, 122, 123, 124, 125].

2.5.5 Curing-based damage healing law

In [6], the authors proposed a new phenomenological damage-healing model applied to polymers. The proposed healing variable concerned the autonomous self-healing concept and was associated with the curing mechanism of the healing agent and the catalyst. In microcapsules-based self-healing concept, the propagated cracks break the microcapsules which results in the release of the healing agent. This latter fills the crack, reacts with the catalyst and they form a solid material in the crack area

(Figure 2.2). It was assumed in this work that the process of cure leads to the mechanical properties variation and stiffness recovery [126]. In this formulation re-damage of the healed material was also considered. As previously shown in equation (2.1) [3], the convolution integral was used to define the healing as follows:

$$h\left(t\right)=\int_{s=t^{c}}^{t}d\left(s\right)\eta_{h}exp\left(-\eta_{h}\left[t-s\right]\right)ds \tag{2.20}$$

where $d(s)$, η_h are the damage variable during the healing period and the parameter that determines the speed of the healing process, respectively. t^c and t are the initial time of the healing and the healing time, respectively. It was assumed that the damage threshold decreases by the introduction of the healing as it is increased due to damage. Therefore, a damage threshold equation was defined which assumes that the behavior of the fully healed material is similar to the original material and the evolution of the healing variable does not affect the increase of the damage variable at constant deformations. The healing was introduced in three cases. The first one concerns the introduction of the healing during the rest period. When the material is loaded and unloaded the healing variable evolves during a rest period. Afterward, the material is reloaded and comparison of the stress-strain response of the healed and original materials is carried out. Figure 2.7 elucidates the stress-strain response of the healed material when the healing is introduced during different rest periods.

In the second example, the healing is introduced when the material is partially damaged while the assumption of its evolution during a required recovery time is kept. It should be noted that in this example the strain is released before the evolution of the healing which means that damage is constant in this phase. The third example concerns the introduction of the healing during a rest period in which the strain is assumed to be constant. For further works on modeling of self-healing polymers and microcapsules-based self-healing, the reader can refer to [127, 128, 129, 130, 131].

2.6 Anisotropic damage-healing formulations

Damage and healing of brittle materials are generally simulated by conventional continuum damage-healing mechanics in which scalar damage and healing variables

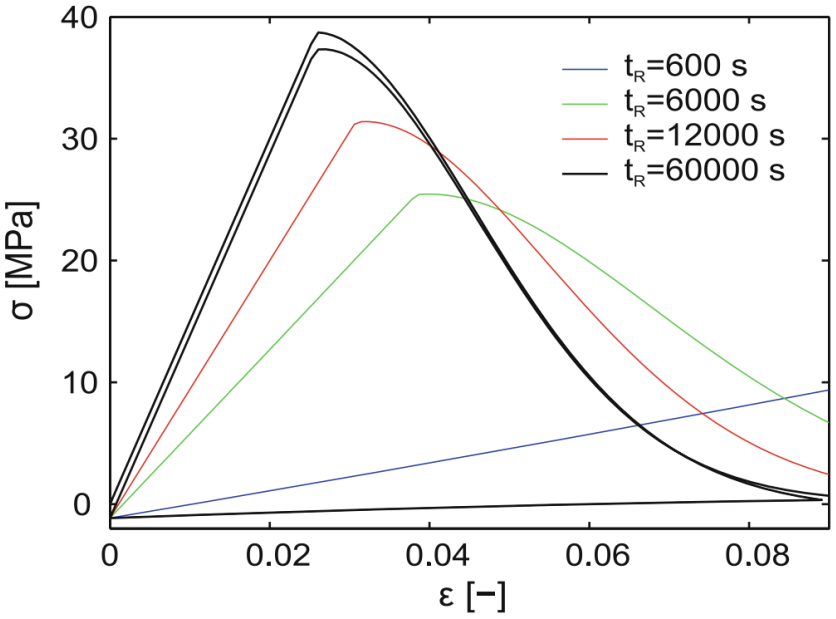

Figure 2.7: Stress-strain response of the healed material with different rest periods [6].

are used to describe the relationship between nominal stress and effective stress; isotropic damage-healing models. In addition, anisotropic damage-healing formulations were also recently proposed and studied using second-order and fourth-order damage and healing tensors. Murakami [132] was the first who generalized the multi-axial anisotropic formulation of the description of the material degradation. Although most of the works conducted on CDHM are based on isotropic presentation, an anisotropic CDHM was also investigated by the introduction of a healing tensor. According to the formulation in [7], the damage variable tensor is expressed as

$$\phi_{ij} n_i = \frac{\left(dA n_j - d\bar{A}\bar{n}_j\right)}{dA}; 0 \leq \left(\phi_{ij}\phi_{ij}\right)^{1/2} \leq 1 \tag{2.21}$$

where dAn_j and $d\bar{A}\bar{n}_j$ are the damage and effective fictitious area vectors, respectively. When the healing is introduced into the material the effective area increases. Figure 2.8 shows the anisotropic damage and healing configurations [7]. According to the presentation in Figure 2.8, the authors in [7] proposed a second rank

anisotropic healing variable tensor as follows:

$$h_{ij}n_i^d = \frac{\left(\phi_{jk}dAn_k - dA^h n_j^h\right)}{dA^d}; 0 \leq (h_{ij}h)^{1/2} \leq 1 \tag{2.22}$$

where h_{ij} describes the relationship between the damaged area vector dAn_i and the effective healed area vector. In the same paper, k_{ijkl} is denoted the fourth-order anisotropic damage variable tensor and describes the elastic modulus degradation as follows

$$\begin{cases} k_{ijkl}^{(1)} = \left(\bar{E}_{ijmn} - E_{ijmn}^d\right)\bar{E}_{mnkl}^{-1} \\ k_{ijkl}^{(2)} = \left(\bar{E}_{mnkl} - E_{mnkl}^d\right)\bar{E}_{ijmn}^{-1} \end{cases} \tag{2.23}$$

where $\bar{E}_{ijkl}$ and E_{ijkl}^d are the undamaged and damaged elastic tensors. The subscripts in equation (2.23) represent the two different mathematical tensorial expressions of the damage tensor. In addition, a new fourth rank healing tensor $h_{ijkl}^{'}$ was also defined to measure the elastic modulus recovery as follows:

$$\begin{cases} h_{ijkl}^{'(1)} = \left(E_{ijmn}^h - E_{ijmn}^d\right)E_{mnkl}^{d^{-1}} \\ h_{ijkl}^{'(2)} = \left(E_{mnkl}^h - E_{mnkl}^d\right)E_{ijmn}^{d^{-1}} \end{cases} \tag{2.24}$$

where E_{ijkl}^h is the healed elastic modulus. It was assumed that the material is undamaged when $h_{ijkl}^{'} = 0_{ijkl}$ (0_{ijkl} is the fourth rank zero tensor), and is fully healed when $h_{ijkl}^{'max} = k_{ijkl}^{max}$.

The generalization of the relational between the effective stress and nominal stress of equation (9) is expressed in the case of anisotropic materials as follows [133]:

$$\bar{\sigma}_{ij} = M_{ijkl}\sigma_{kl} \tag{2.25}$$

where M_{ijkl} represents the fourth-rank damage effect tensor. $\bar{\sigma}_{ij}$ and σ_{kl} are the effective and Cauchy stress tensors, respectively.

The proposed healing tensor was later decomposed to healing tensor for cracks and healing tensor for voids along the lines of the decomposition theory applied on scalar based healing definition in [134, 135]. For more details on the definition of the anisotropic damage variable tensors that were defined based on cross-section area reduction and elastic stiffness degradation, the reader can refer to [82, 89]. The

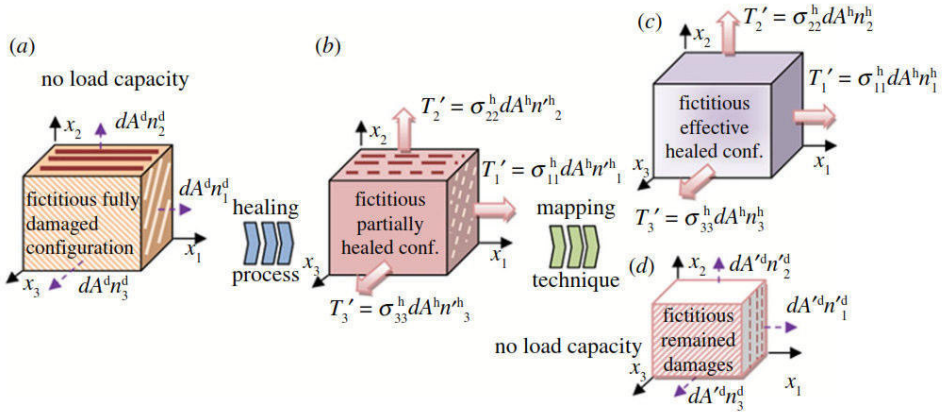

Figure 2.8: (a) fictitious damaged state, (b) fictitious healed state, (c) fictitious effective healed material state and (d) fictitious damaged state [7].

same authors proposed an anisotropic presentation of new damages variables that are called Fabric Tensors [136, 137]. Later on, the same authors in [7] extended their work and proposed a coupled viscoplastic-viscodamage-viscohealing model to study the irregular behavior of glassy polymers [121]. Power function was added to the Frederick-Armstong-Philips-Chaboche (FAPC) model in the expression of the dynamic recovery of the hardening function. This latter results in increase of back stress evolution which cannot describe the irregular responses associated with the inelastic responses of glassy polymers.

Asphalt concrete is a multiphase material and exhibits complicated mechanical behavior and multiple modes of degradation. In [8], the authors developed a viscoelastic-viscoplastic model coupled to anisotropic damage in which a second-order damage tensor was introduced in order to relate the nominal and effective stresses. The damage tensor was divided into permanent and non-permanent parts. The first part represents the classical damage process, while the second part represents the self-healing during unloading and rest period. A creep recovery test was simulated using the healing model. The test concerns the application of a pressure of 1 MPa during 800 s. Afterwards, unloading period of 50 s and rest period of 3000 s were imposed. A reduction of the degradation was observed during the unloading and rest period (Figure 2.9). Some investigations were also carried out in which

anisotropic damage is coupled with a scalar healing variable. In this regard, the authors in [93] developed a thermodynamic damage healing model applied to salt rock with alternative fabric descriptors. Later on, the anisotropy induced by the healing was also simulated in [97]. The effect of crack opening, closure and healing on the stiffness evolution was described by means of a multiscale model. Fabric tensors are used to relate the microcrack evolution with the macroscopic deformation rate. In [138, 139], the anisotropic Cosserat continuum model was used to simulate the damage, healing and plastic of granular materials. Combination of damage and healing was defined in terms of undamaged and damaged elastic moduli tensors. Other investigations on the anisotropic definition of damage variable based on elastic modulus tensor degradation were undertaken. This concerns the decomposition of the stiffness [134], definition of anisotropic damage tensors based on Poisson's ratio, shear modulus and bulk modulus degradation [136], and description of damage in series and damage in parallel [140].

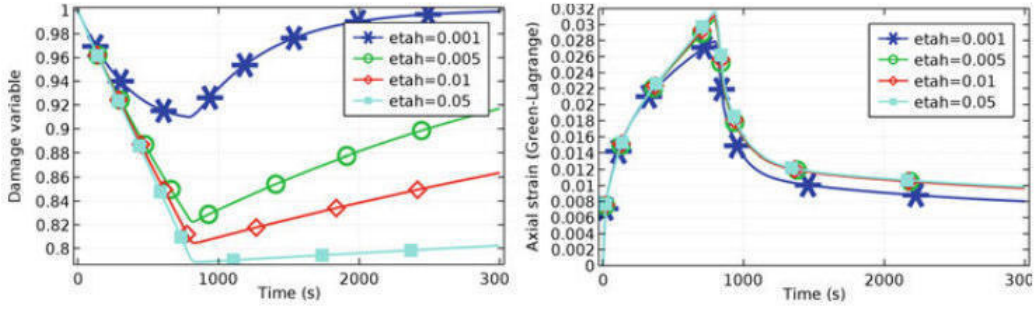

Figure 2.9: Effect of creep recovery load on evolution of degradation (left). Evolution of axial strain due to healing parameter effect resulting of creep-recovery test [8].

Chapter 3

Modeling of damage-healing and nonlinear self-healing concrete behavior

3.1 Introduction

This chapter provides the details of the application of the damage-healing model on concrete material. The derivations of the so-called nonlinear helaing theory is given and comparision to the classical (linear) self-healing model is also carried out.

3.2 Damage and healing variables

In this section, the variables describing damage and healing are reviewed within the framework of continuum damage-healing mechanics. Two definitions of healing variables are defined in the concept of coupled and uncoupled self-healing mechanisms. This section is restricted to the scalar formulation of damage and healing. According to continuum damage mechanics, Figure 3.1 shows the initial, damaged and effective configurations of the material defined by the initial cross-section S_0, damaged cross-section S_φ, effective cross-section $\overline{S}$, respectively. The initial, damaged and effective configurations are also represented by their elastic moduli E_0, E_φ and $\overline{E}$, respectively. The definition of damage will be defined here in terms of

cross-sectional area reduction. In this case, the damage variable can be defined as

$$\varphi = \frac{S_\varphi}{S_0} \quad with\ 0 \leq \varphi \leq 1 \tag{3.1}$$

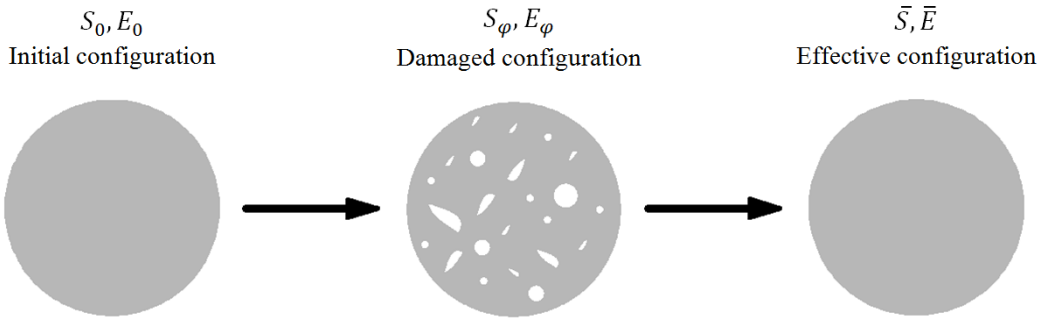

Figure 3.1: Initial, damaged and effective configurations.

It should be noted that the values $\varphi = 0$, $0 < \varphi < 1$, and $\varphi = 1$ represent the undamaged, partially damaged, and fully damaged material states, respectively. Removing all the damaged part (Figure 3.1, right), leads to the relation between the nominal stress σ in the damaged material state and the effective stress $\overline{\sigma}$ in the undamaged state. This relation is given in [141, 142, 143, 144]

$$\overline{\sigma} = \frac{\sigma}{1 - \varphi} \tag{3.2}$$

The healing mechanism affects the damaged sections of the material in which the cracks and voids are filled in two different systems. The first system called coupled self-healing which assumes that the healing occurs at the same time with damage evolution, and the second system called uncoupled self-healing which assumes that the healing occurs when the material is deformed and subjected to a rest period (damage is constant). The coupled self-healing process reflects the activation of the healing process simultaneously with damage and it concerns the autonomous self-healing mechanism based on microcapsules (or hollow fibres). When damage increases and reaches a certain critical value, the microcracks occur and break the microcapsule. Following that, the healing agent is released from the microcapsule, fills the microcracks, reacts with the catalyst and forms a solid material. In the un-

coupled self-healing process the healing is imposed after loading stops or during the unloading phase. In these two phases the damage evolution is deactivated (damage is constant).

Two healing variables are defined for each self-healing process. The coupled healing process is defined by the fact that the damage and healing evolves simultaneously with damage in the material. In this case, the healing variable can take the following form:

$$h_c = \frac{S_h}{S_\varphi} \quad with\ 0 \leq h_c \leq 1 \tag{3.3}$$

where h_c represents the healing variable in the case of coupled self-healing system and S_h is the healed cross-section. It should be noted that the values of $h_c = 0$, $0 < h_c < 1$, and $h_c = 1$ represent the unhealed, partially healed, and fully healed material states, respectively. In the last case, the material recovers its original stiffness and the effective stress becomes similar to the nominal stress ($\overline{\sigma} = \sigma$). Critical damage should occur to break the microcapsules. Therefore, it is supposed that the cracks reflected by the damage variable which is necessary to break the microcapsules evolve before the healing variable.

In the case of uncoupled self-healing system, the damage and healing are activated separately in which the healing is exposed during a rest period (damage evolution is deactivated). Thus, the healing variable can be expressed as follows:

$$h_u = \frac{S_h - S_\varphi}{S_h} \quad with\ 0 \leq h_u \leq 1 \tag{3.4}$$

where h_u represents the healing variable in the case of uncoupled self-healing system. It should be again noted that the values of $h_u = 0$, $0 < h_u < 1$, and $h_u = 1$ represent the case of unhealed, partially healed, and fully healed material states, respectively. It is assumed that the healing effect occurs after loading stops or during the unloading phase. In these two phases the damage evolution is deactivated and the material is exposed to a rest period during which the healing is imposed. The healed configuration can also be defined in terms of its elastic modulus E_h. Figure 3.2 shows the combination of the damaged, partially healed, and effective configurations of the material. In this case the relation in equation (3.2) becomes [23, 84, 86]

$$\overline{\sigma} = \frac{\sigma}{1 - \varphi\,(1 - h)} \tag{3.5}$$

Equation (3.5) is obtained by replacing the damage variable in equation (3.2) by $\varphi\,(1-h)$. This variable is termed in [23] the effective damage variable, and in [86] the combined damage/healing variable. It is called here the eliminated damage variable. It represents the amount of the damage that is eliminated from the total cross-section due to the healing effect.

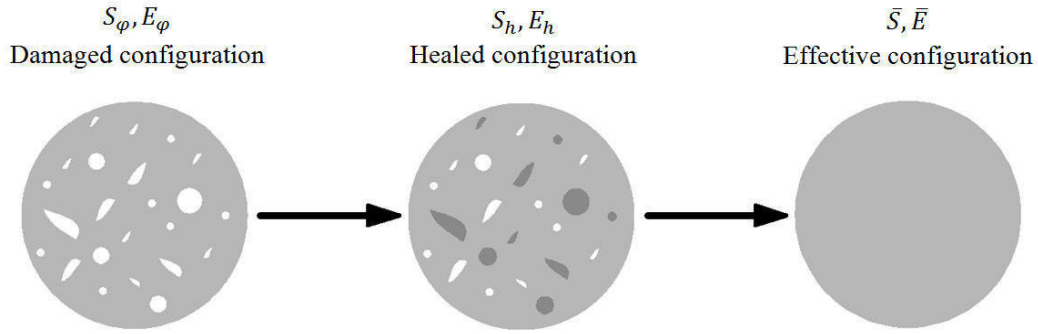

Figure 3.2: Damaged, partially healed, and effective configurations.

3.3 Thermodynamic framework of continuum damage-healing model

In this section, the thermodynamic framework of continuum damage-healing mechanics is reviewed. A certain assumptions regarding the strains in the damaged-partially-healed and effective configurations are needed. Usually, the hypothesis of elastic strain equivalence and the hypothesis of elastic energy equivalence are used. Both types of hypotheses are used by researchers in the field of CDHM. However, because of the involvement of some energy formulations the hypothesis of elastic energy is more appropriate compared to the hypothesis of elastic strain equivalence. Therefore, the second hypothesis listed above is assumed in the present work. The thermodynamic description of CDHM is restricted to small strain and isotropic

material. The damage and healing criteria are presented and the constitutive equations for damage and healing processes are derived. The hypothesis of elastic energy equivalence can be written as follows:

$$U = \frac{1}{2E_h}\sigma^2 = \frac{1}{2\overline{E}}\overline{\sigma}^2 \tag{3.6}$$

From equation (3.5), one substitutes $\overline{\sigma}$ into equation (3.6), and obtains the relation of the elastic modulus in the damaged-partially-healed and effective configurations:

$$E_h = \overline{E}\left(1 - \varphi\left(1 - h\right)\right)^2 \tag{3.7}$$

It should be noted that when the material is fully healed ($h = 1$) the elastic modulus in the healing configuration becomes similar to the elastic modulus in the effective configuration ($E_h = \overline{E}$). On the other hand, when there is no healing ($h = 0$) the elastic modulus in the healing configuration becomes similar to the elastic modulus in the damage configuration ($E_h = \overline{E}(1-\varphi^2)$) which fits the classical results obtained from CDM [141, 142, 143]. The evolution equations of damage and healing processes given in the present section follows the definition presented in [84] adapted with equation (3.5) of the effective stress defined in the present damage-healing model. The thermodynamic damage model is presented based on a scalar function g^{φ} and a generalized thermodynamic force y^{φ} that corresponds to damage variable. A similar healing scalar function g^h and thermodynamic force y^h are defined in order to incorporate the evolution equations of the healing effect. These two criteria are defined as follows:

$$g^{\varphi}\left(y^{\varphi}, s^{\varphi}\right) = \frac{1}{2}y^{\varphi^2} - L^{\varphi}\left(s^{\varphi}\right) \tag{3.8}$$

$$g^{h}\left(y^{h}, s^{h}\right) = \frac{1}{2}y^{h^2} - L^{h}\left(s^{h}\right) \tag{3.9}$$

where $L^{\varphi}\left(s^{\varphi}\right)$ is a damage-strengthening parameter which is a function of the global damage parameter s^{φ}. $L^h(s^h)$ is the healing-strengthening parameter, and s^h is the global healing parameter.

Next, one substitutes the elastic stiffness from equation (3.7) into equation (3.6),

which results in the following expression of the elastic energy in the damage and healing configurations:

$$U = \frac{1}{2}\sigma\varepsilon = \frac{1}{2}E\varepsilon^2 = \frac{1}{2}\overline{E}\left(1-\varphi\left(1-h\right)\right)^2\varepsilon^2 \tag{3.10}$$

After differentiating equation (3.10), one obtains

$$dU = \varphi E(1-\varphi(1-h))\varepsilon^2 dh - E(1-h)(1-\varphi(1-h))^2\varepsilon^2 d\varphi + \overline{E}(1-\varphi(1-h))^2\varepsilon d\varepsilon \tag{3.11}$$

The generalized conjugated thermodynamic forces that correspond to damage and healing are defined as follows:

$$y^{\varphi} = \frac{\partial U}{\partial \varphi} = -\overline{E}\left(1-h\right)\left(1-\varphi\left(1-h\right)\right)\varepsilon^2 \tag{3.12}$$

$$y^{h} = \frac{\partial U}{\partial h} = \varphi\overline{E}\left(1-\varphi\left(1-h\right)\right)\varepsilon^2 \tag{3.13}$$

Next, one uses the power of dissipation definition in the aim to derive the normality rule concerning damage and healing as follows:

$$\Pi = -y^{\varphi}d\varphi + y^{h}dh - L^{\varphi}ds^{\varphi} + L^{h}ds^{h} \tag{3.14}$$

The energy dissipation function Π is subjected to the constraint equations (3.8) and (3.9), and it is minimized with the incorporation of Langrage multipliers, which results in the following expression:

$$\Psi = \Pi - d\lambda^{\varphi}.g^{\varphi} - d\lambda^{h}.g^{h} \tag{3.15}$$

One substitutes equations (3.8), (3.9), and (3.14) into equation (3.15), to obtain

$$\begin{aligned}\Psi = -y^{\varphi}d\varphi + y^{h}dh - L^{\varphi}ds^{\varphi} + L^{h}ds^{h} - d\lambda^{\varphi}(\frac{1}{2}y^{\varphi^2} - L^{\varphi}(s^{\varphi})) \\ -d\lambda^{h}(\frac{1}{2}y^{h^2} - L^{h}(s^{h}))\end{aligned} \tag{3.16}$$

After the application of the stationary conditions of $\frac{\partial\Psi}{\partial y^{\varphi}} = 0$, $\frac{\partial\Psi}{\partial y^{h}} = 0$, $\frac{\partial\Psi}{\partial L^{\varphi}} = 0$,

and $\frac{\partial \Psi}{\partial L^h} = 0$, equation (3.16) results in the following relations:

$$d\varphi = -d\lambda^{\varphi}.y^{\varphi} \tag{3.17}$$

$$dh = d\lambda^{h}.y^{h} \tag{3.18}$$

$$ds^{\varphi} = d\lambda^{\varphi} \tag{3.19}$$

$$ds^{h} = -d\lambda^{h} \tag{3.20}$$

Equations (3.17) and (3.18) represent the evolution equations for damage and healing variables, and equations (3.19) and (3.20) show the relation between damage and healing variables and their corresponding multipliers. One now applies the consistency conditions $dg^{\varphi} = 0$ and $dg^{h} = 0$ in order to obtain the damage and healing variables as follows:

$$\frac{\partial g^{\varphi}}{\partial y^{\varphi}} dy^{\varphi} + \frac{\partial g^{\varphi}}{\partial L^{\varphi}} dL^{\varphi} = 0 \tag{3.21}$$

$$\frac{\partial g^{h}}{\partial y^{h}} dy^{h} + \frac{\partial g^{h}}{\partial L^{h}} dL^{h} = 0 \tag{3.22}$$

Incorporating $dL^{\varphi} = ds^{\varphi} \left(\frac{\partial L^{\varphi}}{\partial s^{\varphi}}\right)$ and $dL^{h} = ds^{h} \left(\frac{\partial L^{h}}{\partial s^{h}}\right)$ into equations (3.21) and (3.22) and using equations (3.8), (3.9), (3.19), and (3.20) results in:

$$ds^{\varphi} = d\lambda^{\varphi} = \frac{y^{\varphi} dy^{\varphi}}{\frac{\partial L^{\varphi}}{\partial s^{\varphi}}} \tag{3.23}$$

$$ds^{h} = -d\lambda^{h} = \frac{y^{h} dy^{h}}{\frac{\partial L^{h}}{\partial s^{h}}} \tag{3.24}$$

Next, one differentiates equations (3.12) and (3.13) to investigate the strain-damage and strain-healing relations as follows:

$$dy^{\varphi} = \overline{E}\left(1-2\varphi+2\varphi h\right)\varepsilon^2 dh + \overline{E}\left(1-h\right)^2\varepsilon^2 d\varphi \\ -2\overline{E}\left(1-h\right)\left(1-\varphi\left(1-h\right)\right)\varepsilon d\varepsilon \tag{3.25}$$

$$dy^{h} = \overline{E}\varphi^2\varepsilon^2 dh + \overline{E}\left(1-2\varphi+2\varphi h\right)\varepsilon^2 d\varphi + 2\overline{E}\varphi\left(1-\varphi\left(1-h\right)\right)\varepsilon d\varepsilon \tag{3.26}$$

Equations (3.23) and (3.24) are substituted into equations (3.17) and (3.18) to obtain the equations in terms of the conjugated forces and strengthening functions as follows:

$$d\varphi = -\frac{\left(y^{\varphi}\right)^2 dy^{\varphi}}{\frac{\partial L^{\varphi}}{\partial s^{\varphi}}} \tag{3.27}$$

$$dh = -\frac{\left(y^{h}\right)^2 dy^{h}}{\frac{\partial L^{h}}{\partial s^{h}}} \tag{3.28}$$

Incorporating equations (3.12), (3.13), (3.25) and (3.26) into equations (3.27) and (3.28) results in the relations of strain-damage and strain-healing as follows:

$$\frac{\partial L^{\varphi}}{\partial s^{\varphi}}d\varphi = \overline{E}^2\left(1-h\right)^2\left(1-\varphi\left(1-h\right)\right)^2\varepsilon^4[\overline{E}\left(1-2\varphi+2\varphi h\right)\varepsilon^2 dh \\ +\overline{E}\left(1-h\right)^2\varepsilon^2 d\varphi - 2\overline{E}\left(1-h\right)\left(1-\varphi\left(1-h\right)\right)\varepsilon d\varepsilon] \tag{3.29}$$

$$\frac{\partial L^{h}}{\partial s^{h}}dh = \overline{E}^2\varphi^2\left(1-\varphi\left(1-h\right)\right)^2\varepsilon^4[\overline{E}\varphi^2\varepsilon^2 dh \\ +\overline{E}\left(1-2\varphi+2\varphi h\right)\varepsilon^2 d\varphi + 2\overline{E}\varphi\left(1-\varphi\left(1-h\right)\right)\varepsilon d\varepsilon] \tag{3.30}$$

In the case of damage without healing, one sets $h = 0$ and $dh = 0$, and equation (3.29) results in:

$$\frac{\partial L^{\varphi}}{\partial s^{\varphi}}d\varphi = \overline{E}^3\varepsilon^5\left(1-h\right)^2\left[2\left(1-\varphi\right)d\varepsilon - \varepsilon d\varphi\right] \tag{3.31}$$

Equation (3.31) shows consistency with the relationship between the damage and

strain according to continuum damage mechanics [84, 142].

3.4 Damage-healing model description

In this section, the formulation of the proposed damage-healing model is described. Mazars damage model for concrete is adopted in the present work [110]. It should be noted that in Mazars damage model the compressive and tensile damage are defined. However, the present model is restricted to only pure tensile loads. The isotropic Mazars damage model is usually defined using an equivalent strain ε_{eq}. The equivalent strain allows reflecting a triaxial state of the material by equivalence to a uniaxial state. In the present work, the model is applied to one-dimensional examples. Therefore, the equivalent strain is termed uniaxial strain and the term ε_u is used rather than ε_{eq}. The damage model is represented by a scalar damage variable φ ($0 \leq \varphi \leq 1$). Again, one should note that $\varphi = 0$, $0 < \varphi < 1$, and $\varphi = 1$ represent the undamaged, partially damaged and fully damaged material states, respectively. The growth of damage is controlled by the damage threshold which is formulated as follows:

$$\Gamma^{\varphi}\left(Y, \kappa\right) \leq 0 \tag{3.32}$$

where Y and κ are the elastic energy and damage threshold, respectively. For $\Gamma^{\varphi} < 0$ there can be no growth of damage ($\dot{\varphi} = 0$) and the material behavior is linear elastic. The magnitude of the loading function is governed by the Kuhn-Tucker relations

$$\Gamma^{\varphi} \leq 0 \ ; \ \dot{k} \geq 0 \ ; \ \dot{\Gamma}^{\varphi} k = 0 \tag{3.33}$$

An initial value k_0 of k determines the initial elastic domain. Damage growth becomes possible ($\dot{\varphi} > 0$) for $\Gamma^{\varphi} = 0$. During damage evolution, the condition $\dot{\Gamma}^{\varphi} = 0$ must be satisfied. The damage variable can be expressed in terms of the loading criterion as follows:

$$\begin{cases} \varphi = 1 - \frac{(1-A)k_0}{k} - Aexp[-\beta(k - k_0)] & if \ k > k_0 \\ \varphi = 0 & if \ k < k_0 \end{cases} \tag{3.34}$$

where A and β are material parameters and k_0 is the strain threshold of damage.

3.4 Damage-healing model description

The damage-healing model is formulated based on the extension of the damage model with the introduction of the healing variable h . The model is applied at the macroscale and damage and healing are described by means of continuum damage and healing variables. The present model describes the healing efficiency in both coupled and uncoupled self-healing mechanisms; the healing occurs in both deformed and undeformed situations. Consequently, the healing process can be considered as autonomous or autogenous. After the introduction of the healing the material recovers its original stiffness and the fully healed material behavior becomes similar to the behavior of the original material. Thus, in this case the elastic moduli of the fully healed and effective configurations are similar. Unlike the damage-healing models existing in literature, the healing effect of the proposed model is described in different loading conditions, namely in loading, unloading and rest period (loading is stopped and considered as neutral loading). This concerns the so-called coupled and uncoupled self-healing mechanisms. In the case of coupled self-healing mechanism, the damage is activated during damage evolution, and in the case of uncoupled self-healing mechanism the healing is activated during the rest period. In addition, the nonlinear healing theory is applied using the present model and comparison with the classical healing theory is performed.

The healing is considered to eliminate the damage effect in the material. The fully healed material is supposed to be similar to the original material in terms of material stiffness. Several parameters influence the healing efficiency such as damage history, rest period and material characteristics. Therefore, the main feature of the proposed healing model is to take into account the parameters that influence the healing efficiency. The material characteristics are defined mathematically using the parameter γ. It should be noted that the material parameter γ defines how fast the healing progresses. Physically, it can be represented by for instance the percentage of microcapsules, shell thickness, healing agent strength, size and percentage of aggregates in concrete, etc. Varying these material characteristics influences the performance of the healing. Inspired from different experimental studies [52, 145, 146], we propose the following time-dependent healing law:

$$h\left(t\right) = f\left(\varphi\left(\varepsilon_u,\ t\right), t\right) \tag{3.35}$$

$$h\left(t\right) = 1 - exp\left[-\gamma\varphi\left(t_h\right)\left(t_{hf} - t_{hi}\right)\right] \tag{3.36}$$

where γ is a material parameter, and $\varphi\left(t_h\right)$ is the damage variable during the healing period t_h . It should be noted that $\varphi\left(t_h\right)$ takes constant values during the time after the unloading phase ($\dot{\varphi} = 0$). Unlike the damage-healing models existing in the literature, the proposed model describes the healing efficiency when the healing is activated during the loading phase; damage and healing evolve simultaneously. In this case $\varphi\left(t_h\right)$ evolves until failure ($\dot{\varphi} > 0$). The material is exposed to healing during the healing time t_h which has initial healing time t_{hi} and final healing time t_{hf} ($t_h \in [\ t_{hi}\ , t_{hf}\ ]$). The healing variable is supposed to take the value $h = 0$ when the material is unhealed and $h = 1$ when the material is fully healed. In the latter case, the material that has been fully healed exhibits the same behavior as the original material. The healing variable defined in equation (3.36) is expected to describe the uncoupled and coupled self-healing behaviour. One may then present the healing variables $h_u\left(t\right)$ and $h_c\left(t\right)$, respectively, of the uncoupled and coupled self-healing mechanisms with respect to damage history as follows:

$$\begin{cases} h_u\left(t\right) = 1 - exp\left[-\gamma\varphi\left(t_h\right)\left(t_{hf} - t_{hi}\right)\right] & if\ \varphi = 0 \\ h_u\left(t\right) = 0 & if\ \varphi > 0 \end{cases} \tag{3.37}$$

$$\begin{cases} h_c\left(t\right) = 1 - exp\left[-\gamma\varphi\left(t_h\right)\left(t_{hf} - t_{hi}\right)\right] & if\ \varphi > 0 \quad and\ \ \varphi \geq \varphi_{cr} \\ h_c\left(t\right) = 0 & if\ \varphi > 0 \quad and\ \ \varphi < \varphi_{cr} \end{cases} \tag{3.38}$$

where φ_{cr} represents the critical damage necessary to induce the healing mechanism. The critical damage variable reflects the effect of the critical cracks necessary to break the microcapsules (or hollow fibres), and consequently induces the healing mechanism. It should be noted that in the present work we use the critical strain (ε_{cr}) instead of critical damage (φ_{cr}) in the application of the coupled damage-healing model for the one-dimensional example. Consequently, one should also note that the coupled healing variable $h_c\left(t\right)$ starts to evolve when the unidirectional strain exceeds the critical strain ($\varepsilon_u \geq \varepsilon_{cr}$). Since the healing variable is defined as an opposite of the damage variable, the damage threshold has to be decreased

under the healing effect. In this case, the damage threshold depends on damage and healing effects, and equation (3.32) is rewritten as follows:

$$\Gamma^{\varphi}[(Y, \kappa(\varphi, h))] \leq 0 \tag{3.39}$$

When the energy exceeds the material damage threshold, damage is initiated and accumulated via the variable φ. The magnitude of the loading function is governed by the Kuhn-Tucker relations

$$\Gamma^{\varphi} \leq 0 \quad ; \quad \dot{k} \geq 0 \quad ; \quad \Gamma^{\varphi}\dot{k} = 0 \tag{3.40}$$

Again, an initial value k_0 of k determines the initial elastic domain. Damage growth becomes possible ($\varphi > 0$) for $\Gamma^{\varphi} = 0$. During damage evolution, the condition $\Gamma^{\varphi} = 0$ must be satisfied. The model has to be specified by the healing evolution equation (3.39) and the damage condition (3.32).

3.5 Application to examples

The proposed damage-healing model is applied to one-dimensional examples. In order to analyse the healing efficiency the influence of the following parameters are taken into account:

- History of loading and damage.
- Rest period between unloading and reloading: In this time period, the material is supposed to be partially or fully healed with varying the rest period.
- Material characteristics: e.g. percentage of microcapsules, shell thickness, healing agent strength, size and percentage of aggregates in concrete, etc. Varying these material characteristics in concrete material influences the performance of the healing [2, 147]. These material characteristics are defined mathematically in the present work with the parameter γ.

A unidirectional strain is prescribed at the end of the one-dimensional element and the evolution of stress-time and stress-strain responses with and without healing are described. The model is applied in the case of uncoupled and coupled self-healing

Table 3.1: Material parameters.

E [MPa]	k_0	A	β	γ
32000	0.000085	0.9	2000	0.0001

mechanisms. In the following sections, three examples will be applied. The first and second ones concern the uncoupled self-healing mechanisms with zero and non-zero strain during the rest period. The third one concerns the coupled self-healing mechanism. Figure 3.3 shows the strain history of the three examples. The material parameters used for the three examples are inspired by concrete material and are presented in Table 3.1. It is important to note that the parameter γ presented in Table 3.1 concerns the first and second examples in which it is constant, while in the third example it varies from 0.0001 to 0.02 in order to study its influence on the healing efficiency.

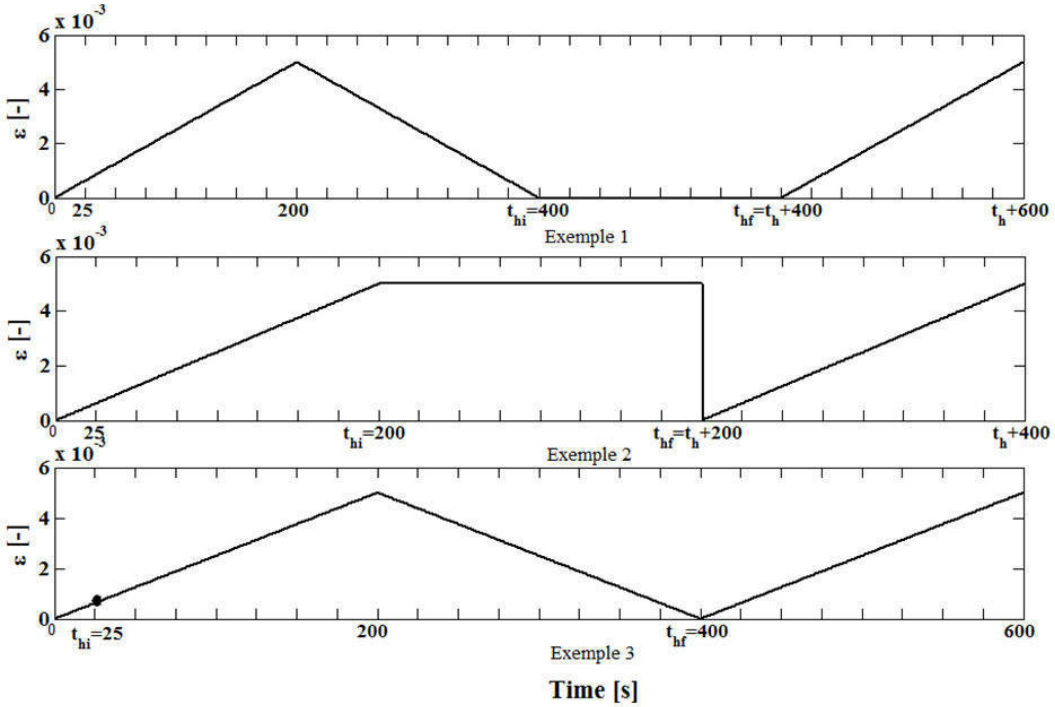

Figure 3.3: Strain history of three examples for coupled and uncoupled self-healing mechanisms.

3.5.1 Uncoupled damage-healing mechanism

As previously presented, two healing variables were defined in Section 2 that measure the healing effect in the case of uncoupled and coupled self-healing mechanisms. The uncoupled self-healing mechanism is characterized by the fact that the healing and damage are activated separately. In this case, the material is exposed to healing during the rest period. The material is supposed to be loaded, unloaded, exposed to rest period and then reloaded. Another example is applied in which the healing is introduced during the rest period with non-zero strain. In this case, the material is supposed to be loaded until the strain reaches the value of 0.005, then it is kept constant during the rest period and afterwards the strain is increased again from a zero value. During the loading phase the damage evolves until failure and becomes constant during unloading and rest period. When the damage evolution becomes deactivated ($\dot{\varphi} = 0$) the healing takes place during the rest period; damage and healing are activated separately. After the material has been exposed to healing it is reloaded in order to analyse the behavior of the healed material. If the material is fully healed it should exhibit similar behavior as the original material and the elastic modulus in this situation becomes similar to the elastic modulus in the effective configuration ($E_h = \overline{E}$). On the other hand, if the material is not healed it should exhibit similar behavior as the damaged material and the elastic modulus in this case becomes similar to the elastic modulus in the damaged situation ($E_h = E_\varphi$).

In the present example, the healing is supposed to take place separately than the damage variable. The strain history of the present example is shown above in Figure 3.3 (Example 1). The element is subjected to prescribed unidirectional strain until failure and then unloaded until the strain reduces to zero. This is followed by a rest time for various periods during which the material is exposed to healing. Afterwards, the material is reloaded and the strain increases again. In the reloading phase, the healing efficiency is analysed and the recovery of stiffness is described by plotting the stress-time and stress-strain responses after healing. During the loading phase the stress increases linearly until the damage threshold is reached. Afterwards, the stress response becomes exponential in softening due to the degradation of the material stiffness. The stress response remains zero in unloading, rest period and reloading phases due to damage. The material is supposed to gain its total original

stiffness after the introduction of the healing effect. Therefore, different periods of rest time are chosen in order to analyse the influence of the rest period on the healing efficiency. The rest period varies from 2000 s until 30000 s. Figures 3.4(a) and 3.4(b) show the stress-time and stress-strain responses of the material behavior after the introduction of the healing in which the response of the healed material is compared to the response of the original material. It should be noted that the stress-strain responses in Figure 3.4(b) are limited to the reloading phase; time interval $\in [t_h + 400\ ,\ t_h + 600]\ s$. In this phase, the material is reloaded after the introduction of the healing in order to analyse the behavior of the healed material.

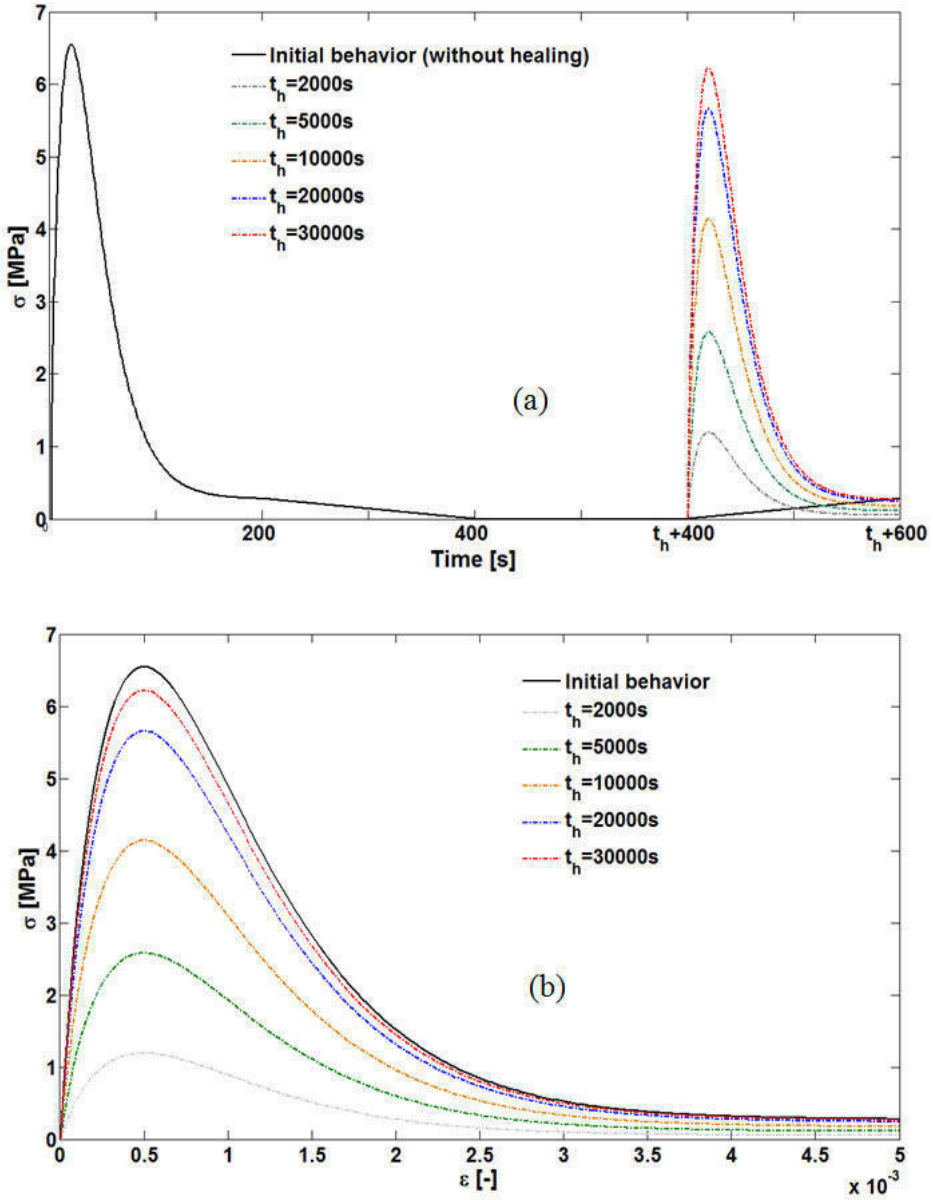

Figure 3.4: (a) Stress-time and (b) stress-strain responses of the uncoupled damage-healing model with various rest period and zero strain.

It can be seen from Figure 3.4 that the recovery of the material stiffness is well described using the damage-healing model. Figure 3.4(a) shows that the material is loaded and unloaded from zero time until 400 s, subjected to different rest periods t_h , and reloaded from the time $(t_h + 400)$ s to $(t_h + 600)$ s. It is clearly shown that when the healing is exposed during a short rest period the material stiffness is not fully recovered. For example with the rest period t_h =2000 s, the material recovers a part of the stiffness which represents 17.14 % of the original stiffness. On the other hand, when the healing is exposed during a long rest period the material recovers its original stiffness as it is shown in the case of the rest period t_h =30000 s. It should be noted that the healing time depends on the material parameter γ which can be adjusted to adapt the numerical results to the experimental studies. It can also be seen that the proposed damage-healing model describes the exact recovery of the failure strength in which the same peak load was reached in the case of t_h =30000 s comparing to the original material. One should note that the introduction of the healing effect to the damaged material is expected to regularize the underlying problem avoiding or at least alleviating the mesh dependency of the solution when local damage models are used.

Several experimental investigations were carried out in literature regarding the uncoupled self-healing mechanism such as [148, 149] in which the self-healing mechanism incorporating thermoplastic particles was studied, and [150] in which a self-healing polymer network was designed by employing thermally reversible covalent bond. The authors in [151] studied the effect of ionomers on the mechanical properties of self-healing. In [152], shape memory polymers were used to study the efficiency of self-healing effect in structural scale. In Figure 3.5, the results of an experimental test on uncoupled self-healing mechanism example are presented [9]. The evolution of the recovery of the stiffness for different periods of time of ageing in water is shown in this figure. This experimental investigation concerned the study of the influence of the healing effect on the mechanical behavior of healed concrete beam subjected to three points bending. The specimens were loaded, unloaded, exposed to several periods of ageing, and then reloaded. Three specimens were stored in air and three others were stored in water during the time periods to induce the healing mechanism. The beams were cracked, and the ageing periods selected were 1, 3, 6, and 10 weeks. The experimental results showed that the recovery of the

mechanical properties of the specimens stored in water increases with the increase of the rest period. From Figure 3.5, it is clearly seen that the material stiffness is recovered due to self-healing, and the stiffness becomes close to the stiffness of the intact material with time.

It is important to note that the stiffness recovery shown in Figure 3.5 corresponds exactly to the stiffness recovery obtained using the developed uncoupled damage-healing model. Then, one can conclude that the experimental results fit the results of the framework of the uncoupled damage-healing model developed in the present work, in which the rest period influences directly the healing efficiency.

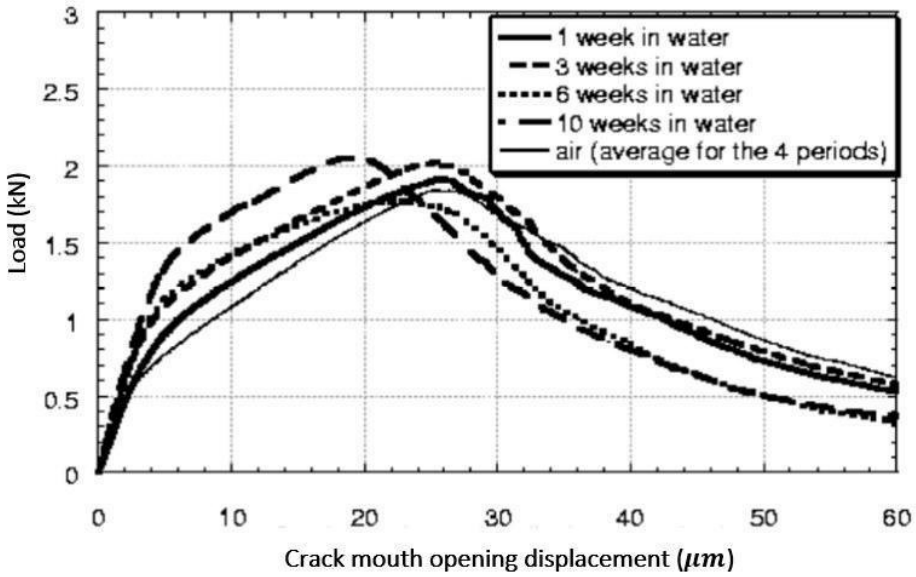

Figure 3.5: Experimental example of the behavior of self-healed specimens for different rest periods [9].

Unlike the previous example, in the next example the healing is supposed to be introduced during the rest period with non-zero strain. The strain is kept constant during the rest period. This kind of loading can be found in the experimental tests of fatigue analysis [17]. The strain history of the example with constant non-zero strain during the rest period is shown above in Figure 3.3 (Example 2). The healing is introduced similarly to the example with zero strain during the similar rest periods which vary from 2000 s to 30000 s. The results of the introduction of the healing

effect during non-zero strain are shown in Figures 3.6(a) and 3.6(b). It is seen from the figures that the stiffness recovery and failure strength of the healed material during the rest period with non-zero strain is similar to the healed material during the rest period with zero strain (Figure 3.4). One can conclude that the healing efficiency is affected by the damage and healing histories and not by the strain history; the material is deformed in both cases of zero and non-zero strain during the rest period.

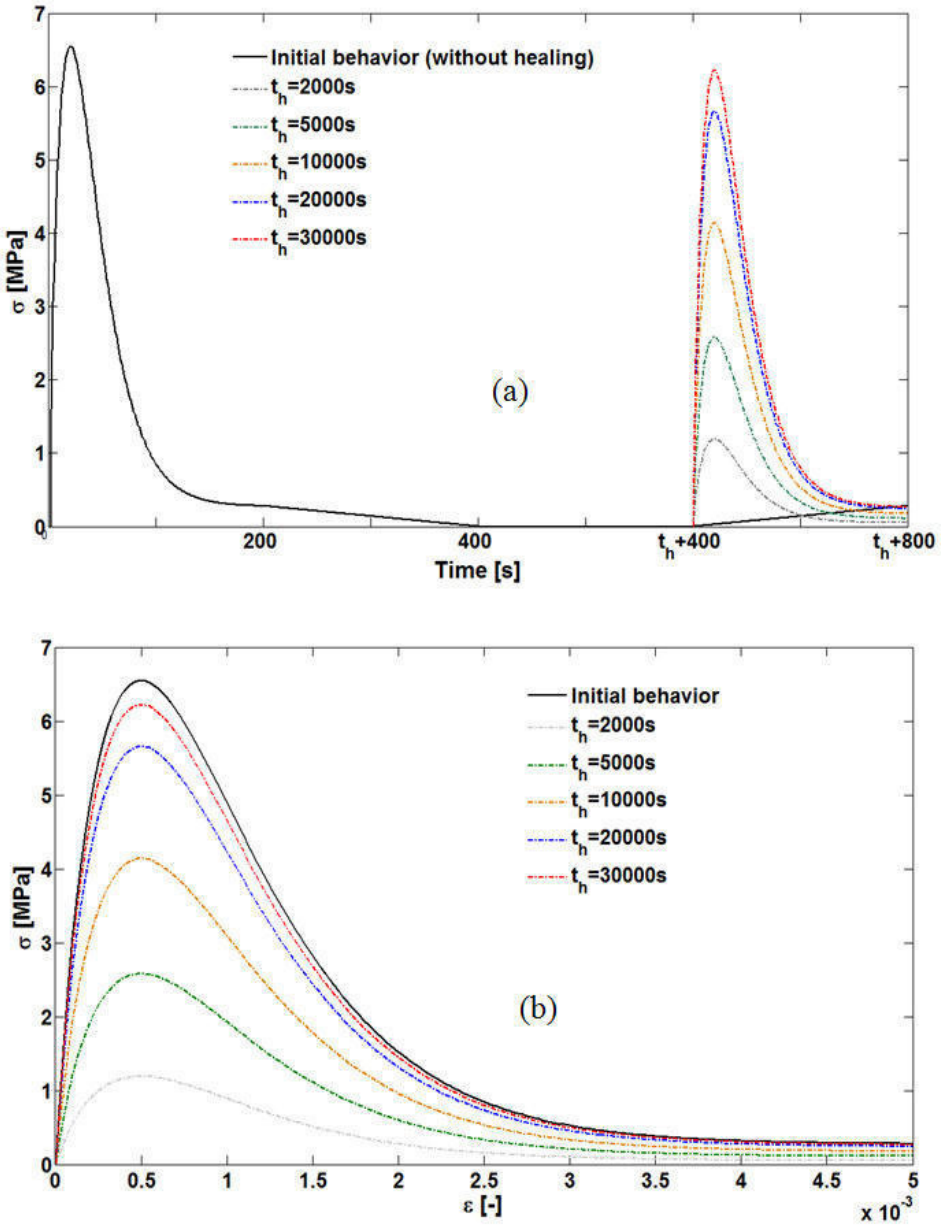

Figure 3.6: (a) Stress-time and (b) stress-strain responses of the of uncoupled damage-healing model with various rest period and non-zero strain.

3.5.2 Coupled damage-healing mechanism

In this section, the concept of coupled self-healing is highlighted. The healing variable defined in equation (3.3) represents the healing that is activated in the system simultaneously with damage evolution. Several experimental investigations were carried out in literature in which the coupled self-healing mechanism represents the autonomous self-healing process such as the microcapsulated self-healing system proposed in [2]. Coupled self-healing mechanism may also use hollow fibres [147, 153] and microvascular system [154, 155]. The challenging issue in numerical analysis of self-healing materials is to describe the healing efficiency of the material before it becomes deformed; damage and healing occur at the same time ($h > 0 \;\; \& \;\; \dot{\varphi} > 0$). In the case of microcapsules-based self-healing mechanism, when damage increases, microcracks occur and break the microcapsules. The healing agent releases from the microcapsules, reacts with the catalyst, forms a solid material and fills the microcracks. Critical microcracks are needed to break the microcapsules. Consequently, the release of the healing agent depends on the density of the microcracks. One can say that if an appropriate distribution of the microcapsules is provided in the material, the cracks can be healed during their propagation.

An example is applied on coupled self-healing mechanism. The strain history of the present example is shown above in Figure 3.3 (Example 3). The loading strain is first increased until it reaches the maximum value of 0.005. It is then decreased to zero and increased afterwards. During the loading phase the damage evolves until failure and becomes constant during the unloading phase. The healing occurs during loading and continues until unloading. Following that, the material is reloaded to analyse the response of the healed material. It is assumed in this example that the critical microcracks that are able to break the microcapsules occur after 25 seconds of loading which corresponds to the value of critical strain $\varepsilon_{cr} = 0.000625$. The black circle in Figure 3.3 (Example 3) represents the beginning time of the healing. The key parameter of the coupled self-healing mechanism is the material characteristics that are defined in the present work mathematically by the material parameter γ. Therefore, in order to describe the influence of the material characteristics on the healing efficiency different values of the material parameter γ are taken in this example. It should be noted that the values of the material parameter γ are adjusted

in the aim to adapt the numerical results to the experimental studies. Figures 3.7(a) and 3.7(b) show the stress-time and stress-strain responses of the healed material with different values of material parameter γ. Comparison of the behavior of the healed material with the behavior of the original material is described. It should be noted that the plot of Figure 3.7(b) is limited to the time interval between 400 s and 600 s during which the healed material is reloaded.

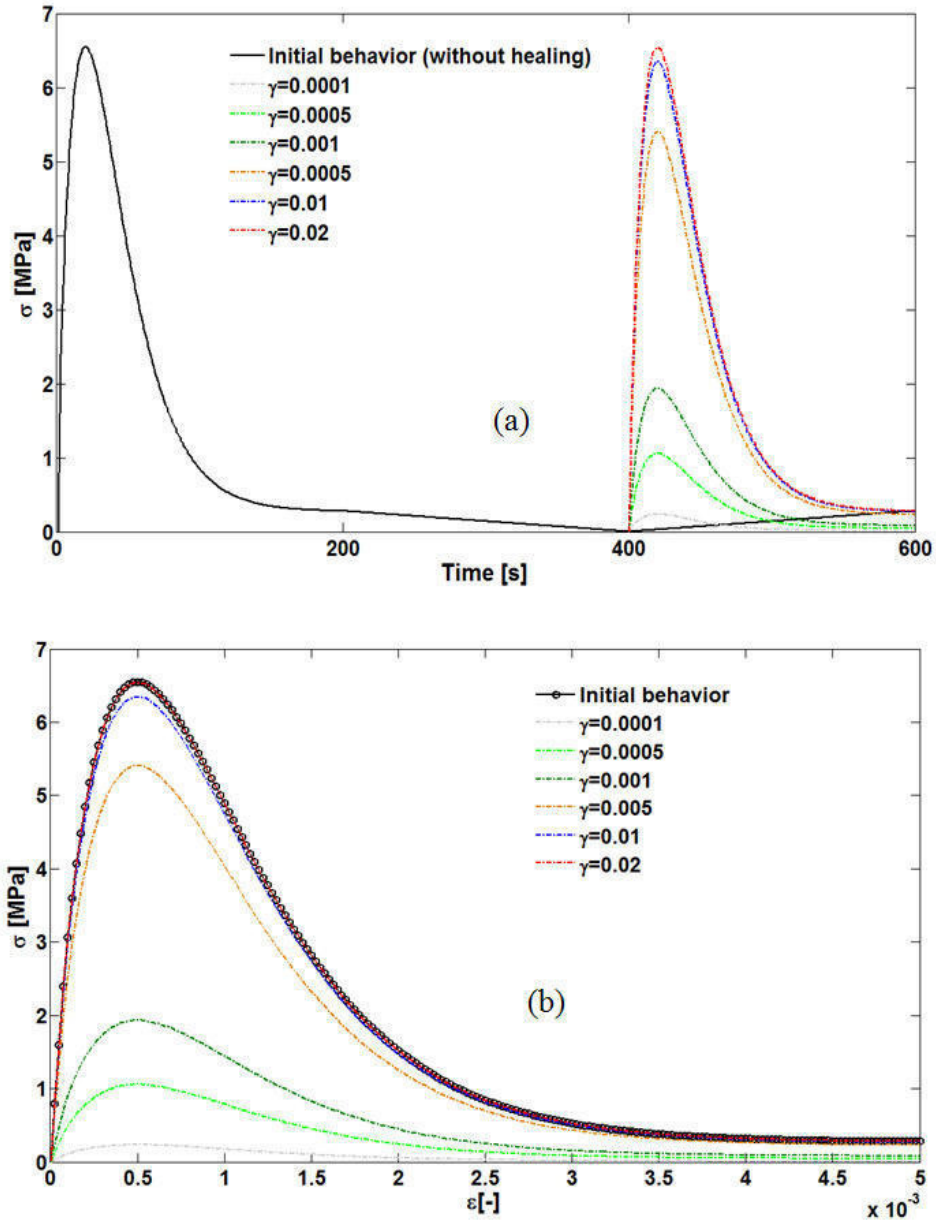

Figure 3.7: (a) Stress-time and (b) Stress-strain responses of the damage-healing model for coupled self-healing mechanism.

It is seen from Figure 3.7 that the model is able to describe the healing of the damaged material even if the healing is exposed during the loading phase. It is clearly shown that the material stiffness is partially recovered when the material parameter γ takes a small value. For example with $\gamma = 0.001$, the material recovers a part of the stiffness which represents 31.20 % of the original stiffness. On the other hand, when the healing is exposed with a large value of the parameter γ the material recovers its original stiffness as it is shown in the case of $\gamma = 0.02$. With the same value of the material parameter γ an exact recovery of the failure strength in which the same peak load was reached comparing to the original material. Since the material parameter γ is supposed to reflect the material characteristics of self-healing material, one can conclude that for instance in the case of microcapsules-based self-healing material an appropriate preparation of microcapsules and materials properties is necessary to achieve the complete recovery of material stiffness. As Figure 3.4 might indicate, for the case of coupled self-healing mechanism the healing effect is expected to regularize the problem of mesh-dependency in brittle material with strain softening. When the critical damage occurs and induces the healing, the latter leads to the minimization or elimination of the damage and the material softening and results in the regularization of the problem.

Figure 3.8 shows experimental evidence that the microcapsule loading percentage influences the crack mouth healing efficiency. The authors in [10] performed an experimental study on microcapsules-based self-healing mortar. Liquid sodium silicate was used as healing agent, and the volume fraction of the microcapsules was varied with respect to the volume of cement. It is clear from the figure that the increase in microcapsule percentage results in the total crack healing and, consequently in stiffness recovery. It should be noted that the crack mouth healing percentage in Figure 3.7 is fully compatible with the healing variable h. One can then conclude that the experimental results fit the results of the framework of the coupled damage-healing model developed in the present work, in which the material parameter has a direct influence on the healing efficiency.

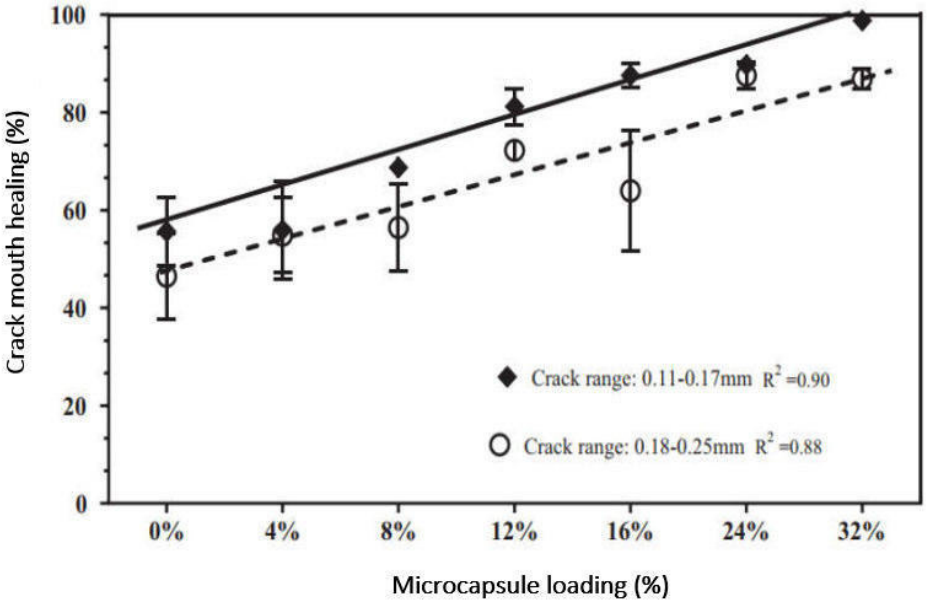

Figure 3.8: Experimental example of the crack mouth healing percentage as function of microcapsule loading percentage [10].

3.6 Nonlinear damage-healing theory

The nonlinear self-healing concept was first proposed in [88]. The linear (classical) self-healing theory is represented in equation (3.5). It is called linear because of the linearity of the equation in h. We will show in this section that the linear healing theory is a special case of the nonlinear healing theory when the damage is small. In this section, the nonlinear self-healing concept is introduced and compared to the linear self-healing model.

From equation (3.5), the eliminated damage variable φ_{hd} is expressed as follows:

$$\varphi_{hd} = \varphi\,(1-h) \tag{3.41}$$

Then, one rewrites equation (5) as follows:

$$\overline{\sigma} = \frac{\sigma}{1-\varphi_{hd}} = \frac{\sigma}{1-\varphi\,(1-h)} \tag{3.42}$$

It is clear from equation (3.42) that the eliminated damage variable φ_{hd} is linear

in h. Consequently, equation (3.42) represents the linear self-healing model. The geometric representation of the nonlinear healing theory is elucidated in Figure 3.9. In the left part of the figure the state of the damaged material is shown by the classical damage variable φ while in the right part of the figure the state of partially healed material is shown by the healing variable h. In the nonlinear healing theory, only a partial set of the damaged area is considered to be healed. One can clearly see from right part of Figure 3.9 that the size of the healed area S_h is less than the size of the damaged area S_φ.

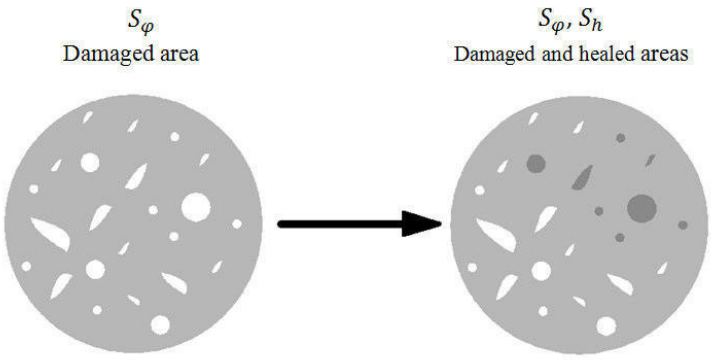

Figure 3.9: Geometric representation of nonlinear healing concept.

The nonlinear self-healing theory is applied following the mathematical derivation along with the same definition introduced in [88]. This theory was defined based on the decomposition of damage variable given in [156]:

$$\varphi = \varphi_1 + \varphi_2 - \varphi_1\varphi_2 \tag{3.43}$$

where φ_1 and φ_2 represent, respectively, the first and second damage processes acting in series. The healing variable is introduced to the decomposition equation according to the following conditions:

$$\varphi_1 = h\varphi \tag{3.44}$$

$$\varphi_2 = \varphi_{hd} \tag{3.45}$$

Table 3.2: Boundary conditions of equation (3.47).

Variables	Zero healing	Complete healing
φ	> 0	0
h	0	1
φ_{hd}	φ	0

The first condition in equation (3.44) represents the first stage of the healing which is the healed damage while the second condition in equation (3.45) represents the second stage of the healing which is the effective damage stage. After Substituting equations (3.44) and (3.45) into equation (3.43), the following equation is obtained:

$$\varphi = h\varphi + \varphi_{hd} - h\varphi\varphi_{hd} \tag{3.46}$$

From equation (3.46), the expression of the eliminated damage variable in the case of generalized nonlinear healing model takes the following form:

$$\varphi_{hd} = \frac{\varphi\,(1-h)}{1-h\varphi} \tag{3.47}$$

Equation (3.47) represents the expression of the nonlinear healing generalization of equation (3.41). This equation is nonlinear because of the nonlinearity of the variable φ_{hd} in h. It is important to note that for the nonlinear healing theory, equation (3.47) satisfies the two boundary conditions of self-healing theory as shown in Table 3.2:

Following the expressions of the nonlinear healing theory in equation (3.47) and the effective stress in equation (3.5), one then writes the equation of the effective stress of the generalized nonlinear healing model as follows:

$$\overline{\sigma} = \frac{\sigma\,(1-h\varphi)}{1-\varphi} \tag{3.48}$$

Next, one shows that the linear healing model is a special case of the nonlinear healing model. Therefore, Taylor series expansion around the point $h = 0$ is

calculated as follows:

$$\frac{1}{1-h\varphi} = 1 + h\varphi + h^2\varphi^2 + h^3\varphi^3 + h^4\varphi^4 + ... \tag{3.49}$$

Substituting only the first two terms of the series on the right-hand side of equation (3.49) into equation (3.47) results in the following form:

$$\varphi_{hd} = \varphi\,(1-h)\,(1+\varphi h) \tag{3.50}$$

After simplification of equation (3.50), one obtains

$$\varphi_{hd} = \varphi\,(1-h) + \varphi^2 h\,(1-h) \tag{3.51}$$

If the quadratic term in φ on the right-hand side of equation (3.51) is ignored for the case of small damage, the following equation is obtained:

$$\varphi_{hd} = \varphi\,(1-h) \tag{3.52}$$

From equation (3.52), it is clearly seen that it represents exactly the equation of the eliminated damage variable defined in equation (3.41). Therefore, it is demonstrated that the linear healing model is a special case of the nonlinear healing model for the case of small damage. We will next present the quadratic healing model which is a special case of the nonlinear healing model.

3.7 Quadratic self-healing

Quadratic healing model represents a special case of the nonlinear healing model. Equation (3.41) can be rewritten as follows

$$\varphi_{hd} = \varphi - \varphi h \tag{3.53}$$

It should be noted that the term φh represents the subtraction of the healed damage part from φ . As already applied for nonlinear healing model, one rewrites equation (3.47) using the Taylor series expansion as follows [88]:

$$\varphi_{hd} = \varphi(1-h)(1+\varphi h+\varphi^2 h^2 \ +\varphi^3 h^3+...) \tag{3.54}$$

Considering only the first two terms and neglecting the higher order terms of equation (3.54) result in the following equation:

$$\varphi_{hd} = (\varphi - h\varphi)\,(1+\varphi h) \tag{3.55}$$

After expansion, equation (3.55) can be written as follows:

$$\varphi_{hd} = (\varphi - h\varphi) + \left(h\varphi^2 - h^2\varphi^2\right) \tag{3.56}$$

Equation (3.56) represents the quadratic healing because the variable φ_{hd} is a quadratic function of the healing variable h . Two parts are defined in equation (3.56). The first part $(\varphi - h\varphi)$ represents the linear damage variable that is unhealed, and the second part $(h\varphi^2 - h^2\varphi^2)$ represents the quadratic damage that is unhealed. Using equation (3.50) for the quadratic healing, the effective stress is written as follows:

$$\overline{\sigma} = \frac{\sigma}{1-(\varphi - h\varphi)\,(1+\varphi h)} \tag{3.57}$$

3.8 Coupled and uncoupled non-linear self-healing models

In this section, application of the nonlinear healing theory in the case of coupled and uncoupled self-healing mechanisms is carried out. The generalized nonlinear and quadratic healing models are applied to one-dimensional examples subjected to a prescribed unidirectional strain. The healing efficiency is described by comparison of the stress-time and stress-strain responses with and without healing. The same material parameters presented above in Table 3.1 are used for the examples of nonlinear healing models.

3.8.1 Uncoupled nonlinear self-healing model

Following the definition of the healing variable in equation (3.4), the material is exposed to healing during the rest period. In this case, damage and healing are activated separately. The material is supposed to be loaded, unloaded, exposed to rest period and then reloaded. In order to analyse the behavior of the healed material, this latter is reloaded after it has been exposed to healing during the rest period.

The healing effect in the case of uncoupled self-healing mechanism is introduced when the material if deformed. Observing equation (3.48) of the generalized non-linear healing model one can see that if the healing is introduced in the damaged state material the effective stress approaches infinity which is contradictory with the self-healing theory. Consequently, one can say that the generalized nonlinear self-healing model cannot be used when the material is damaged and the material in this case remains unhealed. Therefore, equation (3.57) of the quadratic healing model is used in the case of uncoupled self-healing mechanism. It should be noted that the material is subjected to the same strain history shown above in Figure 3.3 (Example 1). The one-dimensional element is subjected to unidirectional strain until failure and then reloaded until the strain reduces to zero. Afterwards, the material is subjected to various rest periods during which the material is exposed to healing. Then, the strain increases again in the reloading phase. In this phase, the material is analysed to describe the recovery stiffness and healing efficiency. The same rest periods of time are used in this example (from 200 s to 30000 s). It should be noted that the example of the non-zero strain during the rest period is not applied in the uncoupled nonlinear self-healing model because it is concluded that the healing efficiency is affected by the damage and healing histories and not by the strain history (see above Section 5.1). Figures 3.10(a) and 3.10(b) show the stress-time and stress-strain responses of the material behavior after the introduction of the healing effect and the comparison to the damaged and original material responses. It should be again noted that the plot of the stress-strain responses in Figure 3.10(b) are limited to the reloading phase (time interval $[t_h + 400\ ,\ t_h + 600]$ s). In this phase, the material is reloaded after the introduction of the healing in order to analyse the response of the healed material.

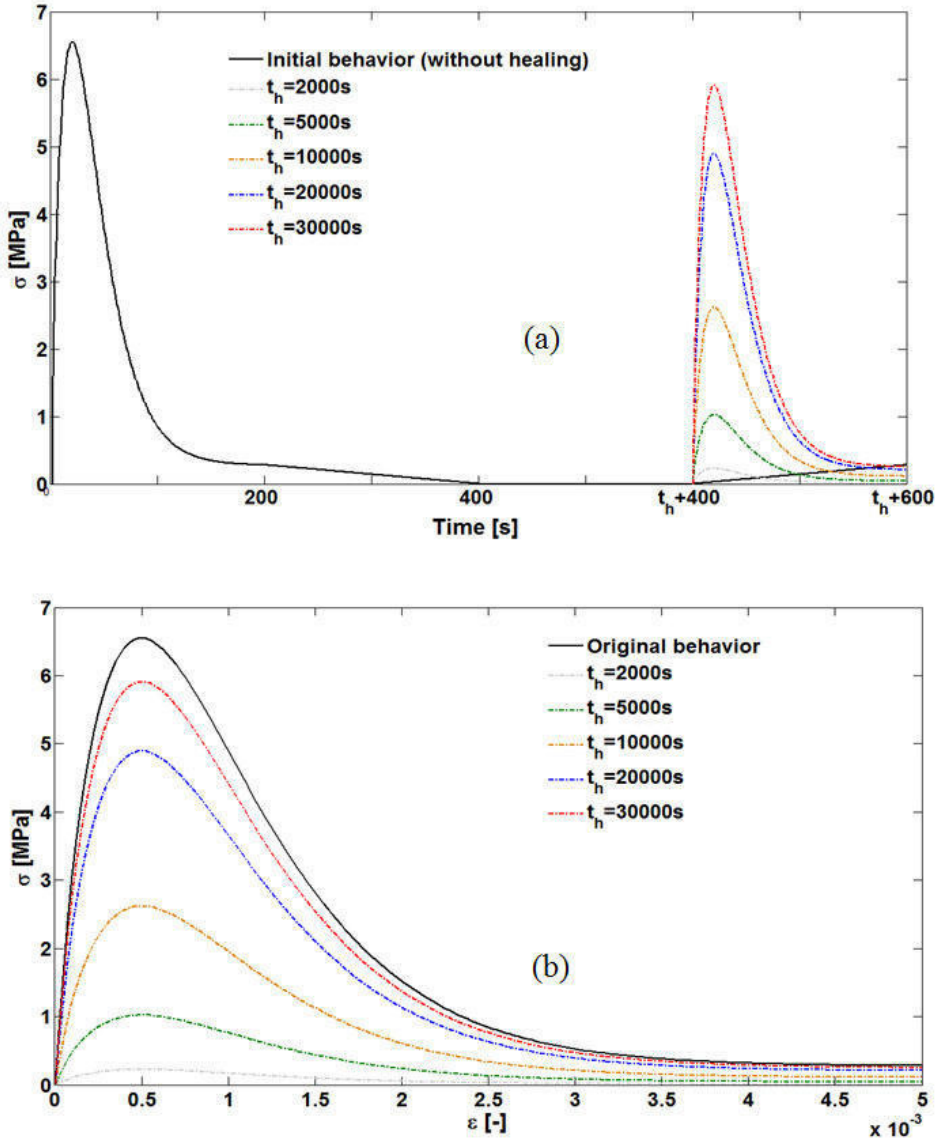

Figure 3.10: (a) Stress-time and (b) stress-strain responses of the quadratic damage-healing model with various intervals of rest period.

It can be observed from Figure 3.10 that the quadratic damage-healing model describes the recovery of the material stiffness. It is shown that the material stiffness is not fully recovered when the healing is exposed during a short interval of rest period. On the other hand, a large stiffness is recovered when the healing is exposed during a long interval of rest period. Comparing Figure 3.4(b) of the uncoupled linear damage-healing model and Figure 3.10(b) of the uncoupled quadratic damage-healing model, one can observe that the healed material response in Figure 3.4(b) with 2000 s of rest period exhibits similar behavior as the healed material in Figure 3.10(b) with 5000 s of rest period, with 17.14 % of the original stiffness recovered. Consequently, one can say that the stiffness recovery using the linear damage-healing model is larger than the stiffness recovery using the quadratic damage-healing model. It is then concluded that the quadratic damage-healing model underestimates the healing efficiency, and the hypothesis of nonlinear healing theory is confirmed in which only a part of the damaged material is healed compared to the classical (linear) damage-healing model. It should be again noted that the healing time depends on the material parameter γ which can be adjusted to adapt the numerical results to the experimental studies.

3.8.2 Coupled nonlinear self-healing model

In this section, the coupled nonlinear damage-healing model is applied. Following the definition of the healing variable in equation (3.3), the material is exposed to healing during damage evolution. In this case, damage and healing are activated simultaneously. The material is supposed to be loaded, unloaded and reloaded. In the reloading phase, the response of the healed material is analyzed and compared to the damaged and original material responses. In the case of coupled self-healing mechanism the healing is introduced in the undeformed material state. The damage evolves first and the healing starts to evolve after the critical damage needed to break the microcapsules occurs. The coupled self-healing mechanism is reflected by the autonomous self-healing process such as the microcapsules-based self-healing system. In this system, critical microcracks are needed to break the microcapsules. Following that, the healing agent releases, reacts with the catalyst and forms a solid material that fills the microcracks.

Equation (3.48) of the generalized nonlinear healing model is used in this section. The material is subjected to the same strain history shown above in Figure 3.3 (Example 3). The one-dimensional element is subjected to unidirectional strain until failure, unloaded and then reloaded. In the reloading phase, the healed material is analysed to describe the recovery of the material stiffness and the healing efficiency. In this example, it is also assumed that the critical microcracks needed to break the microcapsules occur after 25 seconds of loading which corresponds to the value of the critical strain $\varepsilon_{cr} = 0.000625$. The healing is exposed during loading and continued until unloading. The same values of the material parameter γ used in the example of linear damage-healing model are used in this section. Figures 3.11(a) and 3.11(b) show the stress-time and stress-strain responses of the healed material with different values of the material parameter γ.

From Figure 3.11, one can see that the nonlinear damage-healing model is able to describe the coupled self-healing mechanism. Unlike the results of the coupled linear self-healing model elucidated in Figure 3.7, it is clearly shown in Figure 3.11 that the material is not able to recover its stiffness with the values of the material parameter γ 0.0001, 0.0005, 0.001, and 0.005, while the material stiffness is partially recovered with the value of γ =0.01. However, 75 % of the original material stiffness is recovered with the value of γ =0.02. On the other hand, with the same value of the material parameter γ =0.02 full recovery of the material stiffness was reached using the linear self-healing model (Figure 3.7). One can conclude that the generalized nonlinear self-healing model underestimates the healing efficiency, and again the hypothesis of nonlinear healing theory is confirmed in which only a part of damaged material is healed compared to the classical (linear) damage-healing model.

3.9 Conclusion

We have presented in this chapter the damage-healing law proposed in the present work which is based in the continuum damage-healing mechanics framework. We have demonstrated that the proposed model is able to describe the autonomous and autogenous healing mechanisms and stiffness recovery in concrete material. Comparison of the classical (linear) and nonlinear self-healing models showed that in both coupled and uncoupled self-healing theories the generalized nonlinear and quadratic healing models underestimate the healing efficiency comparing to the linear healing model. Qualitative comparison of the results of the developed model with the results of the experimental investigations was also discussed.

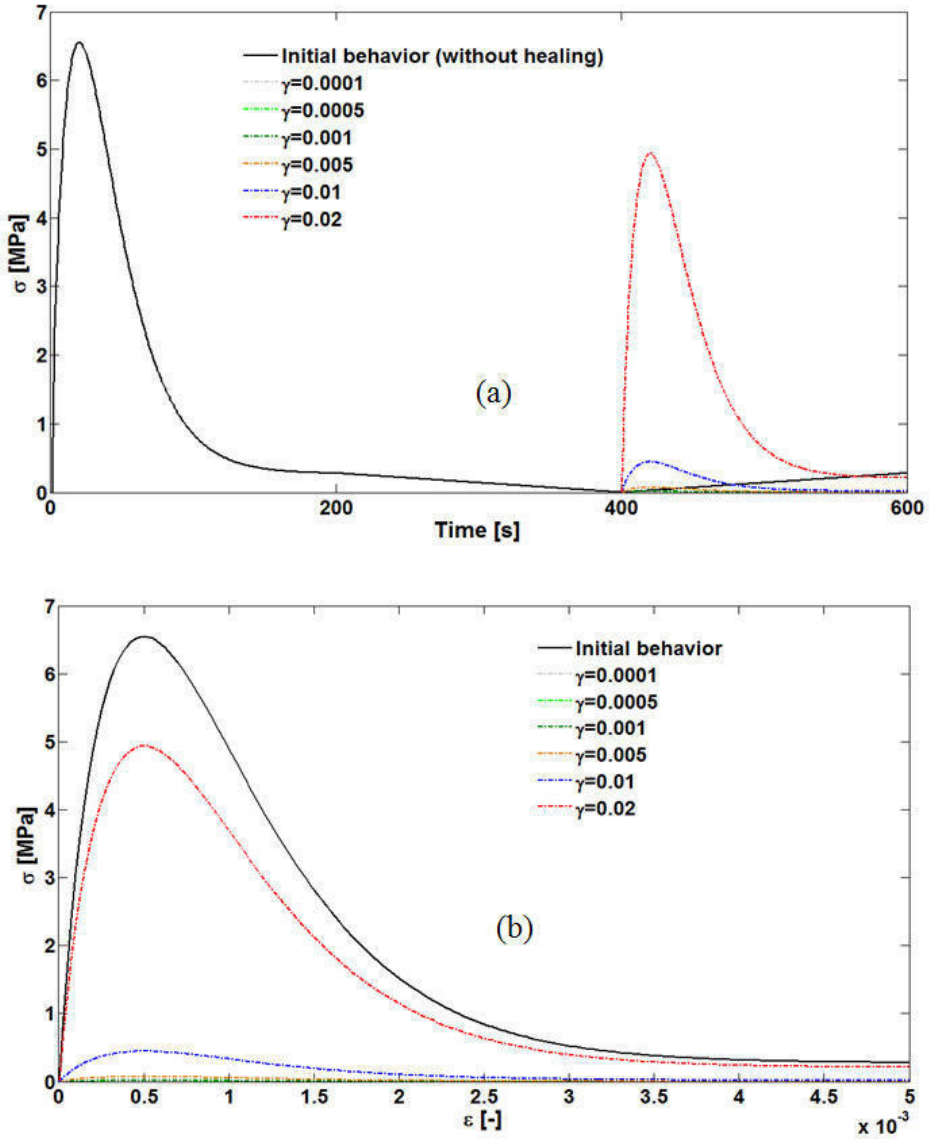

Figure 3.11: (a) Stress-time and (b) stress-strain responses of the generalized non-linear damage-healing model for coupled self-healing mechanism.

Chapter 4

Plane stress, plane strain and isotropic elasticity healing formulations

4.1 Introduction

In this chapter we present a theoretical formulation of different self-healing variables. Healing variables based on the recovery in elastic modulus, shear modulus, Poisson's ratio, and bulk modulus are defined. The formulation is presented in both scalar and tensorial cases. A new healing variable based on elastic stiffness recovery in proposed which is consistent with the continuum damage-healing mechanics. The evolution of the healing variable calculated based on cross-section as function of the healing variable calculated based on elastic stiffness is presented in both hypotheses of elastic strain equivalence and elastic energy equivalence. The components of the fourth-rank healing tensor are also obtained in the case of plane stress, plane strain and isotropic elasticity.

4.2 Elastic-stiffness-based healing variable

In the previous chapter, we called φ_{hd} the eliminated damage variable which is equal to $(1-h)$. In this section, a combined damage-healing elastic modulus E_c is proposed

which is a function of damage and healing variables l and r, respectively. It should be noted that the damage and healing variables l and r are calculated based on elastic modulus reduction and recovery, respectively. The proposed expression is written as:

$$E_c = \overline{E}\,(1 - l + r) \tag{4.1}$$

It should be noted that equation (4.1) is defined such that the variation of the elastic modulus fits the boundary conditions of the healing mechanism. When the material is totally healed ($r = l$), it means that that no damage exists in the material ($l = 0$), then the combined damage-healing elastic modulus becomes similar to the effective elastic modulus ($E_c = \overline{E}$). When the material is not healed ($r = 0$), the combined damage-healing elastic modulus becomes $E_c = \overline{E}\,(1 - l)$ which is consistent with the damage formulation defined in [7].

4.3 Hypothesis of elastic strain equivalence

Using the hypothesis of elastic strain equivalence, the strain in the healed material state is assumed to be equal to the strain in the effective material state $\overline{\varepsilon}$:

$$\varepsilon = \overline{\varepsilon} \tag{4.2}$$

$$\sigma = E_c \varepsilon \tag{4.3}$$

$$\overline{\sigma} = \overline{E}\overline{\varepsilon} \tag{4.4}$$

Substituting for $\overline{\sigma}$ and σ using equations (3.5) and (4.2), respectively, into equation (4.4), the following expression of the effective elastic modulus is obtained:

$$\overline{E} = \frac{E_c}{1 - \varphi\,(1 - h)} \tag{4.5}$$

Next, using equations (4.1) and (4.5) the relation between the damage and healing variables φ, h, l and r can be expressed as follows:

$$h = \frac{\varphi - l + r}{\varphi} \tag{4.6}$$

From equation (4.6), one can observe that when $r = l$ the healing variable h becomes $h = 1$, which is found consistent with the CDHM. It means that when the material is totally healed in terms of elastic modulus ($r = l$) , it becomes also totally healed in terms of cross-section ($h = 1$). From equation (4.6), one can extract the expression of r as follows:

$$r = \varphi\,(h - 1) + l \tag{4.7}$$

The objective of the self-healing is to recover the material stiffness such that the healed material reacts similarly to the original (intact) material. Since the healing is a multi-physic complicated process, experimental researches reveal that in order to obtain a complete healing, appropriate conditions of the chemical and mechanical properties of the material should be considered [57, 145, 157, 158]. These conditions can be reflected for instance by the healing time, degree of damage, material mixture, chemical contents, microcapsules percentage, . . .etc. Based on this conclusion, we will consider the partial healing case which seems more realistic. Thus, we assume that the maximum damage variable is 0.3 ($0 \leq l \leq 0.3$) and the maximum healing variable is 0.15 ($0 \leq r \leq 0.15$). Based on this assumption, we plot the expression in equation (4.6) as shown in Figure 4.1. We take example of different values of l equals to 0.2, 0.25 and 0.3. According to CDM, and equating the two expressions $E_\varphi = \overline{E}\,(1 - \varphi)$ from [85] and equation (4.1) without healing ($E_l = \overline{E}\,(1 - l)$), one finds that $\varphi = l$. Thus, equation (4.6) becomes

$$h = \frac{r}{l} \tag{4.8}$$

From equation (4.8), one can observe that there is consistency between the geometrical healing h and the material stiffness healing r. If the material is totally healed in terms of material stiffness ($r = l$), one finds that the material becomes totally healed in terms of geometry ($h = 1$). On the other hand, the material cannot be geometrically healed ($h = 0$) if it is not healed in terms of material stiffness.

It is observed from Figure 4.1 that when the healing variable $h = 0$ we finds

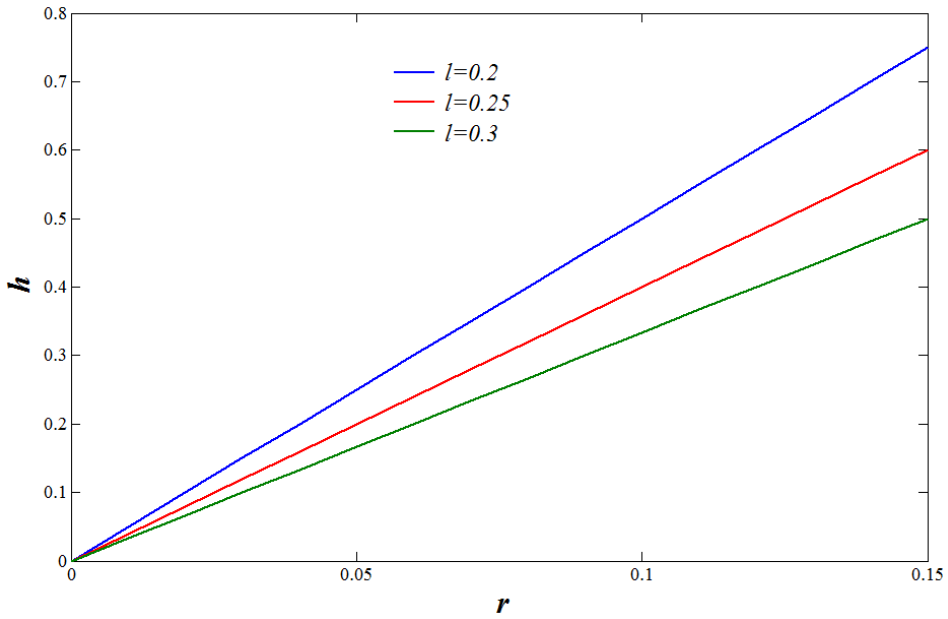

Figure 4.1: Variation of the healing variable h as function of r with different values of damage variable l using stain equivalence hypothesis.

$r = 0$, and the maximum healing variable h changes with the change of the damage variable l . The healing variable h is found to have maximum values equal to 0.75, 0.6 and 0.5 in the cases of the damage values $l = 0.2$, $l = 0.25$ and $l = 0.3$, respectively. One can say that the recovery in the cross-section is overestimated comparing to the recovery in the elastic stiffness. It is concluded that the material damage is reflected mostly by the reduction in its geometry. Accordingly, when self-healing is introduced the recovery in the cross-section is found greater than the recovery in the elastic stiffness.

4.4 Hypothesis of elastic energy equivalence

Using the hypothesis of elastic energy equivalence, the elastic energy in the healed material state is assumed to be equal to the elastic energy in the effective material state:

$$\frac{\sigma^2}{2E_l} = \frac{\overline{\sigma}^2}{2\overline{E}} \tag{4.9}$$

Substituting equations (4.5) into equation (4.9), the following expression is obtained:

$$\overline{E} = \frac{E_c}{(1-\varphi\,(1-h))^2} \tag{4.10}$$

Next, using equations (4.1) and (4.10) the relation between the variables φ, h , l and r can be expressed as follows:

$$h = \frac{\varphi - 1 + \sqrt{1-l+r}}{\varphi} \tag{4.11}$$

Equation (4.11) can be rewritten as:

$$r = (1-\varphi\,(1-h))^2 + l - 1 \tag{4.12}$$

From equation (4.11), it can also be observed that when the material is totally healed in terms of elastic modulus ($r = l$) , it becomes also totally healed in terms of cross-section $h = 1$.

The healing variable h in Equation (4.11) is plotted in Figure 4.2. It should be noted that according to the damage mechanics and the elastic energy equivalence, and equating equations (4.1) and (4.10) without considering the healing variable r , one obtains $\varphi = (1 - \sqrt{1-l}\,)$. From Figure 4.2, one can see that at the healing value $r = 0$, the healing variable h is equal to zero. On the other hand, it is found that the healing variable h takes the maximum values of 0.76, 0.61 and 0.52 when the damage variable l is equal to 0.2, 0.25 and 0.3, respectively. Again, it is observed from Figure 4.2 that the healing due to cross-section recovery is overestimated comparing to the healing due to elastic stiffness recovery. On the other hand, there is a short overestimation of the healing due to cross-section using the hypothesis of elastic energy equivalence comparing to the hypothesis of elastic strain equivalence.

Next, we will define three other healing variables in terms of the recovery of the shear modulus G, Possion's ratio ν, and the bulk modulus K. The relations between these three variables and the healing variable r will also be given.

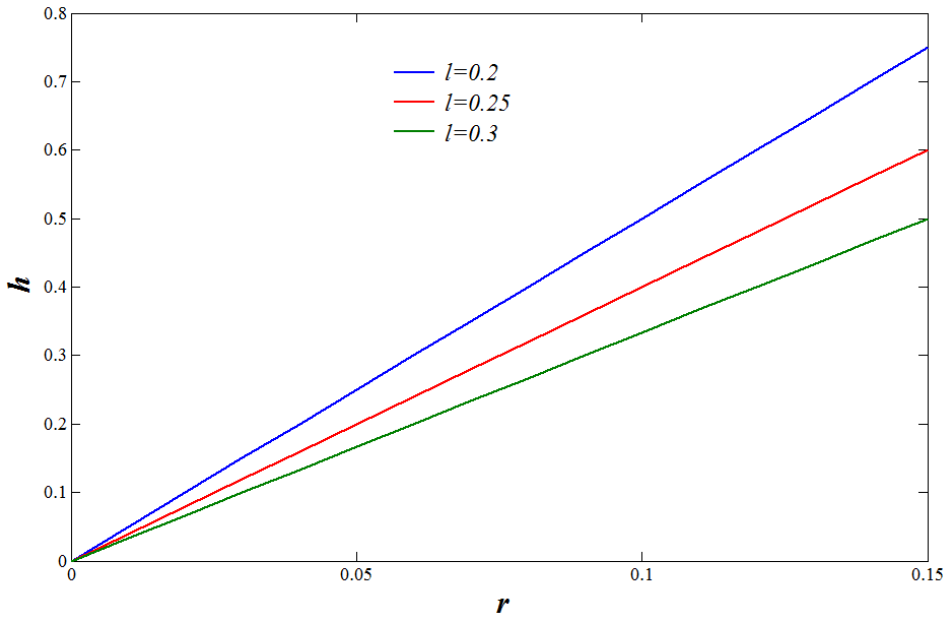

Figure 4.2: Variation of the healing variable h as function of r with different values of damage variable l using energy equivalence hypothesis.

We denote β and s respectively the damage and healing variables calculated based on the shear modulus G changes. Equation (4.1) can be expressed in terms of the shear modulus as follows

$$G_c = \overline{G}\,(1 - \beta + s) \tag{4.13}$$

where G_c and $\overline{G}$ are the damage-healing shear modulus and effective shear modulus, respectively. It should be noted that $0 \leq s \leq \beta$. The damage and healing variables calculated based on the recovery of Poisson's ratio are denoted α and p, respectively. The combined damage-healing Poissons ratio can also be expressed as:

$$\nu_c = \overline{\nu}\,(1 - \alpha + p) \tag{4.14}$$

where ν_c and $\overline{\nu}$ are the damage-healing Poisson's ratio and effective Poisson's ratio, respectively, and $0 \leq p \leq \alpha$.

Next, we will define the relation between the damage and healing variables φ, β, α, r, s, and p. In order to obtain this relation, the following two equations are used:

$$G_c = \frac{E_c}{2\left(1+\nu_c\right)} \tag{4.15}$$

$$\overline{G} = \frac{\overline{E}}{2\left(1+\overline{\nu}\right)} \tag{4.16}$$

Dividing equation (4.16) by equation (4.5), and using equations (4.1) and (4.12), one obtains the following expression:

$$\frac{1+\overline{\nu}}{1+\nu_c} = \frac{1-\beta+s}{1-l+r} \tag{4.17}$$

Substituting equation (4.14) into equation (4.17), one obtains

$$p = \frac{\left(1-l+r\right)\left(\nu_c-\alpha+1\right)-\left(1-\beta+s\right)\left(1+\nu_c\right)\left(1-\alpha\right)}{\left(1+\nu_c\right)\left(1-\beta+s\right)-\left(1-l+r\right)} \tag{4.18}$$

If we assume that the damage variable due to the shear modulus β equals to the damage variable due to the elastic modulus l, one can observe from equation (4.17) that the healing variable calculated based on the shear modulus recovery s is greater than the healing variable calculated based on the elastic modulus recovery r. This can be explained by the fact that there is recovery in the Poisson's ratio ν due to the effect of E and G. On the other hand, when the healing variable calculated based on elastic modulus recovery is greater than the healing variable calculated based on the shear modulus recovery ($r > s$), we will obtain $\nu_c > \overline{\nu}$, which means that there is an increase in the Poisson's ratio due to the healing effects of E and G. In addition, if the healing variable s equals to the healing variable r we will have

$$\nu_c = \overline{\nu} \tag{4.19}$$

This means that there is a complete recovery of Poisson's ratio and $p = 1$.

Next, we denote ω and b the damage and healing variables calculated based on the bulk modulus, respectively.

$$4.20K_c = \overline{K}\left(1-\omega+b\right) \tag{4.20}$$

where K_c and $\overline{K}$ are the damage-healing and effective bulk moduli, respectively, and $0 \leq b \leq \omega$. Using the elastic constants in the following equations:

$$K_c = \frac{G_c E_c}{9G_c - 3E_c} \tag{4.21}$$

$$\overline{K} = \frac{\overline{GE}}{9\overline{G} - 3\overline{E}} \tag{4.22}$$

and dividing equation (4.22) by equation (4.21) along with the use of equations (4.1), (4.13), (4.15) and (4.16), the following expression is obtained:

$$\frac{1 - 2\overline{\nu}}{1 - 2\nu_c} = \frac{1 - \omega + b}{1 - l + r} \tag{4.23}$$

Substituting for equation $\overline{\nu}$ using equation (4.14), one obtains

$$b = \frac{(1 - 2\nu_c)(1 - l + r) + (1 - 2\nu_c)(\omega - 1)}{1 - 2\nu_c} \tag{4.24}$$

From equation (4.23), one can observe that the healing due to the bulk modulus is greater than the healing due to the elastic modulus if the damage variables due to the bulk and elastic moduli are equal, which can also be explained by the fact that there is recovery in the Poisson's ratio due to K and E. On the other hand, it can also be observed that if the healing due to the elastic modulus is greater than the healing due to the bulk modulus, the material is exhibited to the super healing mechanism ($\nu_c > \overline{\nu}$). One can conclude from equations (4.17) and (4.23) in the domain of the self-healing that the healing due to the elastic modulus is always underestimated comparing to the healing due to the shear and bulk moduli. On the other hand, if the healing variable r is greater than the healing variable b, one finds ($\overline{\nu} > \nu_c$), which means that there is an increase in the Poisson's ratio due to the healing effects of E and G.

4.5 Tensorial healing variables

In this section, equations (3.5) and (4.1) will be generalized in the case of anisotropic materials. Therefore, scalar variables are replaced with tensors, and the tensors are presented by vectors (defined by braces) and matrices (defined by brackets). The tensorial formulation of equation (3.5) is defined as follows:

$$\{\overline{\sigma}\} = [Q]\{\sigma\} \tag{4.25}$$

where $\{\sigma\}$ and $\{\overline{\sigma}\}$ are the damage-healing and effective stress tensors, respectively. $[Q]$ is the fourth-rank healing tensor and is expressed as

$$[Q] = \left([M]^{-1} + ([I] - [M]^{-1})[H]^{-1}\right)^{-1} \tag{4.26}$$

where I is the fourth-rank identity tensor. M and H are the damage and healing effect tensors, respectively. It was shown based on equation (4.26) that the expression $\varphi(1-h)$ is generalized to become $\left([I] - [M]^{-1}\right)\left([I] - [H]^{-1}\right)$ and the expression of healing is obtained using the fact that the components of M correspond to $1/(1-\varphi)$ and the components of H correspond to $1/h$.

The scalar damage and healing variables in equation (4.1) can be generated in three dimensions respectively using the following expressions:

$$[L] = ([\overline{E}] - [E_L])[\overline{E}]^{-1} \tag{4.27}$$

$$[R] = ([E_C] - [E_L])[\overline{E}]^{-1} \tag{4.28}$$

where $[L]$ and $[R]$ are the fourth-rank damage and healing tensors calculated in terms of elastic modulus. $[E_L]$, $[E_C]$ and $[\overline{E}]$ are the damaged, combined damage-healing, and effective elasticity tensors, respectively. From equation (4.28), it can be observed that when the material is totally healed ($[R] = [L]$), the combined damage-healing elasticity tensor becomes similar to the effective elasticity tensor ($[E_C] = [\overline{E}]$) which is physically consistent with the self-healing theory. On the other hand, for no healing ($[E_C] = [E_L]$), one obtains $R = 0$. Equation (4.28) can be rewritten as:

$$[E_C] = [R][\overline{E}] + [E_L] \tag{4.29}$$

where

$$[E_L] = [\overline{E}]([I] - [L]) \tag{4.30}$$

4.5.1 Hypothesis of elastic strain equivalence

Equation (4.2) can be generalized as follows:

$$\{\overline{\varepsilon}\} = \{\varepsilon\} \tag{4.31}$$

Substituting equations (4.29) and (4.30) into equation (4.31) along with the use of equation (4.25), one obtains

$$[Q] = [R] + [E_L]^{-1}\,[\overline{E}] \tag{4.32}$$

Equation (4.32) can be rewritten as

$$[R] = [Q] - [E_L]^{-1}\,[\overline{E}] \tag{4.33}$$

Substituting equation (4.26) into equation (4.33), one finds

$$[R] = \left([M]^{-1} + ([I] - [M]^{-1})\,[H]^{-1}\right)^{-1} - [E_L]^{-1}\,[\overline{E}] \tag{4.34}$$

Equation (4.32) represents the fourth-rank healing effect tensor in the case of elastic stain equivalence. From this equation, it is observed that when the material is only damaged ($[R] = [0]$) & ($[E_c] = [E_\varphi]$), $[Q]$ becomes similar to the fourth-rank damage effect tensor $[M]$, which is consistent with the damage definition in equation (4.27) and in [136]. On the other hand, when the material is totally healed ($[R] = [L]$ & $[E_C] = [E_L] = [\overline{E}]$) , and according to equations (4.27) and (4.32), one finds that $[Q]$ becomes similar to $[I]$, which leads to the similarity of $\{\overline{\sigma}\}$ and $\{\sigma\}$ in equation (4.25).

4.5.2 Hypothesis of elastic energy equivalence

In this case, equation (4.9) is generalized as follows:

$$\frac{1}{2}\,\{\overline{\sigma}\}\,[\overline{E}]^{-1}\,\{\overline{\sigma}\} = \frac{1}{2}\,\{\sigma\}\,[E_C]^{-1}\,\{\sigma\} \tag{4.35}$$

Substituting equations (4.29) and (4.30) into equation (4.35) along with the use of equation (4.25), one obtains

$$[Q]\,[Q] = [R] + [E_L]^{-1}\,[\overline{E}] \tag{4.36}$$

Equation (4.36) can be rewritten as

$$[R] = [Q]\,[Q] - [E_L]^{-1}\,[\overline{E}] \tag{4.37}$$

Substituting equation (4.26) into equation (4.37), one finds

$$\begin{aligned} R = ([M]^{-1} + ([I] - [M]^{-1})[H]^{-1})^{-1}([M]^{-1} \\ +([I] - [M]^{-1})[H]^{-1})^{-1} - [E_L]^{-1}[\overline{E}] \end{aligned} \tag{4.38}$$

4.6 Isotropic elasticity application

In the case of isotropic elasticity the matrices of $[E_C]$ and $[\overline{E}]^{-1}$ are defined as follows:

$$[E_C] = \begin{bmatrix} \lambda_c + 2\mu_c & \lambda_c & \lambda_c & 0 & 0 & 0 \\ \lambda_c & \lambda_c + 2\mu_c & \lambda_c & 0 & 0 & 0 \\ \lambda_c & \lambda_c & \lambda_c + 2\mu_c & 0 & 0 & 0 \\ 0 & 0 & 0 & 2\mu_c & 0 & 0 \\ 0 & 0 & 0 & 0 & 2\mu_c & 0 \\ 0 & 0 & 0 & 0 & 0 & 2\mu_c \end{bmatrix} \tag{4.39}$$

$$[\overline{E}]^{-1} = \begin{bmatrix} \frac{1}{\overline{E}} & \frac{-\overline{v}}{\overline{E}} & \frac{-\overline{v}}{\overline{E}} & 0 & 0 & 0 \\ \frac{-\overline{v}}{\overline{E}} & \frac{1}{\overline{E}} & \frac{-\overline{v}}{\overline{E}} & 0 & 0 & 0 \\ \frac{-\overline{v}}{\overline{E}} & \frac{-\overline{v}}{\overline{E}} & \frac{1}{\overline{E}} & 0 & 0 & 0 \\ 0 & 0 & 0 & \frac{1}{2\overline{G}} & 0 & 0 \\ 0 & 0 & 0 & 0 & \frac{1}{2\overline{G}} & 0 \\ 0 & 0 & 0 & 0 & 0 & \frac{1}{2\overline{G}} \end{bmatrix} \tag{4.40}$$

It should be noted that equation (4.39) represents the elasticity matrix in the damage-healing configuration. Thus, according to equations (4.1), (4.13) and (4.14) E_c, υ_c and G_c are summarized in the case of damage and healing, respectively, as follows:

$$E_c = \overline{E}\,(1 - l + r) \tag{4.41}$$

$$G_c = \overline{G}\,(1 - \beta + s) \tag{4.42}$$

$$\upsilon_c = \overline{\upsilon}\,(1 - \alpha + p) \tag{4.43}$$

λ_c and μ_c are the damage-healing Lame's constants expressed as:

$$\lambda_c = \frac{\upsilon_c E_c}{(1 + \upsilon_c)\,(1 - 2\upsilon_c)} \tag{4.44}$$

$$\mu_c = G_c = \overline{G}\,(1 - \beta + s) \tag{4.45}$$

Equation (4.29) can be rewritten as

$$[R] = [E_C]\,[\overline{E}]^{-1} + [L] - [I] \tag{4.46}$$

Before calculation of the components of the healing matrix $[R]$, one should calculate the components of the damage matrix $[L]$. Therefore, equation (4.30) can be rewritten as

$$[L] = [I] - [E_L]\,[\overline{E}]^{-1} \tag{4.47}$$

where equation (4.40) is replaced by the elasticity matrix in the damage configuration $[E_L]$, and the expressions in equations (4.41), (4.42) and (4.43) become in the case of damage as follows:

$$E_c = \overline{E}\,(1 - l) \tag{4.48}$$

$$G_c = \overline{G}\,(1 - \beta) \tag{4.49}$$

$$\upsilon_c = \overline{\upsilon}\,(1 - \alpha) \tag{4.50}$$

Substituting equations (4.39) and (4.40) in the case of damage configuration into equation (4.47) along with the use of equations (4.48), (4.49) and (4.50), one obtains the expression of the components of the fourth-rank damage tensor $[L]$ as follows:

$$[L] = \begin{bmatrix} l_{11} & l_{12} & l_{13} & l_{14} & l_{15} & l_{16} \\ l_{21} & l_{22} & l_{23} & l_{24} & l_{25} & l_{26} \\ l_{31} & l_{32} & l_{33} & l_{34} & l_{35} & l_{36} \\ l_{41} & l_{42} & l_{43} & l_{44} & l_{45} & l_{46} \\ l_{51} & l_{52} & l_{53} & l_{54} & l_{55} & l_{56} \\ l_{61} & l_{62} & l_{63} & l_{64} & l_{65} & l_{66} \end{bmatrix} \tag{4.51}$$

$$l_{11} = \frac{(\alpha - 1)\left(2\upsilon_c^2 + l\upsilon - l\right) - 2\upsilon_c^2\left(l - 1\right)}{\left(2\upsilon_c - 1\right)\left(\upsilon_c + 1\right)\left(\alpha - 1\right)} \tag{4.52a}$$

$$l_{12} = \frac{\upsilon_c \alpha \left(1 - l\right)}{\left(2\upsilon_c - 1\right)\left(\upsilon_c + 1\right)\left(\alpha - 1\right)} \tag{4.52b}$$

$$l_{13} = l_{12} = l_{21} = l_{23} = l_{31} = l_{32} \tag{4.52c}$$

$$l_{11} = l_{33} \tag{4.52d}$$

$$l_{14} = l_{41} = l_{15} = l_{51} = l_{16} = l_{61} = 0 \tag{4.52e}$$

$$l_{24} = l_{42} = l_{25} = l_{52} = l_{26} = l_{62} = 0 \tag{4.52f}$$

$$l_{34} = l_{43} = l_{35} = l_{53} = l_{36} = l_{63} = 0 \tag{4.52g}$$

$$l_{44} = l_{55} = l_{66} = \beta \tag{4.52h}$$

From equation (4.52a), one can observe that if $\upsilon_c = 0$ we will obtain $l_{11} = l$. This is consistent with the scalar definition of the damage variables in Section 4.4.

Next, one calculates the components of the fourth-rank healing tensor $[R]$ using equation (4.46). Substituting equations (4.39) and (4.40) into equation (4.46) along with the use of equations (4.41), (4.42), (4.43) and (4.51), one obtains the components of $[R]$ as:

$$[R] = \begin{bmatrix} r_{11} & r_{12} & r_{13} & r_{14} & r_{15} & r_{16} \\ r_{21} & r_{22} & r_{23} & r_{24} & r_{25} & r_{26} \\ r_{31} & r_{32} & r_{33} & r_{34} & r_{35} & r_{36} \\ r_{41} & r_{42} & r_{43} & r_{44} & r_{45} & r_{46} \\ r_{51} & r_{52} & r_{53} & r_{54} & r_{55} & r_{56} \\ r_{61} & r_{62} & r_{63} & r_{64} & r_{65} & r_{66} \end{bmatrix} \tag{4.53}$$

$$r_{11} = \frac{2\upsilon_c^2 (r - l + 1) + r (\upsilon_c - 1)(p - \alpha + 1)}{(2\upsilon_c - 1)(\upsilon_c + 1)(p - \alpha + 1)} - \frac{2\upsilon_c^2 (l - 1)}{(2\upsilon_c - 1)(\upsilon_c + 1)(\alpha + 1)} \tag{4.54a}$$

$$r_{12} = \frac{\upsilon_c (r - l + 1)}{(2\upsilon_c - 1)(\upsilon_c + 1)(p - \alpha + 1)} - \frac{\upsilon_c (l - r + \alpha r - 1)}{(2\upsilon_c - 1)(\upsilon_c + 1)(\alpha + 1)} \tag{4.54b}$$

$$r_{13} = r_{23} = r_{31} = r_{32} \tag{4.54c}$$

$$r_{11} = r_{33} \tag{4.54d}$$

$$r_{14} = r_{41} = r_{15} = r_{51} = r_{16} = r_{61} = 0 \tag{4.54e}$$

$$r_{24} = r_{42} = r_{25} = r_{52} = r_{26} = r_{62} = 0 \tag{4.54f}$$

$$r_{34} = r_{43} = r_{35} = r_{53} = r_{36} = r_{63} = 0 \tag{4.54g}$$

$$r_{44} = r_{55} = r_{66} = s \tag{4.54h}$$

The fourth-rank healing matrix $[R]$ reduces to the following expression:

$$[R] = \begin{bmatrix} r_{11} & r_{12} & r_{12} & 0 & 0 & 0 \\ r_{12} & r_{11} & r_{12} & 0 & 0 & 0 \\ r_{12} & r_{12} & r_{11} & 0 & 0 & 0 \\ 0 & 0 & 0 & r_{44} & 0 & 0 \\ 0 & 0 & 0 & 0 & r_{55} & 0 \\ 0 & 0 & 0 & 0 & 0 & r_{66} \end{bmatrix} \tag{4.55}$$

where r_{11} , r_{12} and r_{44} are found as follows:

$$r_{11} = \frac{2\upsilon_c^2 (r - l + 1) + r (\upsilon_c - 1)(p - \alpha + 1)}{(2\upsilon_c - 1)(\upsilon_c + 1)(p - \alpha + 1)} - \frac{2\upsilon_c^2 (l - 1)}{(2\upsilon_c - 1)(\upsilon_c + 1)(\alpha + 1)} \tag{4.56a}$$

$$r_{12} = \frac{\upsilon_c\,(r - l + 1)}{(2\upsilon_c - 1)\,(\upsilon_c + 1)\,(p - \alpha + 1)} - \frac{\upsilon_c\,(l - r + \alpha r - 1)}{(2\upsilon_c - 1)\,(\upsilon_c + 1)\,(\alpha + 1)} \tag{4.56b}$$

$$r_{44} = s \tag{4.56c}$$

From equation (4.56a), one can observe that if $\upsilon_c = 0$ we will obtain $r_{11} = r$. This is consistent with the scalar definition of the healing variables in Section 4.4.

4.7 Plane stress application

In this section, special case of plane stress will be applied. According to the plane stress formulation, equations ((4.39) and (4.40) become:

$$[E_C] = \frac{E_c}{1 - \upsilon_c^2} \begin{bmatrix} 1 & \upsilon_c & 0 \\ \upsilon_c & 1 & 0 \\ 0 & 0 & \frac{1-\upsilon_c}{2} \end{bmatrix} \tag{4.57}$$

$$[\overline{E}]^{-1} = \begin{bmatrix} \frac{1}{\overline{E}} & \frac{-\overline{\upsilon}}{\overline{E}} & 0 \\ \frac{-\overline{\upsilon}}{\overline{E}} & \frac{1}{\overline{E}} & 0 \\ 0 & 0 & \frac{1}{\overline{G}} \end{bmatrix} \tag{4.58}$$

Substituting equations (4.57) and (4.58) in the case of damage configuration into equation (4.47) along with the use of equations (4.48), (4.49) and (4.50), one obtains the expression of the components of the fourth-rank damage tensor $[L]$ for plane strain case as follows:

$$[L] = \begin{bmatrix} l_{11} & l_{12} & l_{13} \\ l_{21} & l_{22} & l_{23} \\ l_{31} & l_{32} & l_{33} \end{bmatrix} \tag{4.59}$$

where

$$l_{11} = \frac{(\alpha - l)(\upsilon_c^2 - 1) - \alpha(1 - l)}{(\upsilon_c^2 - 1)(\alpha - 1)} \tag{4.60a}$$

$$l_{22} = l_{11} \tag{4.60b}$$

$$l_{12} = \frac{\upsilon_c \alpha (1 - l)}{(\upsilon_c^2 - 1)(\alpha - 1)} \tag{4.60c}$$

$$l_{21} = l_{12} \tag{4.60d}$$

$$l_{33} = \beta \tag{4.60e}$$

$$l_{13} = l_{23} = l_{31} = l_{32} = 0 \tag{4.60f}$$

From equation (4.60a), one can observe that if $\upsilon_c = 0$ we will obtain $l_{11} = l$. This is also consistent with the scalar definition of the damage variables in Section 4.4.

Next, one calculates the components of the fourth-rank healing tensor $[R]$ using equation (4.46). Substituting equations (4.57) and (4.58) into equation (4.46) along with the use of equations (4.41), (4.42), (4.43) and (4.59), one obtains the components of $[R]$ as:

$$[R] = \begin{bmatrix} r_{11} & r_{12} & r_{12} \\ r_{12} & r_{11} & r_{12} \\ r_{12} & r_{12} & r_{11} \end{bmatrix} \tag{4.61}$$

where

$$r_{11} = \frac{-r\,(p-\alpha+1) - \upsilon_c^2\,(r-l-1)}{(\upsilon_c-1)\,(\upsilon_c+1)\,(p-\alpha+1)} - \frac{\upsilon_c^2\,(l-1)}{(\upsilon_c-1)\,(\upsilon_c+1)\,(\alpha-1)} \tag{4.62a}$$

$$r_{22} = r_{11} \tag{4.62b}$$

$$r_{12} = \frac{\upsilon_c\,(r-l+1)}{(\upsilon_c-1)\,(\upsilon_c+1)\,(p-\alpha+1)} - \frac{\upsilon_c\,(l-r+\alpha r-1)}{(\upsilon_c-1)\,(\alpha-1)} \tag{4.62c}$$

$$r_{21} = r_{12} \tag{4.62d}$$

$$r_{33} = s \tag{4.62e}$$

$$r_{13} = r_{23} = r_{31} = r_{32} = 0 \tag{4.62f}$$

The fourth-rank matrix $[R]$ reduces to the following expression:

$$[R] = \begin{bmatrix} r_{11} & r_{12} & 0 \\ r_{12} & r_{11} & 0 \\ 0 & 0 & r_{33} \end{bmatrix} \tag{4.63}$$

where r_{11}, r_{12} and r_{33} are found as follows:

$$r_{11} = \frac{-r\,(p-\alpha+1) - \upsilon_c^2\,(r-l-1)}{(\upsilon_c-1)\,(\upsilon_c+1)\,(p-\alpha+1)} - \frac{\upsilon_c^2\,(l-1)}{(\upsilon_c-1)\,(\upsilon_c+1)\,(\alpha-1)} \tag{4.64a}$$

$$r_{12} = \frac{\upsilon_c\,(r - l + 1)}{(\upsilon_c - 1)\,(\upsilon_c + 1)\,(p - \alpha + 1)} - \frac{\upsilon_c\,(l - r + \alpha r - 1)}{(\upsilon_c - 1)\,(\alpha - 1)} \tag{4.64b}$$

$$r_{33} = s \tag{4.64c}$$

From equation (4.64a), one can observe that if $\upsilon_c = 0$ we will obtain $r_{11} = r$. This is consistent with the scalar definition of the healing variables in Section 4.4.

4.8 Plane strain application

In this section, special case of plane strain will be applied. According to the plane strain formulation, equations (4.39) and (4.40) become:

$$[E_C] = \frac{E_c}{(1+\upsilon_c)(1-2\upsilon_c)} \begin{bmatrix} 1-\upsilon_c & \upsilon_c & 0 \\ \upsilon_c & 1-\upsilon_c & 0 \\ 0 & 0 & \frac{1-2\upsilon_c}{2} \end{bmatrix} \tag{4.65}$$

$$[\overline{E}]^{-1} = \frac{1+\overline{\upsilon}}{\overline{E}} \begin{bmatrix} 1-\overline{\upsilon} & -\overline{\upsilon} & 0 \\ -\overline{\upsilon} & 1-\overline{\upsilon} & 0 \\ 0 & 0 & 2 \end{bmatrix} \tag{4.66}$$

Substituting equations (4.65) and (4.66) in the case of damage configuration into equation (4.47) along with the use of equations (4.48), (4.49) and (4.50), one obtains the expression of the components of the fourth-rank damage tensor $[L]$ for plane strain case as follows:

$$[L] = \begin{bmatrix} l_{11} & l_{12} & l_{13} \\ l_{21} & l_{22} & l_{23} \\ l_{31} & l_{32} & l_{33} \end{bmatrix} \tag{4.67}$$

where

$$l_{11} = \frac{2\upsilon_c^2 + l\upsilon_c - l}{(2\upsilon_c - 1)(\upsilon_c + 1)} - \frac{2\upsilon_c^2 - 2\upsilon_c^2 l + \alpha(\upsilon_c^2 l - \upsilon_c^2)}{(2\upsilon_c - 1)(\upsilon_c + 1)(\alpha - 1)^2} \tag{4.68a}$$

$$l_{22} = l_{11} \tag{4.68b}$$

$$l_{12} = \frac{\upsilon_c \alpha (1 - l)(\upsilon_c - \alpha + 1)}{(2\upsilon_c - 1)(\upsilon_c + 1)(\alpha - 1)^2} \tag{4.68c}$$

$$l_{21} = l_{12} \tag{4.68d}$$

$$l_{33} = \beta \tag{4.68e}$$

$$l_{13} = l_{23} = l_{31} = l_{32} = 0 \tag{4.68f}$$

From equation (4.68a), one can see again that if $\upsilon_c = 0$ we will obtain $l_{11} = l$, which is consistent with the scalar definition of the damage variables in Section 4.4.

Next, one calculates the components of the fourth-rank healing tensor $[R]$ using equation (4.46). Substituting equations (4.65) and (4.66) into equation (4.46) along with the use of equations (4.41), (4.42), (4.43) and (4.67), one obtains the components of $[R]$ as:

$$[R] = \begin{bmatrix} r_{11} & r_{12} & r_{12} \\ r_{12} & r_{11} & r_{12} \\ r_{12} & r_{12} & r_{11} \end{bmatrix} \tag{4.69}$$

where

$$r_{11} = \frac{\upsilon_c^2 (r - l + 1)(\upsilon_c + p - \alpha + 1)}{(2\upsilon_c - 1)(\upsilon_c + 1)(p - \alpha + 1)} + \frac{r(\upsilon_c - 1)}{(2\upsilon_c - 1)(\upsilon_c + 1)} - \frac{\upsilon_c^2 (\upsilon_c - 1)(r - l + 1)}{(p - \alpha + 1)^2 (2\upsilon_c - 1)(\upsilon_c + 1)} + \frac{\upsilon_c^2 (l - 1)(2 - \alpha)}{(2\upsilon_c - 1)(\upsilon_c + 1)(\alpha - 1)^2} \tag{4.70a}$$

$$r_{22} = r_{11} \tag{4.70b}$$

$$r_{12} = \frac{(l - 1)(\upsilon_c^2 \alpha - \upsilon_c \alpha + \upsilon_c)}{(\alpha - 1)^2 (2\upsilon_c - 1)(\upsilon_c + 1)} - \frac{\upsilon_c r}{(2\upsilon_c - 1)(\upsilon_c + 1)} + \frac{(r - l + 1)(\upsilon_c^2 (\alpha - p) + \upsilon_c (p - \alpha) + \upsilon_c)}{(p - \alpha + 1)^2 (2\upsilon_c - 1)(\upsilon_c + 1)} \tag{4.70c}$$

$$r_{21} = r_{12} \tag{4.70d}$$

$$r_{33} = s \tag{4.70e}$$

$$r_{13} = r_{23} = r_{31} = r_{32} = 0 \tag{4.70f}$$

The fourth-rank healing matrix $[R]$ reduces to the following expression:

$$[R] = \begin{bmatrix} r_{11} & r_{12} & 0 \\ r_{12} & r_{11} & 0 \\ 0 & 0 & r_{33} \end{bmatrix} \tag{4.71}$$

where r_{11}, r_{12} and r_{33} are found as follows:

$$r_{11} = \frac{\upsilon_c^2 (r - l + 1)(\upsilon_c + p - \alpha + 1)}{(2\upsilon_c - 1)(\upsilon_c + 1)(p - \alpha + 1)} + \frac{r(\upsilon_c - 1)}{(2\upsilon_c - 1)(\upsilon_c + 1)} - \frac{\upsilon_c^2 (\upsilon_c - 1)(r - l + 1)}{(p - \alpha + 1)^2 (2\upsilon_c - 1)(\upsilon_c + 1)} + \frac{\upsilon_c^2 (l - 1)(2 - \alpha)}{(2\upsilon_c - 1)(\upsilon_c + 1)(\alpha - 1)^2} \tag{4.72a}$$

$$r_{12} = \frac{(l - 1)(\upsilon_c^2 \alpha - \upsilon_c \alpha + \upsilon)}{(\alpha - 1)^2 (2\upsilon_c - 1)(\upsilon_c + 1)} - \frac{\upsilon_c r}{(2\upsilon_c - 1)(\upsilon_c + 1)} + \frac{(r - l + 1)(\upsilon_c^2 (\alpha - p) + \upsilon_c (p - \alpha) + \upsilon_c)}{(p - \alpha + 1)^2 (2\upsilon_c - 1)(\upsilon_c + 1)} \tag{4.72b}$$

$$r_{33} = s \tag{4.72c}$$

From equation (4.72a), one can observe that if $\upsilon_c = 0$ we will obtain $r_{11} = r$. This is consistent with the scalar definition of the healing variables in Section 4.4.

4.9 Conclusion

Definition of different healing variables in terms of different elastic constants recovery in scalar and tensorial formulations was given in this chapter. The healing variables were defined based on the recovery in elastic modulus, Poisson's ratio, shear modulus and bulk modulus, and the relationships between these variables were obtained. Plane stress, plane strain and isotropic elasticity derivations were also given along with the definition of the fourth-rank healing tensor. In addition, both hypotheses of elastic strain and elastic energy equivalence were used to illustrate the relationship between the healing variable calculated based on cross-section and the healing variable calculated based on elastic stiffness. It was found that the healing variable calculated based on elastic stiffness is greater than the one calculated based on cross-section in the case of hypothesis of elastic energy equivalence. It was also shown that the healing tensor fits the boundary conditions of the healing variable in the case of scalar formulation.

Chapter 5

Contribution to the design of new strengthening theory based on super healing materials

5.1 Introduction

The present chapter focuses on a crucial solution for the strengthening of materials which is based on super healing materials. Once the stiffness of the material is recovered, further healing can result as a strengthening process. This chapter presents a new theoretical framework of the super healing model within the framework of continuum damage-healing mechanics. The proposed theory is extended from linear to nonlinear super healing theory.

5.2 Super healing mechanism

The idea of super healing materials was first proposed in [86]. The main idea is to give the material the ability not only to heal itself, but also to strengthen itself. In this case, the value of the healing variable increases beyond what is necessary to recover the original stiffness of the material. It is clear from equation (3.5) that when the material is fully healed the healing variable h takes the value of 1. In the theory of super healing, once the material recovers its original stiffness (E_0) the

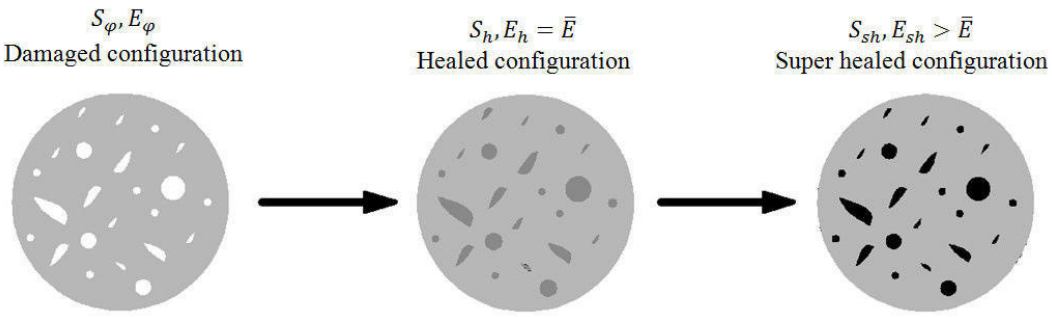

Figure 5.1: Damaged, healed, and super healed configurations.

healing is supposed to be continued ($h > 1$). In this case, the healing will not be actually healing but some form of strengthening and enhancing the stiffness of the material. Figure 5.1 shows the state of the material in the case of super healing. The super healed material is characterized by its higher elastic modulus E_{sh} which is higher than the elastic modulus of the healed and original materials ($E_{sh} > \overline{E}$).

Figure 5.2 shows the chart of the variation of the elastic modulus of the material in different states. In the initial state the material is intact and its stiffness is represented by the original elastic modulus E_0. Once the material is subjected to external loading and after the energy exceeds the material threshold, damage is initiated and accumulated via the variable φ. In this case the material is damaged and its stiffness is represented by the elastic modulus E_φ, which is inferior to the original stiffness. The elastic moduli E_{ph} and E_{fh} represent the stiffness of the partially and fully healed material, respectively. Introducing the super healing material leads to the enhancing and strengthening of the material stiffness in which the elastic modulus of the super-healed/strengthened material is higher than the elastic modulus of the fully healed and original materials.

5.3 Linear refined super healing mechanics

In this section, the proposed refined super healing theory is presented. This presentation is based on the linear formulation that follows the classical definition of self-healing existing in the literature which is described in equation (3.5).

According to continuum damage-healing mechanics, it is well known that the

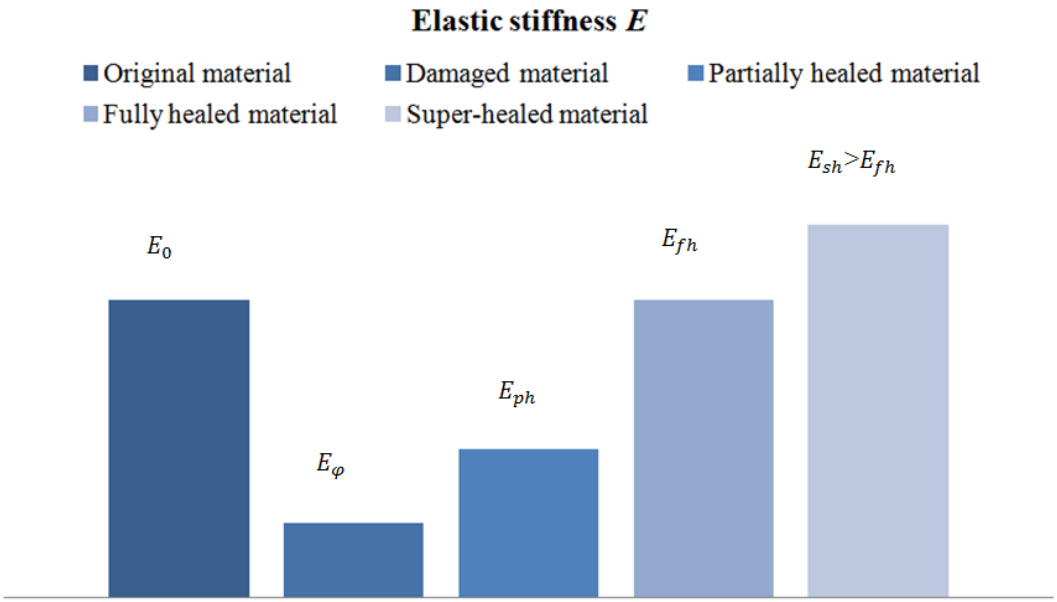

Figure 5.2: Variation of material stiffness from initial to super healed state.

healing mechanism is applied to eliminate the damage effect in the material and to recover its original stiffness. Since the fully damaged material state is represented by its maximum damage variable $\varphi = 1$, the fully healed material state should be represented by its maximum healing variable $h = 1$, while the undamaged and unhealed material states are represented by the values $\varphi = 0$ and $h = 0$, respectively. In order to describe the healing effect on recovering the stiffness of the material, the material should be reloaded. After reloading, comparison between the healed material stiffness E_h and the original material stiffness E_0 is necessary. If the headed material stiffness E_h is similar to the original material stiffness E_0 one can say that the material is fully healed ($h = 1$). On the other hand, if the healed material stiffness E_h is similar to the damaged material stiffness E_φ one can say that the material is unhealed ($h = 0$). It should be noted that the effective configuration ($\varphi = 0$) is similar to the initial configuration. Then, since the behavior of the material in the fully healed configuration is similar to the behavior of the material in the initial configuration, the behavior of the material in the fully healed and effective configurations are also similar (see above Figure 5.2).

5.3 Linear refined super healing mechanics

In the present theory, it is supposed that once the material recovers its original stiffness, the healing is continued beyond its maximal value $h = 1$. In this phase, the healing variable will reach large values such as 2, 3, 4,. . . ., x in which the healing will not act as actually healing but some form of strengthening and enhancing the stiffness of the material. In this case, x represents the maximal value of super healing that can be applied. The super healing variable is denoted by h_s in the proposed refined theory. This notation is adopted in order to differentiate between the healing variable and the super healing variable (or may be to differentiate between the two phases).

Two mechanisms of super healing are described in this theory. The first concerns super healing when the variable h_s takes a single large value and acts at only one point of the material. This is called here the single super healing mechanism. This mechanism can be applied in reality for example in the case of microcapsules-based self-healing concrete [2, 52, 159]. In this case, when only one single crack appears in the material and is healed further due to self-healing, the strengthening of this material due to super healing material should take one large single value of h_s that enhances the stiffness of the material in the area of the single crack. The second mechanism concerns super healing when the variable h_s ($h_s \geq 1$) takes small values and acts at different points of the material. This case can be applied for example when the concrete is damaged in different points (multiple cracks). Once the material recovers its original stiffness due to self-healing, super healing can be applied with small values of h_s at these points. The value of h_s in this case depends on the number of the cracks that are healed in the damaged material. The cracks that are healed are further supposed to be super healed. Therefore, in this case the number of super healing variables is called n. The limitation of the second mechanism is that the variable h_s is able to take only one value that is constant at every point in the material. It should be noted that the present work aims to present theoretically the new theory of strengthening of materials. Therefore, it is hoped that future research will be physically carried out to demonstrate that the super healing variable h_s can take different values at the same time.

In the present refined theory a formulation is proposed which represents both single and multiple super healing mechanisms. It will be shown that the super healing variable h_s may not be restricted to only integer values, however it can also

take non-integer values. It is assumed in this theory that the material used for super healing (strengthening material) is supposed to be the same material used for self-healing. It is not the intention of the present work to characterize the material used for super healing but only to point the way of the concept and the possible realization of the proposed theory. We hope that this material will be produced in the future and applied in the manufacturing technology along the lines of the present theory.

In the case of multiple super healing mechanisms, the super healing variable h_s occurs at the same time, takes the same values of 1, 2, 3, ... , x and increases through $x+1$. In this case, the super healing parameter h_s takes small values, while for single super healing mechanism h_s takes large value with $n = 0$. It is proposed in the present refined super healing theory that the following expression is applicable:

$$\overline{\sigma} = \frac{\sigma}{1 + [h_s (n+1) - 1] \varphi} \tag{5.1}$$

where h_s is the variable characterizing the super healing material ($h_s \geq 1$) while n is the number of the super healing variables that can occur at the same time. It should be noted that the variable h_s is supposed to take only one value (1 or 2 or 3 . . . and so on). Equation (5.1) represents the main result governing the proposed theory of super healing. One can see from equation (5.1) that as the number of the super healing parameters n approaches infinity, the value of the effective stress approaches zero and is irrespective of the damage and super healing variables. This is the main result when the mechanical properties of a material are enhanced due to the application of a strengthening material of structural elements. Thus, one can conclude that the first characteristic of the proposed theory is its accordance with the theory of strengthening materials [160].

From equation (3.2), one can see that when the damage variable $\varphi = 1$, the effective stress explodes and goes to infinity indicating the complete rupture of the material, while in equation (5.1) when the damage variable $\varphi = 1$ the effective stress retains a finite value. This can be explained by the fact that in the reloading phase, the material will not rupture even though the damage variable is high. This is due to the effect of super healing that enhances the material stiffness comparing to the stiffness of the healed and original materials.

Following the concept of multiple super healing mechanisms, one replaces the healing variable h of equation (3.5) by a resultant super healing variable h_r defined as the sum of the multiple super healing variables h_1 , h_2 , h_3 , . . ., h_{n+1} as follows:

$$h_r = h_1 + h_2 + h_3 + ... + h_{n+1} \tag{5.2}$$

In this case, equation (3.5) becomes

$$\overline{\sigma} = \frac{\sigma}{1 - \varphi\,(1 - h_1 - h_2 - h_3 - \ . \ .. - h_{n+1})} \tag{5.3}$$

It should be noted that equation (5.2) can be used in the case of a single super healing mechanism with setting $n = 0$. In this case, h_r represents only one single large value of super healing. The important feature of the present theory is that the super healing variables of equation (5.2) are not restricted to a value of 1 or 2 only but they can take any positive integer or non-integer values. One supposes that the multiple healing mechanism is applied in which these variables are operating at the same time with each one having a value of 1. If one substitutes the value of 1 for each super healing variable into equation (5.3), one will obtain the governing equation of super healing defined by equation (5.1).

5.4 Linear refined anisotropic super healing mechanics

In this section, the refined theory of super healing is generalized to anisotropic damage and healing formulations [7, 118]. In the case of isotropic damage mechanics, the damage variable is presented by a scalar (equation (3.2)), while tensors are used to present the damage in the case of anisotropic damage mechanics. The tensors are denoted in this section by capital letters and are represented by matrices.

Let Hs denote the fourth-rank super healing tensor corresponding to the super healing variables h_r defined in equation (5.1). Following the concept of multiple super healing mechanisms as shown in the present theory, the norm of the fourth-rank super healing tensor Hs increases beyond the value of the norm of the fourth-rank identity tensor I ($\|Hs\| \geq \|I\|$). The norm of the fourth-rank identity tensor

I is 1, which is the maximum value of the healing variable in equation (3.5). It should be noted that the norm of the identity tensor represents the fully healed state material. In this case, $\|Hs\| = \|I\|$ denotes that the original stiffness of the material is fully recovered. According to equation (5.2), one can assume that multiple fourth-rank healing tensors are operating at the same time while their components increase through $(n+1)\, I_{ijkl}$ $(Hs1_{ijkl}, Hs2_{ijkl}, Hs3_{ijkl}, (n+1)\, Hs_{ijkl})$. It should be noted that in the case of single super healing mechanism, one sets $n = 0$ while the components of the fourth-rank super healing tensor Hs take large values. The anisotropic formulation of equation (5.1) is written as the following expression:

$$\overline{\sigma}_{ij} = \left[M^{-1}_{ijkl} + (n+1)\, Hs^{-1}_{ijmn} : \left(I_{mnkl} - M^{-1}_{mnkl}\right)\right]^{-1} \sigma_{kl} \tag{5.4}$$

It is seen from equation (5.4) that for the case of multiple super healing mechanisms, when the number of healing variables n goes to infinity, the effective stress approaches zero. This can be found also when the norm of the fourth-rank super healing tensor Hs goes to infinity. It should be noted that this cannot be achieved in reality, but n and Hs can take large values which leads to the minimization of the effective stress. This minimization is due to the strengthening of the material that can support more loading comparing to the original material without super healing effect. This is the same conclusion obtained by equation (5.1) in the case of isotropic damage-healing mechanics.

5.5 Refined super healing in plane stress

In this section, the proposed refined theory of super healing is solved for the special case of plane stress based on continuum damage-healing mechanics. Plane stress is considered in x and y directions and it is supposed that the stress components σ_{13}, σ_{23} and σ_{33} vanish. This leads to $\sigma_{13} = \sigma_{23} = \sigma_{33} = 0$. Therefore, the tensors in equation (5.4) are presented by matrices [142]:

$$\{\sigma\} = \begin{Bmatrix} \sigma_{11} \\ \sigma_{22} \\ \sigma_{12} \end{Bmatrix} \tag{5.5}$$

$$\{\overline{\sigma}\} = \begin{Bmatrix} \overline{\sigma}_{11} \\ \overline{\sigma}_{22} \\ \overline{\sigma}_{12} \end{Bmatrix} \tag{5.6}$$

$$I = \begin{bmatrix} 1 & 0 & 0 \\ 0 & 1 & 0 \\ 0 & 0 & 1 \end{bmatrix} \tag{5.7}$$

$$M = \frac{1}{\Delta} \begin{bmatrix} \psi_{22} & 0 & \varphi_{12} \\ 0 & \psi_{11} & \varphi_{12} \\ \frac{\varphi_{12}}{2} & \frac{\varphi_{12}}{2} & \frac{\psi_{11}+\psi_{22}}{2} \end{bmatrix} \tag{5.8}$$

where $\psi_{11} = 1 - \varphi_{11}$ and $\psi_{22} = 1 - \varphi_{22}$. The denominator Δ is given in [142]:

$$\Delta = \psi_{11}\psi_{22} - \varphi_{12}^2 \tag{5.9}$$

Next, one demonstrates the definition of the super healing matrix of equation (5.1) in the case of plane stress. It should be noted that the super healing matrix follows the same definition of the healing matrix. However, the values of the components of the super healing matrix are greater than the values of the components of the healing matrix. Equation (5.4) can be written as follows:

$$\overline{\sigma}_{ij} = Q_{ijkl}\sigma_{kl} \tag{5.10}$$

where Q_{ijkl} is the fourth-rank damage healing transformation tensor. Q_{ijkl} can be rewritten similarly to equation (4.26) as follows:

$$Q_{ijkl} = \left(M_{ijkl}^{-1} + \left(I_{ijmn} - M_{ijmn}^{-1}\right) H_{mnkl}^{-1}\right)^{-1} \tag{5.11}$$

Applying the equivalence elastic energy between the real and effective configurations, the following relationship is obtained

$$Q_{ijuw}Q_{klpq} = \left(h_{mnij}E_{klmn}^{d} + E_{klij}^{d}\right)\overline{E}_{uwpq}^{-1} \tag{5.12}$$

where h_{ijkl}, E_{ijkl}^{d} and $\overline{E}_{ijkl}$ are the fourth-rank healing variable tensor, the damaged elastic modulus and the elastic modulus in effective configuration, respectively. The

authors in [7] proposed the representation of the fourth-rank tensors M_{ijkl} and H_{ijkl} to be written as follows:

$$M_{ijkl} = \left[\left(I_{ij} - \varphi_{ij}\right)\left(I_{kl} - \varphi_{kl}\right)\right]^{-1/2} \quad and \quad H_{ijkl} = \left[h_{ij}h_{kl}\right]^{-1/2} \tag{5.13}$$

Substituting Q_{ijkl} from equation (5.11) into equation (5.12), one obtains

$$\begin{aligned}\left(M^{-1}_{ijuw} + \left(I_{ijmn} - M^{-1}_{ijmn}\right) H^{-1}_{mnuw}\right)^{-1} \left(M^{-1}_{klpq} + \left(I_{klmn} - M^{-1}_{klmn}\right) H^{-1}_{mnpq}\right)^{-1} \\ = \left(h_{mnij}E^{d}_{klmn} + E^{d}_{klij}\right) \overline{E}^{-1}_{uwpq}\end{aligned} \tag{5.14}$$

According to [161], the following form of the effective elastic modulus is obtained:

$$\overline{E}_{uwpq} = M^{-1}_{ijuw} E^{d}_{ijkl} M^{-T}_{klpq} \tag{5.15}$$

where the superscript $-T$ indicates transpose of the inverse of the tensor. Next, one substitutes M_{ijkl} and H_{ijkl} from equation (5.13) into equation (5.14) to obtain the relationship between the second rank damage variable tensor, φ_{ij}, and the healing variable tensor, h_{ij}, with the fourth-rank damage tensor, φ_{ijkl}, and the healing variable tensor, h_{ijkl}. By knowing one set of damage-healing variables, the other set can be obtained from equation (5.14). The results lead to the following super healing matrix in the case of plane stress. It should be noted that the healing and super healing present the same definition of their matrix representation.

$$Hs^{-1} = \begin{bmatrix} hs_{11} & 0 & hs_{12} \\ 0 & hs_{22} & hs_{12} \\ hs_{12} & hs_{12} & \frac{hs_{11}+hs_{22}}{2} \end{bmatrix} \tag{5.16}$$

It should be also noted that the form of the inverse super healing matrix in equation (5.16) is similar to the form of the damage matrix of equation (5.8). Substituting equations (5.5) to (5.16) into equation (5.4) and after simplification, one finds the following relation of the effective stress:

$$\{\sigma\} = [A]\,\{\overline{\sigma}\} \tag{5.17}$$

Using the MATLAB Symbolic Math Toolbox and after simplification, one can

write the following components of the fourth-rank tensor $[A]$ of equation (5.17):

$$A_{11} = (3\varphi_{11} + \varphi_{22} - \varphi_{11}\varphi_{22} - \varphi_{11}^2 + \varphi_{12}^2 - \varphi_{12}^2 hs_{11}(n+1) + \varphi_{11} hs_{11} n \\ +1)(\varphi_{11} + \varphi_{22} - 2) + \varphi_{12} hs_{12}(\varphi_{11} + 1)(n+1) - 2)/(\varphi_{11} + \varphi_{22} - 2) \tag{5.18a}$$

$$A_{12} = (\varphi_{12}(\varphi_{12} hs_{11} - hs_{12} - \varphi_{12} + \varphi_{12} hs_{12} - nhs_{12} + n\varphi_{12} hs_{11} \\ +n\varphi_{22} hs_{12}))/(\varphi_{11} + \varphi_{22} - 2) \tag{5.18b}$$

$$A_{13} = (2\varphi_{12} hs_{11}(\varphi_{11} - 1)(n+1)(\varphi_{11} + \varphi_{22} - 2) - (n+1) hs_{12}(\varphi_{11} \\ +\varphi_{22} - 2\varphi_{11}\varphi_{22}) - 2\varphi_{12}(\varphi_{11} - 1))/(\varphi_{11} + \varphi_{22} - 2) \tag{5.18c}$$

$$A_{21} = (\varphi_{12}(\varphi_{11} hs_{12} - hs_{12} - \varphi_{12} + \varphi_{12} hs_{22} - nhs_{12} + n\varphi_{11} hs_{12} \\ +n\varphi_{12} hs_{22}))/(\varphi_{11} + \varphi_{22} - 2) \tag{5.18d}$$

$$A_{22} = (\varphi_{11} + 3\varphi_{22} - \varphi_{11}\varphi_{22} + \varphi_{22}^2 - \varphi_{12}^2 - \varphi_{12}^2 hs_{22}(n+1) + \varphi_{22} hs_{22}(n \\ +1)(\varphi_{11} + \varphi_{22} - \ \ 2) + \varphi_{12} hs_{12}(\varphi_{22} - 1)(n+1) - 2)/(\varphi_{11} + \varphi_{22} - 2) \tag{5.18e}$$

$$A_{23} = (2(n+1)\varphi_{12} hs_{22}(\varphi_{22} - 1) - (n+1) hs_{12}(\varphi_{11} + \varphi_{22} - 2\varphi_{11}\varphi_{22} \\ -2\varphi_{12}(\varphi_{22} - 1))/(\varphi_{11} + \varphi_{22} - 2) \tag{5.18f}$$

$$A_{31} = (n+1)\varphi_{11} hs_{12} + (\varphi_{12}(\varphi_{11} - 1)(hs_{11} + hs_{22} + nhs_{11} + nhs_{22} \\ -2))/(2(\varphi_{11} + \varphi_{22} - 2)) \tag{5.18g}$$

$$A_{32} = (n+1)\varphi_{22} hs_{12} + (\varphi_{12}(\varphi_{22} - 1)(hs_{11} + hs_{22} + nhs_{11} + nhs_{22} \\ -2))/(2(\varphi_{11} + \varphi_{22} - \ \ 2)) \tag{5.18h}$$

$$A_{33} = -(4(2\varphi_{11}-1)(\varphi_{22}-1) - 4\varphi_{12}hs_{12}(\varphi_{11}-1)(n+1) - 4\varphi_{12}hs_{12}(\varphi_{22} -1)(n+1) + ((hs_{11}+hs_{22})(n+1)(\varphi_{11}+\varphi_{22}-2)(\varphi_{11} +\varphi_{22}-2\varphi_{11}\varphi_{22}))/2)/(2(\varphi_{11}+\varphi_{22}-2)) \quad (5.18i)$$

In order to proceed further, one needs to make a simplifying assumption. If one simplifies equations (5.18) and considers the case of principal components, one set $\varphi_{12} = \varphi_{21} = 0$ and $hs_{12} = hs_{21} = 0$. Then, one substitutes the simplified equations into equation (5.17). After some algebraic manipulations one obtains the following expressions:

$$\overline{\sigma}_{11} = \frac{\sigma_{11}}{1 + [hs_{11}(n+1) - 1]\varphi_{11}} \quad (5.19)$$

$$\overline{\sigma}_{22} = \frac{\sigma_{22}}{1 + [hs_{22}(n+1) - 1]\varphi_{22}} \quad (5.20)$$

$$\overline{\sigma}_{12} = \frac{2\sigma_{12}(\varphi_{11}+\varphi_{22}-2)}{-4(\varphi_{11}-1)(\varphi_{22}-1) - (hs_{11}+hs_{22})(n+1)(\varphi_{11}+\varphi_{22}-2\varphi_{11}\varphi_{22})} \quad (5.21)$$

It can be seen from equations (5.19) and (5.20) that the equations of damage and super healing in the principal components for the case of plane stress reduce to the expression of the scalar case of equation (5.1). One can say that the proposed refined theory of super healing is valid in the case of plane stress. One now considers a special case when the damage and super healing in both x and y directions are similar. In this case, one assumes in equations (5.21) that $\varphi_{11} = \varphi_{22}$ and $hs_{11} = hs_{22}$. After some algebraic manipulations, one obtains the following expression:

$$\overline{\sigma}_{22} = \frac{\sigma_{22}}{1 + [hs_{22}(n+1) - 1]\varphi_{22}} \quad (5.22)$$

It is found that equation (5.21) becomes equivalent to equation (5.20) after considering similarity of damage and super healing in both directions. This proves that the refined theory of super healing material can be applied in the case of plane stress and it can be reduced to a simple case.

5.6 Refined super healing in plane strain

In this section, the linear super healing theory is applied in the case of plane strain using equation (5). Plane strain is considered in x and y directions and it is supposed that the strain components ε_{13} , ε_{23} and ε_{33} vanish. This leads to $\varepsilon_{13} = \varepsilon_{23} = \varepsilon_{33} = 0$. Replacing the tensors in equation (21) with the matrices, one can write [162]

$$\{\sigma\} = \begin{Bmatrix} \sigma_{11} \\ \sigma_{22} \\ \sigma_{33} \\ \sigma_{12} \end{Bmatrix} \tag{5.23}$$

$$\{\overline{\sigma}\} = \begin{Bmatrix} \overline{\sigma}_{11} \\ \overline{\sigma}_{22} \\ \overline{\sigma}_{33} \\ \overline{\sigma}_{12} \end{Bmatrix} \tag{5.24}$$

$$I = \begin{bmatrix} 1 & 0 & 0 & 0 \\ 0 & 1 & 0 & 0 \\ 0 & 0 & 1 & 0 \\ 0 & 0 & 0 & 1 \end{bmatrix} \tag{5.25}$$

$$M = \frac{1}{\Delta} \begin{bmatrix} \psi_{22} & 0 & 0 & \varphi_{12} \\ 0 & \psi_{11} & 0 & \varphi_{12} \\ 0 & 0 & \frac{\Delta}{1-\varphi_{33}} & 0 \\ \frac{\varphi_{12}}{2} & \frac{\varphi_{12}}{2} & 0 & \frac{\psi_{11}+\psi_{22}}{2} \end{bmatrix} \tag{5.26}$$

In the present work, we propose a super healing matrix in the case of plane strain to in the following form:

$$Hs^{-1} = \begin{bmatrix} hs_{11} & 0 & 0 & hs_{12} \\ 0 & hs_{22} & 0 & hs_{12} \\ 0 & 0 & hs_{33} & 0 \\ hs_{12} & hs_{12} & 0 & \frac{hs_{11}+hs_{22}}{2} \end{bmatrix} \tag{5.27}$$

Substituting equations (5.24), (5.25) and (5.27) into equation (5.4), the following

relation of the effective stress is obtained:

$$\{\sigma\} = [D]\{\sigma\} \tag{5.28}$$

The components of the tensor $[D]$ are obtained using the MATLAB Symbolic Math Toolbox. The following components of the tensor $[L]$ are as follows:

$$\begin{aligned} D_{11} = -(\varphi_{22} - 1)/((hs_{22}(n+1) - 1)\varphi_{12}^2 - \varphi_{11} - \varphi_{22} + \varphi_{11}\varphi_{22} \\ +\varphi_{11} hs_{22}(n+1) - \varphi_{11}\varphi_{22} hs_{22}(n+1)n + 1) \end{aligned} \tag{5.29a}$$

$$D_{12} = D_{13} = D_{14} = D_{21} = 0 \tag{5.29b}$$

$$\begin{aligned} D_{11} = -(\varphi_{22} - 1)/((hs_{22}(n+1) - 1)\varphi_{12}^2 - \varphi_{11} - \varphi_{22} + \varphi_{11}\varphi_{22} \\ +\varphi_{11} hs_{22}(n+1) - \varphi_{11}\varphi_{22} hs_{22}(n+1)n + 1) \end{aligned} \tag{5.29c}$$

$$D_{23} = D_{24} = D_{31} = D_{32} = 0 \tag{5.29d}$$

$$D_{33} = 1/(\varphi_{33}(hs_{33}(n+1) - 1) + 1) \tag{5.29e}$$

$$D_{34} = D_{41} = D_{42} = D_{43} = 0 \tag{5.29f}$$

$$\begin{aligned} D_{44} = -(2(\varphi_{11} + \varphi_{22} - 2))/(4\varphi_{11}\varphi_{22} - 4\varphi_{22} - 4\varphi_{11} - 4\varphi_{12}^2 \\ +\varphi_{11} hs_{11}(n+1) + \varphi_{11} hs_{22}(n+1) + \varphi_{22} hs_{11}(n+1) \\ +\varphi_{22} hs_{22}(n+1) + 2\varphi_{12}^2 hs_{11}(n+1) + 2\varphi_{12}^2 hs_{22}(n+1) \\ -2\varphi_{11}\varphi_{22} hs_{11}(n+1) - 2\varphi_{11}\varphi_{22} hs_{22}(n+1) + 4) \end{aligned} \tag{5.29g}$$

If one makes a simplifying assumption of equations (31) and considers the case of principal components $\varphi_{12} = \varphi_{21} = 0$ and $hs_{12} = hs_{21} = 0$. The following expressions are obtained:

$$\overline{\sigma}_{11} = \frac{\sigma_{11}}{1 + [hs_{11}(n+1) - 1]\varphi_{11}} \tag{5.30}$$

$$\overline{\sigma}_{22} = \frac{\sigma_{22}}{1 + [hs_{22}(n+1) - 1]\varphi_{22}} \tag{5.31}$$

$$\overline{\sigma}_{33} = \frac{\sigma_{33}}{1 + [hs_{33}(n+1) - 1]\varphi_{33}} \tag{5.32}$$

$$\begin{aligned} \overline{\sigma}_{12} = [-(2(\varphi_{11} + \varphi_{22}2))/(4\varphi_{11}\varphi_{22}4\varphi_{22}4\varphi_{11} + \varphi_{11} hs_{11}(n+1) \\ +\varphi_{11} hs_{22}(n+1) + \varphi_{22} hs_{11}(n+1) + \varphi_{22} hs_{22}(n+1) \\ 2\varphi_{11}\varphi_{22} hs_{11}(n+1) - 2\varphi_{11}\varphi_{22} hs_{22}(n+1) + 4)]^{-1}\sigma_{12} \end{aligned} \tag{5.33}$$

It is clear from equations (5.30), (5.31) and (5.32) that the equations of the linear super healing in the principal components reduce to the scalar case of equation (5.1). One can say that the linear super healing theory is valid in the case of plane strain. Now, one considers the special case when the damage and super healing variables in equation (5.33) are similar in both directions ($\varphi_{11} = \varphi_{22}$ and $hs_{11} = hs_{22}$). After simplification, the following expression is obtained:

$$\sigma_{22} = \frac{\sigma_{22}}{1 + [hs_{22}(n+1) - 1]\varphi_{22}} \tag{5.34}$$

One can see that equation (5.34) reduces to the scalar formulation in equation

(5.1) after the assumption of simplicity of damage and super healing in both directions. This confirms that the linear super healing theory is applicable in the case of plane strain.

5.7 One-dimensional example of refined super healing

In this section, we apply the concept of the refined theory of super healing material to a one-dimensional element using damage-healing mechanics. Figure 5.3 shows the strain history example that is applied to the one-dimensional element. The element is supposed to be loaded until it reaches a strain value of 0.005, unloaded until zero strain, and afterward reloaded. During the loading phase the damage evolves until failure and becomes constant during unloading. When the damage evolution becomes deactivated ($\dot{\varphi} = 0$) the healing takes place during the unloading phase. The material should be reloaded after it has been exposed to healing in order to analyze the behavior of the healed material. If the material is fully healed the healed material exhibits similar behavior as the original material and the elastic modulus in this situation becomes similar to the elastic modulus in the effective configuration ($E_{fh} = E_0$) (see Figure 5.2 above). On the other hand, if the material is not healed it exhibits similar behavior as the damaged material and the elastic modulus in this case becomes similar to the elastic modulus in the damaged situation ($E_h = E_\varphi$).

When self-healing is imposed, the material recovers its original stiffness. Figure 5.4 shows the effect of self-healing mechanism with healing variables $h = 0.5$ and $h = 0.99$. The red curve represents the behavior of the totally damaged material ($h = 0$) in which the material stiffness approaches zero. When the healing is introduced with $h = 0.5$, the material recovers half of its stiffness (blue curve), while the total stiffness is recovered with $h = 0.99$ (green curve). The black curve represents of behavior of the original material.

Figure 5.5 shows the behavior of the material after the refined super healing theory is imposed according to equation (5.1). In this example the multiple super healing mechanism is applied in which one sets the super healing variable $h_s = 1$ and the number of super healing variables $n = 3$. The super healing material is

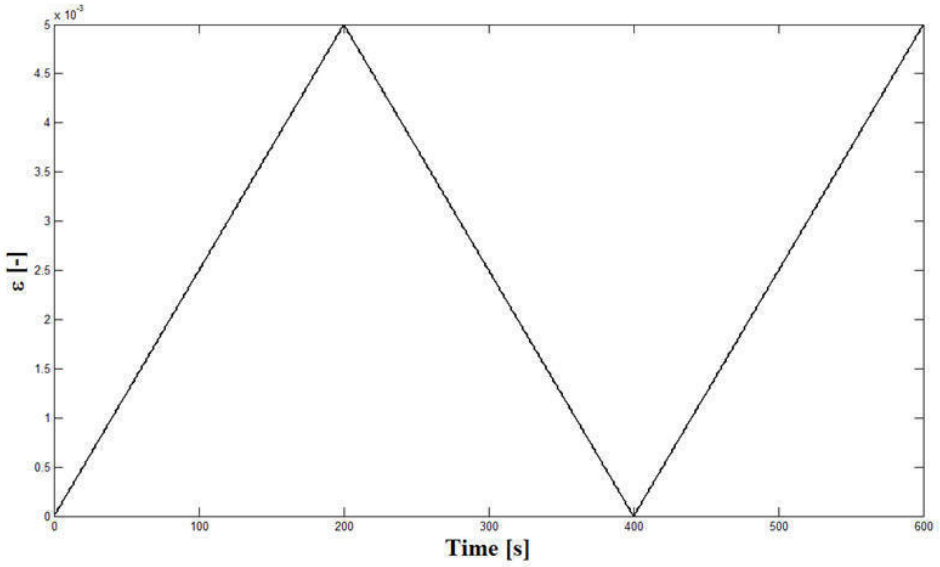

Figure 5.3: Loading (strain) history.

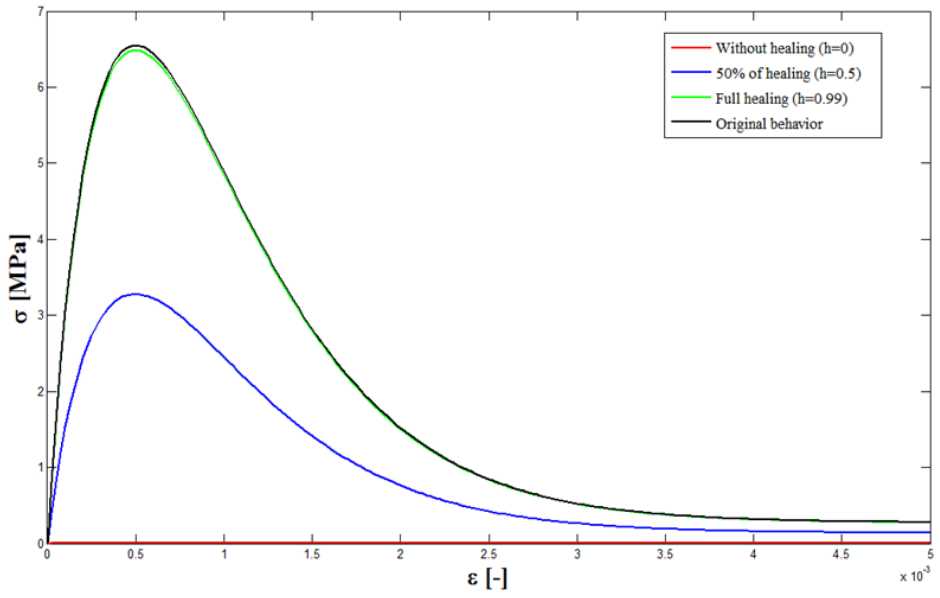

Figure 5.4: Effect of self-healing mechanism.

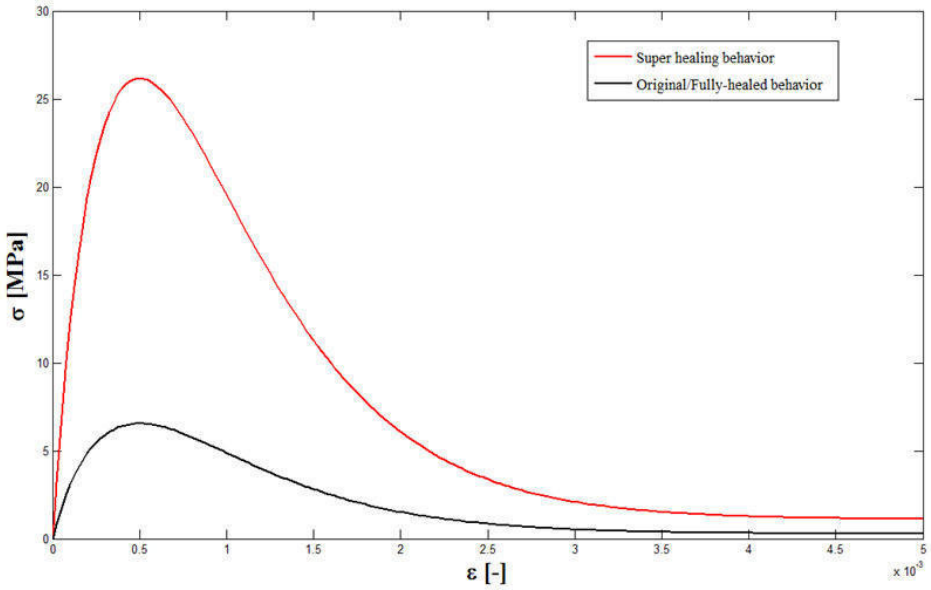

Figure 5.5: Effect of refined super-healing mechanism.

expected to enhance the material stiffness. One can see from Figure 5.5 that the stiffness of the material is enhanced due to super healing effect. It should be noted that the present example aims only to highlight the theoretical framework of the proposed theory. The present theory can be applied in the case of for example microcapsules based super healing concrete. Appropriate healing agent should be chosen in which it acts as both healing and super healing materials. When critical damage appears and breaks the microcapsules, the healing agent is released from the microcapsule, reacts with the catalyst, fills the cracks and forms a solid material. The same healing material after reaction with appropriate chemical components forms the super healing material which acts as strengthening material. The resulting is characterized by its higher stiffness comparing to the healed and original material. In the future it is hoped that experimental investigations will be carried out and new materials which behave according to the same mechanical properties of the proposed theory of super healing will be produced.

5.8 Nonlinear super healing

In this section, the generalized nonlinear super healing (GNSH) and quadratic super healing (QSH) models are introduced which will be compared with the linear refined super healing model. From equation (5.1), φ_{sd} is denoted as the combined super-healing/damage variable which takes the following form:

$$\varphi_{sd} = [1 - h_s\,(n+1)]\,\varphi \tag{5.35}$$

The generalized nonlinear super healing model as formulated in this work follows the same concept of the generalized nonlinear self-healing described above in Figure (3.9) with replacing the healed part S_h with the super healed part S_{sh} . The left part of the figure shows the damage state described by the classical damage variable φ, while the right part of the figure shows the super healed (strengthened) state. It is clear from Figure (3.9) that the super healed area S_{sh} is much less in size than the damaged area S_φ. This is in accordance with the nonlinear healing and super healing theory. It is considered that only a partial set of the damaged area is subjected to healing and consequently to super healing.

Following mathematical derivation made along the same lines introduced in Section 3.6, the following expressions of the combined super-healing/damage variable and effective stress are found in the case of generalized nonlinear super healing thery:

$$\varphi_{sd} = \frac{\varphi\,[1 - h_s\,(n+1)]}{1 - h_s\,(n+1)\,\varphi} \tag{5.36}$$

$$\overline{\sigma} = \frac{\sigma\,[1 - h_s\,(n+1)\,\varphi]}{1 - \varphi} \tag{5.37}$$

In addition, the expressions in the case of quadratic self-helaing theory are as follows:

$$\varphi_{sd} = (\varphi - h_s\,(n+1)\,\varphi)(1 + \varphi h_s\,(n+1) \tag{5.38}$$

$$\overline{\sigma} = \frac{\sigma}{1 - (\varphi - h_s\,(n+1)\,\varphi)\,(1 + \varphi h_s\,(n+1))} \tag{5.39}$$

It should be noted that the generalized super healing model is nonlinear because

φ_{sd} is a nonlinear function of h_s, and equation (5.38) represents the quadratic super healing because the effective damage variable φ_{sd} is a quadratic function of the super healing parameter $h_s\,(n+1)$.

5.9 Anisotropic nonlinear refined super healing

In this section, one generalizes equation (5.37) for the effective stress in the case of anisotropic materials. In this case, one uses tensors instead of scalars. It should be noted that the tensors are represented by vector and matrix notations. In the case of anisotropic material, equation (5.37) of the generalized nonlinear super healing model takes the following expression

$$\{\overline{\sigma}\} = [M]\left([I] - (n+1)\left([I] - [M]^{-1}\right)[Hs]^{-1}\right)\{\sigma\} \tag{5.40}$$

where the vectors $\{\sigma\}$ and $\{\overline{\sigma}\}$ represent the nominal stress tensor and the effective stress tensor, respectively. It should be noted that the anisotropic equation (5.40) reduces to the isotropic equation (5.37) when the substitutions $[M] = 1/(1-\varphi)$, $[Hs] = 1/h_s$ and $[I] = 1$ are made.

The anisotropic generalization of equation (5.39) for the quadratic nonlinear super healing leads to the following expression:

$$\begin{aligned}\{\overline{\sigma}\} \;= [[I] - ([I] - [M]^{-1})([I] - (n+1)[Hs]^{-1})([I] \\ +(n+1)([I] - [M]^{-1})[Hs]^{-1}]^{-1}\{\sigma\}\end{aligned} \tag{5.41}$$

It should be noted that the anisotropic equation (5.41) of the quadratic super healing model reduces to the isotropic equation (5.39) when the substitutions $[M] = \frac{1}{1-\varphi}$, $[Hs] = \frac{1}{h_s}$ and $[I] = 1$ are made.

5.9.1 Generalized nonlinear refined super healing in plane stress

The generalized nonlinear refined super healing is applied in this section for the case of plane stress. Plane stress is considered in x and y directions and it is supposed

that the stress components σ_{13}, σ_{23} and σ_{33} vanish ($\sigma_{13} = \sigma_{23} = \sigma_{33} = 0$). It should be noted that the Tensors in equation (5.40) are presented by matrices. The same vectors and matrices in equations (5.5) to (5.16) are used in this section. Substituting these equations into equation (5.40) and after simplification, one finds the following relation of the effective stress:

$$\{\overline{\sigma}\} = [B]\,\{\sigma\} \tag{5.42}$$

Using the MATLAB Symbolic Math Toolbox and after simplification, one can write the following components of the fourth-rank tensor $[B]$ of equation (5.42):

$$\begin{aligned} B_{11} = (\varphi_{22} + hs_{11} - \varphi_{22}hs_{11} + nhs_{11} + \varphi_{12}(hs_{12} + nhs_{12}) - n\varphi_{22}hs_{11} \\ +(n+1)hs_{11}(\varphi_{12}^2 + \varphi_{22} - \varphi_{11}(\varphi_{22} - 1) - 1) - 1)/(\varphi_{12}^2 + \varphi_{22} \\ -\varphi_{11}(\varphi_{22} - 1) - 1) \end{aligned} \tag{5.43a}$$

$$B_{12} = ((n+1)\varphi_{12}hs_{12})/(\varphi_{12}^2 + \varphi_{11} - \varphi_{22}(\varphi_{11} - 1) - 1) \tag{5.43b}$$

$$\begin{aligned} B_{13} = (n+1)hs_{12} + (hs_{12} + \varphi_{12}(hs_{11}/2 + hs_{22}/2 + nhs_{11}/2 \\ +nhs_{22}/2 - 1) - \varphi_{22}hs_{12} + nhs_{12} - n\varphi_{22}hs_{12})/(\varphi_{12}^2 + \varphi_{22} \\ -\varphi_{11}(\varphi_{22} - 1) - 1) \end{aligned} \tag{5.43c}$$

$$B_{21} = ((n+1)\varphi_{12}hs_{12})/(\varphi_{12}^2 + \varphi_{11} - \varphi_{22}(\varphi_{11} - 1) - 1) \tag{5.43d}$$

$$\begin{aligned} B_{22} = (\varphi_{11} + hs_{22} - \varphi_{11}hs_{22} + nhs_{22} + \varphi_{12}(hs_{12} + nhs_{12}) \\ -n\varphi_{11}hs_{22} + (n+1)hs_{22}(\varphi_{12}^2 + \varphi_{11} - \varphi_{22}(\varphi_{11} - 1) - 1) \\ -1)/(\varphi_{12}^2 + \varphi_{11} - \varphi_{22}(\varphi_{11} - 1) - 1) \end{aligned} \tag{5.43e}$$

$$B_{23} = (n+1)hs_{12} + (hs_{12} + \varphi_{12}(hs_{11}/2 + hs_{22}/2 + nhs_{11}/2 + nhs_{22}/2 - 1) - \varphi_{11}hs_{12} + nhs_{12} - n\varphi_{11}hs_{12})/(\varphi_{12}^2 + \varphi_{11} - \varphi_{22}(\varphi_{11} - 1) - 1) \tag{5.43f}$$

$$B_{31} = (n+1)hs_{12} - (\varphi_{12}/2 - hs_{12} + (\varphi_{11}hs_{12})/2 - (\varphi_{12}hs_{11})/2 + (\varphi_{22}hs_{12})/2 - nhs_{12} + (n\varphi_{11}hs_{12})/2 - (n\varphi_{12}hs_{11})/2 + (\varphi_{22}hs_{12})/2)/(\varphi_{12}^2 + \varphi_{11} + \varphi_{22} - \varphi_{11}\varphi_{22} - 1) \tag{5.43g}$$

$$B_{32} = (n+1)hs_{12} - ((\varphi_{11}hs_{12})/2 - \varphi_{12}(hs_{12}/2 + (nhs_{22})/2 - 1/2) - hs_{12} + (\varphi_{22}hs_{12})/2 - nhs_{12} + (n\varphi_{11}hs_{12})/2 + (n\varphi_{22}hs_{12})/2)/(\varphi_{12}^2 + \varphi_{11} + \varphi_{22} - \varphi_{11}\varphi_{22} - 1) \tag{5.43h}$$

$$B_{33} = ((hs_{11} + hs_{22})(n+1))/2 - ((\varphi_{11}hs_{11}/4 - \varphi_{22}/2 - hs_{11}/2 - hs_{22}/2 - \varphi_{11}/2 + (\varphi_{11}hs_{22})/4 + (\varphi_{22}hs_{11})/4 + (\varphi_{22}hs_{22})/4 - (nhs_{11})/2 - (nhs_{22})/2 - \varphi_{12}(hs_{12} + nhs_{12}) + (n\varphi_{11}hs_{11})/4 + (n\varphi_{11}hs_{22})/4 + (n\varphi_{22}hs_{11})/4 + (n\varphi_{22}hs_{22})/4 + 1)/(\varphi_{12}^2 + \varphi_{11} + \varphi_{22} - \varphi_{11}\varphi_{22} - 1) \tag{5.43i}$$

Next, one considers a special case of principal components. Therefore, one sets $\varphi_{12} = \varphi_{21} = 0$ and $hs_{12} = hs_{21} = 0$. Then, one substitutes the simplified equations into equation (5.42). After some algebraic manipulations one obtains the following expressions:

$$\overline{\sigma}_{11} = \frac{\sigma_{11}\left[1 - hs_{11}\left(n+1\right)\varphi_{11}\right]}{1 - \varphi_{11}} \tag{5.44}$$

$$\overline{\sigma}_{22} = \frac{\sigma_{22}\left[1 - hs_{22}\left(n+1\right)\varphi_{22}\right]}{1 - \varphi_{22}} \tag{5.45}$$

$$\begin{aligned}\overline{\sigma}_{12} = \sigma_{12}[(hs_{11}/4 + hs_{22}/4 + (nhs_{11})/4 + (nhs_{22})/4 - 1/2)/((\varphi_{11} - 1) \\ -(hs_{11} + hs_{22} - 2\varphi_{22}hs_{11} - 2\varphi_{22}hs_{22} + nhs_{11} + nhs_{22} + 2n\varphi_{22}hs_{11} \\ -2n\varphi_{22}hs_{22} + 2)/(4(\varphi_{22} - 1))]\end{aligned} \tag{5.46}$$

It can be seen from equations (5.44) and (53) that the equations of damage and super healing in the principal components for the case of plane stress reduce to the expression of the scalar case of equation (5.37). Therefore, one can say that the generalized nonlinear refined super healing model is valid in the case of plane stress.

One now considers a special case when the damage and super healing in both x and y directions are similar. In this case, one assumes in equation (5.46) that $\varphi_{11} = \varphi_{22}$ and $hs_{11} = hs_{22}$. After some algebraic manipulations, one obtains the following expression:

$$\overline{\sigma}_{22} = \frac{\sigma_{22}\left[1 - hs_{22}\left(n+1\right)\varphi_{22}\right]}{1 - \varphi_{22}} \tag{5.47}$$

It is found that equation (5.46) becomes equivalent to equation (5.45) after considering the similarity in damage and super healing. This proves that the nonlinear refined theory of super healing model can be applied in the case of plane stress and it can be reduced to a simple case.

5.9.2 Generalized nonlinear refined super healing in plane strain

In this section, the generalized nonlinear super healing theory is applied in the case of plane strain for the case of anisotropic material based on CDHM. Substituting equations (5.25), (5.26) and (5.27) into equation (5.40) leads to the following relation of the effective stress:

$$\{\sigma\} = [F]\{\sigma\} \tag{5.48}$$

Using the MATLAB Symbolic Math Toolbox and after simplification, one can write the following components of the fourth-rank tensor $[F]$ of equation (5.48):

$$F_{11} = hs_{22}(n+1) + (\varphi_{22} + hs_{22}(n+1) - \varphi_{22}hs_{22}(n+1) - 1)/(\varphi_{12}^2 + \varphi_{22} - \varphi_{11}(\varphi_{22} - 1) - 1) \tag{5.49a}$$

$$F_{12} = (\varphi_{12}hs_{12}(n+1))/(\varphi_{12}^2 + \varphi_{11} - \varphi_{22}(\varphi_{11} - 1) - 1) \tag{5.49b}$$

$$F_{13} = 0 \tag{5.49c}$$

$$F_{14} = hs_{12}(n+1) + (-\varphi_{12} + (\varphi_{12}hs_{22}(n+1)/2 - \varphi_{22}hs_{12}(n+1) + hs_{12}(n+1) + (\varphi_{12}h11(n+1)/2 - \varphi_{22})/(\varphi_{12}^2 + \varphi_{22} - \varphi_{11}(\varphi_{22} - 1) - 1) \tag{5.49d}$$

$$F_{21} = (\varphi_{12}hs_{12}(n+1))/(\varphi_{12}^2 + \varphi_{11} - \varphi_{22}(\varphi_{11} - 1) - 1) \tag{5.49e}$$

$$F_{22} = hs_{11}(n+1) + (\varphi_{11} + hs_{11}(n+1) - \varphi_{11}hs_{11}(n+1) + \varphi_{12}hs_{12}(n+1) - 1)/(\varphi_{12}^2 + \varphi_{11} - \varphi_{22}(\varphi_{11} - 1) - 1) \tag{5.49f}$$

$$F_{23} = 0 \tag{5.49g}$$

$$F_{24} = hs_{12}(n+1) + (-\varphi_{12} + hs_{12}(n+1) - \varphi_{11}hs_{12}(n+1) + (\varphi_{12}hs_{11}(n+1))/2 + (\varphi_{12}h22(n+1))/2)/(\varphi_{12}^2 + \varphi_{11} - \varphi_{22}(\varphi_{11} - 1) - 1) \tag{5.49h}$$

$$F_{31} = F_{32} = 0 \tag{5.49i}$$

$$F_{33} = (\varphi_{33} hs_{33}(n+1) - 1)/(\varphi_{33} - 1) \tag{5.49j}$$

$$\begin{aligned} F_{41} = hs_{12}(n+1) - (\varphi_{12}/2 - hs_{12}(n+1) + (\varphi_{11} hs_{12}(n+1))/2 \\ -(\varphi_{12} hs_{22}(n+1))/2 + (\varphi_{22} hs_{12}(n+1))/2)/(\varphi_{12}^2 + \varphi_{11} + \varphi_{22} \\ -\varphi_{11}\varphi_{22} - 1) \end{aligned} \tag{5.49k}$$

$$\begin{aligned} F_{41} = hs_{12}(n+1) - (\varphi_{12}/2 - hs_{12}(n+1) + (\varphi_{11} hs_{12}(n+1))/2 \\ -(\varphi_{12} hs_{22}(n+1))/2 + (\varphi_{22} hs_{12}(n+1))/2)/(\varphi_{12}^2 + \varphi_{11} + \varphi_{22} \\ -\varphi_{11}\varphi_{22} - 1) \end{aligned} \tag{5.49l}$$

$$\begin{aligned} F_{42} = hs_{12}(n+1) - (\varphi_{12}/2 - hs_{12}(n+1) + (\varphi_{11} hs_{12}(n+1))/2 \\ -(\varphi_{12} hs_{11}(n+1))/2 + (\varphi_{22} hs_{12}(n+1))/2)/(\varphi_{12}^2 + \varphi_{11} + \varphi_{22} \\ -\varphi_{11}\varphi_{22} - 1) \end{aligned} \tag{5.49m}$$

$$F_{42} = 0 \tag{5.49n}$$

$$\begin{aligned} F_{44} = ((hs_{11} + hs_{22})(n+1))/2 - \varphi_{22}/2 - \varphi_{11}/2 \ - (hs_{11}(n+1))/2 \\ -hs_{22}(n+1)/2 + (\varphi_{11} hs_{11}(n+1))/4 - \varphi_{12}\varphi_{12}(n+1) + (\varphi_{11} hs_{22}(n \\ +1))/4 + (\varphi_{22} hs_{11}(n+1))/4 + (\varphi_{22} hs_{22}(n+1))/4 + 1)/(\varphi_{12}^2 \\ +\varphi_{11} + \varphi_{22} - \varphi_{11}\varphi_{22} - 1) \end{aligned} \tag{5.49o}$$

Next, one considers a special case of principal components. Therefore, one sets $\varphi_{12} = \varphi_{21} = 0$ and $hs_{12} = hs_{21} = 0$. Then, one substitutes the simplified equations into equations (5.49). After some algebraic manipulations one obtains the following expressions:

$$\overline{\sigma}_{11} = \frac{\sigma_{11}\left[1 - hs_{11}\left(n+1\right)\varphi_{11}\right]}{1-\varphi_{11}} \tag{5.50}$$

$$\overline{\sigma}_{22} = \frac{\sigma_{22}\left[1 - hs_{22}\left(n+1\right)\varphi_{22}\right]}{1-\varphi_{22}} \tag{5.51}$$

$$\overline{\sigma}_{33} = \frac{\sigma_{33}\left[1 - hs_{33}\left(n+1\right)\varphi_{33}\right]}{1-\varphi_{33}} \tag{5.52}$$

$$\begin{aligned}\overline{\sigma}_{12} = \sigma_{12}[((((2(\varphi_{12}^2 + \varphi_{11} + \varphi_{22} - \varphi_{11}\varphi_{22} - 1))/(\varphi_{11} + \varphi_{22} - 2) - 1)(n \\ +1)(hs_{11}/2 + hs_{22}/2) + 1)(\varphi_{11}/2 + \varphi_{22}/2 - 1))/(\varphi_{12}^2 - (\varphi_{11} - 1)(\varphi_{22} - 1)]\end{aligned} \tag{5.53}$$

It can be clearly seen that the equations (5.50), (5.51) and (5.52) of the generalized nonlinear super healing theory in the principal components for the case of plane strain reduce to the expression of the scalar case of equation (5.37). Therefore, one can say that the generalized nonlinear refined super healing model is valid in the case of plane strain.

One now considers a special case when the damage and super healing in both and directions are similar. In this case, one assumes in equation (5.53) that $\varphi_{11} = \varphi_{22}$ and $hs_{11} = hs_{22}$. After some algebraic manipulations, one obtains the following expression:

$$\overline{\sigma}_{22} = \frac{\sigma_{22}\left[1 - hs_{22}\left(n+1\right)\varphi_{22}\right]}{1-\varphi_{22}} \tag{5.54}$$

It is found that equation (5.54) reduces to the scalar formulation in equation (5.37) after considering the similarity in damage and super healing. This proves that the generalized nonlinear theory of super healing model can be applied in the case of plane strain and it can be reduced to a simple case.

5.9.3 Quadratic refined super healing in plane stress

In this section, the quadratic refined super healing model is applied in the case of plane stress. Therefore, the tensors in equation (5.41) are presented by matrices. Because of the long expressions of the analytical solution, the results of the plane stress example will be briefly presented in this section. The same vectors and matrices in equations (5.5) to (5.16) are used in this section.

Equation (5.39) can be rewritten as follows:

$$\sigma = \left[1 - \left(\varphi - h_s \left(n+1\right) \varphi\right) \left(1 + \varphi h_s \left(n+1\right)\right)\right] \overline{\sigma} \tag{5.55}$$

Substituting equations (5.5) to (5.16) into equation (5.41), one finds the following relation of the effective stress:

$$\{\overline{\sigma}\} = [C] \{\sigma\} \tag{5.56}$$

Using the MATLAB Symbolic Math Toolbox, if one considers a simplified case of principal components where $\varphi_{12} = \varphi_{21} = 0$ and $hs_{12} = hs_{21} = 0$, and substitutes the components of the solutions of the fourth-rank tensor $[C]$ into equation (5.55), one finds, after algebraic manipulations, the following expressions:

$$\sigma_{11} = \left[1 - \left(\varphi_{11} - hs_{11} \left(n+1\right) \varphi_{11}\right) \left(1 + \varphi_{11} hs_{11} \left(n+1\right)\right)\right] \overline{\sigma}_{11} \tag{5.57}$$

$$\sigma_{22} = \left[1 - \left(\varphi_{22} - hs_{22} \left(n+1\right) \varphi_{22}\right) \left(1 + \varphi_{22} hs_{22} \left(n+1\right)\right)\right] \overline{\sigma}_{22} \tag{5.58}$$

$$\begin{aligned} \sigma_{12} = [((((2 \left(\varphi_{22} - 1\right)^2 / (\varphi_{11} + \varphi_{22} - 2) + 1) \left(n+1\right) (hs_{11}/2 + hs_{22}/2) \\ +1)(2\varphi_{22}^2 - 3\varphi_{22} + \varphi_{11})((n+1) hs_{11} + (n+1) \varphi_{22} \ - 2))/(2 \ \varphi_{11} \\ +\varphi_{22} - 2)) + 1]\overline{\sigma}_{12} \end{aligned} \tag{5.59}$$

It can be seen from equations (5.57) and (5.58) that the equations of damage and super healing in the principal components for the case of plane stress reduce to the expression of the scalar case of equation (5.39). Therefore, one can say that the quadratic refined super healing model is valid in the case of plane stress.

One now considers a special case when the damage and super healing in both x and y directions are similar. In this case, one assumes in equations (5.59) that $\varphi_{11} = \varphi_{22}$ and $hs_{11} = hs_{22}$. After some algebraic manipulations, one obtains the following expression:

$$\sigma_{22} = \left[1 - \left(\varphi_{22} - hs_{22}\left(n+1\right)\varphi_{22}\right)\left(1 + \varphi_{22} hs_{22}\left(n+1\right)\right)\right]\overline{\sigma}_{22} \tag{5.60}$$

It is found that equation (5.60) becomes equivalent to equation (5.58) after considering the similarity in damage and super healing. This proves that the quadratic refined theory of super healing model can be applied in the case of plane stress and it can be reduced to a simple case.

5.9.4 Quadratic refined super healing in plane strain

In this section, the quadratic super healing theory is applied in the case of plane strain. Substituting equations (5.25), (5.26) and (5.27) into equation (5.39), one obtains the following relation of the effective stress:

$$\{\overline{\sigma}\} = [J]\{\sigma\} \tag{5.61}$$

The components of the tensor $[J]$ are obtained using the MATLAB Symbolic Math Toolbox. Due to the long expressions of the components of the tensor $[J]$, one considers the case of the principal components where $\varphi_{12} = \varphi_{21} = 0$ and $hs_{12} = hs_{21} = 0$, and substitutes the components of the solutions of the fourth-rank tensor $[J]$ into equation (5.61). After algebraic manipulations, the following expressions are obtained:

$$\sigma_{11} = [1 - (\varphi_{11} - hs_{22}(n+1)\varphi_{11}) - (hs_{22}(n+1)\varphi_{11}^2 - hs_{22}^2(n+1)^2\varphi_{11}^2)]\overline{\sigma}_{11} \tag{5.62}$$

$$\sigma_{22} = [1 - (\varphi_{22} - hs_{11}(n+1)\varphi_{22}) - (hs_{11}(n+1)\varphi_{22}^2 - hs_{11}^2(n+1)^2\varphi_{22}^2)]\overline{\sigma}_{22} \tag{5.63}$$

$$\sigma_{33} = [1 - (\varphi_{33} - hs_{33}(n+1)\varphi_{33}) - (hs_{33}(n+1)\varphi_{33}^2 - hs_{33}^2(n+1)^2\varphi_{33}^2)]\overline{\sigma}_{33} \quad (5.64)$$

$$\begin{aligned}\sigma_{12} = [(((((2(\varphi_{11} + \varphi_{22} - \varphi_{11}\varphi_{22} - 1))))/(\varphi_{11} + \varphi_{22} - 2) - 1)(n+1)(hs_{11}/2 \\ +\varphi_{22}/2) - 1))(\varphi_{11} + \varphi_{22} - 2\varphi_{11}\varphi_{22})(hs_{11}(n+1) + \varphi_{22}(n+1) \\ -2))))/(2(\varphi_{11} + \varphi_{22} - 2)) + 1]\overline{\sigma}_{12}\end{aligned} \quad (5.65)$$

It can be clearly observed that the equations (5.62), (5.63) and (5.64) of the quadratic super healing in the principal components for the case of plane strain reduce to the expression of the scalar case of equation (5.39).Therefore, one can say that the quadratic super healing model is valid in the case of plane strain.

Again, one considers a special case in equation (5.65) when both damage and super healing variables are similar in both directions ($\varphi_{11} = \varphi_{22}$ and $hs_{11} = hs_{22}$). After algebraic manipulations, the following expression is obtained:

$$\sigma_{22} = [1 - (\varphi_{22} - hs_{11}(n+1)\varphi_{22}) - (hs_{11}(n+1)\varphi_{22}^2 - hs_{11}^2(n+1)^2\varphi_{22}^2)]\overline{\sigma}_{22} \quad (5.66)$$

It can be observed that equation (5.66) reduces to the scalar formulation in equation (5.39). It is demonstrated that the quadratic super healing theory can be applied in the case of plane strain.

5.10 Concept of non-super-healed damage

As it was that shown there is a difference between linear and nonlinear healing models, it will be shown in this section that there is also a difference between the linear super healing model of equation (5.1) and the nonlinear generalized super healing model in equation (5.37). According to equations (5.35) and (5.36), it is seen that in both models when the material is undamaged ($\varphi = 0$) the combined super-healing/damage material is equal to zero ($\varphi_{sd} = 0$). However, when the material

is damaged ($\varphi = 1$) the combined super-healing/damage variable becomes $\varphi_{sd} = 1 - h_s\,(n+1)$ in the case of linear super healing model (equation (5.35)). However, in the case of the generalized super healing, one obtains $\varphi_{sd} = 1$ irrespective of the value of the super healing parameter $h_s\,(n+1)$. This can be explained that some form of damage that is not healed and consequently not subjected to super healing remains in the material. The remaining damaged material is the main feature of the nonlinear super healing model and makes this theory distinct and different from the linear super healing model. In order to get complete super healing, the process of super healing has to complete before the material becomes damaged. Therefore, as it was proposed for the nonlinear healing model, the same proposition is adopted for super healing in which complete super healing occurs at a specific value of damage $\varphi < 1$. In this case, equation (5.35) is modified to account for the fact that the damage is not subjected to super healing. The modification proposed for nonlinear healing is adopted here which can be written as the following expression:

$$\varphi_{sd} = [1 - h_s\,(n+1) + \alpha h_s\,(n+1)] \tag{5.67}$$

where α is called here the non-super-healable damage parameter. When the value of α is zero, equation (5.67) becomes equivalent to equation (5.35) with no remaining damage. However, when $\alpha \neq 0$, the material still contains remaining non-super-healed damage.

5.11 Comparison of super healing models

Table 5.1 shows the summary of the comparison between the equations of the linear, generalized nonlinear and quadratic nonlinear super healing models. For the comparison the ratios $\frac{\varphi_{sd}}{\varphi}$ and $\frac{\overline{\sigma}}{\sigma}$ are used.

Figure 5.6 shows the curves representing the expressions of the ratio $\overline{\sigma}/\sigma$ of Table 5.1. In the Figures 5.6(a) and 5.6(b) the features of the linear, generalized nonlinear and quadratic nonlinear self-healing and super healing models are illustrated, respectively. Figure 5.6(a) describes the healing process in every model. In order to plot the curves of the three expressions in Table 5.1, one utilizes an example in which the damage variable $\varphi = 0.5$, and the super healing variable h_s takes the

Table 5.1: Comparison between the super healing models.

Super healing models	Equation of the ratio $\frac{\varphi_{sd}}{\varphi}$	Equation of the ratio $\frac{\overline{\sigma}}{\sigma}$
Linear super healing (LSH)	$\frac{\varphi_{sd}}{\varphi} = 1 - h_s\,(n+1)$	$\frac{\overline{\sigma}}{\sigma} = \frac{1}{1-[1-h_s(n+1)]\varphi}$
Generalized nonlinear super healing (GNSH)	$\frac{\varphi_{sd}}{\varphi} = \frac{1-h_s(n+1)}{1-\varphi h_s(n+1)}$	$\frac{\overline{\sigma}}{\sigma} = \frac{1-h_s(n+1)\varphi}{1-\varphi}$
Quadratic super healing (QSH)	$\frac{\varphi_{sd}}{\varphi} = 1 - h_s\,(n+1) + \varphi h_s\,(n+1) - \varphi h_s^2\,(n+1)^2$	$\frac{\overline{\sigma}}{\sigma} = \frac{1}{1-\left[1-h_s(n+1)+\varphi h_s(n+1)-\varphi h_s^2(n+1)^2\right]\varphi}$

value of 1 with $n = 3$. It is seen from Figure 5.6(a) that for the three models where the material is unhealed ($h_s\,(n+1) = 0$), one obtains the ratio $\overline{\sigma}/\sigma = 2$. This means that the effective stress is greater (double) than the nominal stress which describes the damaged state of the material. In this example, the maximum values of self-healing and super healing parameters $h_s\,(n+1)$ are 1 and 4, respectively. It should be noted that the parameter $h_s\,(n+1)$ represents the healing effect in Figure 5.6(a). It is also observed that the nonlinear healing models produce higher ratio $\overline{\sigma}/\sigma$ comparing with the linear healing model. Furthermore, it is found that the generalized nonlinear healing model produces higher ratio $\overline{\sigma}/\sigma$ compared to the quadratic healing model. On the other hand, when the material is fully healed ($h_s\,(n+1) = 1$), it is seen that the three models meet at one single point. At this point the effective stress is equal to the nominal stress ($\overline{\sigma}/\sigma = 1$). One can observe that all the three models are appropriate to describe the healing concept in which the parameter $h_s\,(n+1)$ represents the healing variable and varies from 0 to 1. In this case, one sets $n = 0$ and $h_s \in [0, 1]$.

The super healing models in Figure 5.6(b) represent the state of the material when the super healing is applied in the case of the linear, generalized nonlinear and quadratic super healing models. The same example is applied in which the super healing parameter takes the values from 1 to 4 ($1 \leq h_s\,(n+1) \leq 4$). It is seen

from the figure that at $\varphi = 0.5$ and $h_s(n+1) = 4$ the values of the ratio $\overline{\sigma}/\sigma$ in the linear and quadratic super healing models are 0.4 and 0.18, respectively. It is observed that the quadratic super healing model produces lower values of the ratio $\overline{\sigma}/\sigma$ compared to the linear super healing model. This means that the performance of the super healing efficiency is overestimated with the quadratic super healing model. For the generalized nonlinear super healing model, one observes that the ratio $\overline{\sigma}/\sigma$ approaches zero with lower value of the super healing parameter supposed in the example comparing with linear and quadratic super healing models. It is found that with the proposed parameters of the present example ($h = 1$, $n = 3$, and $\varphi = 0.5$) the ratio $\overline{\sigma}/\sigma$ will approaches zero when $h_s(n+1) = 2$. If the values of these parameters change, the ratio $\overline{\sigma}/\sigma$ will approach zero in a different value of super healing parameter. It should be noted that the present example aims only to describe the comparison of the theoretical behavior of the super healing models. It is hoped that future research will be undertaken to describe and demonstrate the physical behavior of the super healing models.

From Figure 5.6(b), one can also observe that the generalized nonlinear super healing model reaches the minimum ratios of the linear and quadratic super healing models with 1.6 and 1.82 of the super healing parameters, respectively. Thus, comparing with the linear and quadratic super healing models the generalized nonlinear super healing model overestimates the performance of the super healing efficiency with a difference of 25 % and 9.9 %, respectively. It should be noted that the linear healing and super healing models are illustrated with a curve according to equation (5.1), and the nonlinear healing and super healing models are illustrated with a straight line in Figure 5.6 according to equation (5.37). This is because the nonlinear super healing theories were proposed and defined based on the decomposition of the damage variable to nominal damage and combined super-healing/damage variables (equations (3.43), (3.44), and (3.45)). This is reflected by the linearity and nonlinearity of the ratio φ_{sd}/φ in Table 5.1 for the linear and generalized nonlinear super healing models, respectively.

In the following, the maximum difference between the super healing models is computed using the first derivative of the difference function. The difference will be calculated based on the equations of the ratio φ_{sd}/φ.

One denotes R the parameter of super healing where $R = h_s(n+1)$ and $f_1(R)$

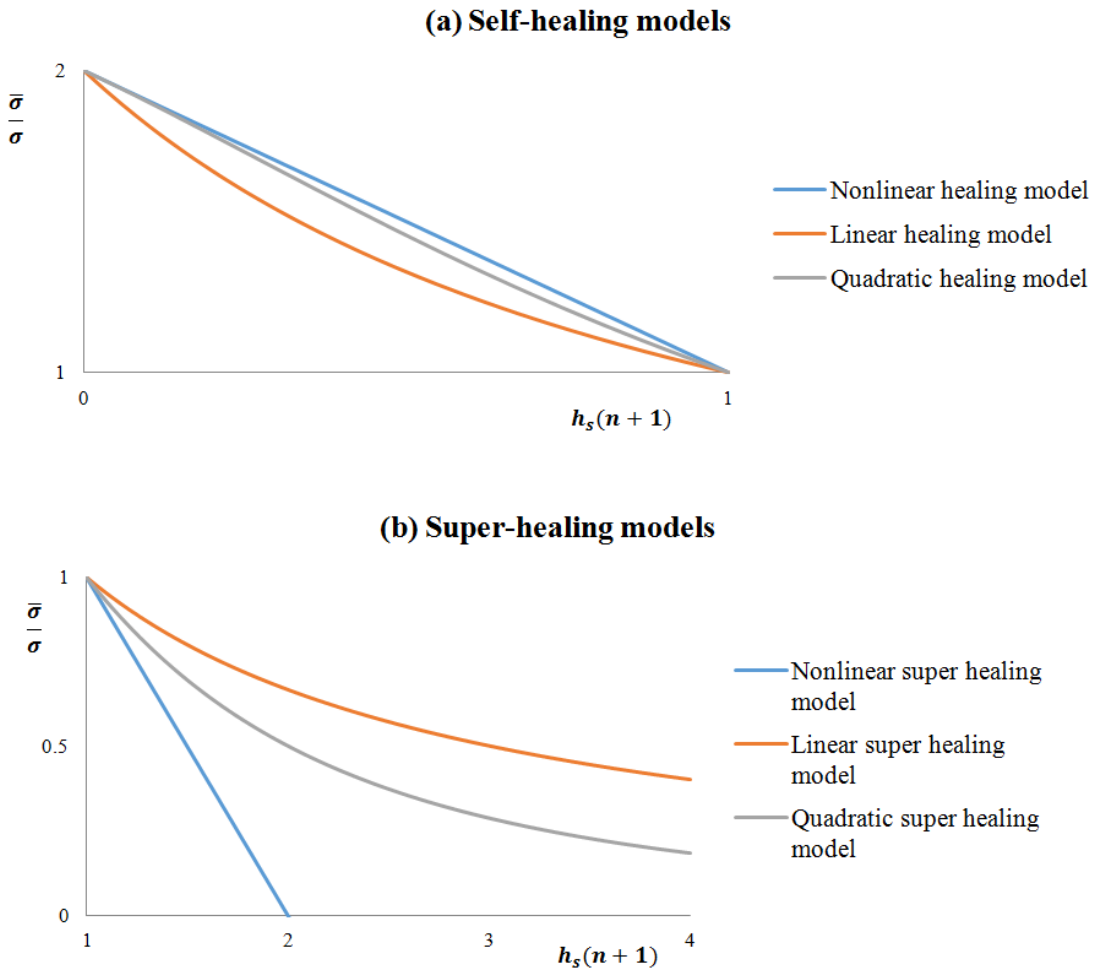

Figure 5.6: Comparison between linear, generalized nonlinear and quadratic models: (a) self-healing models, (b) super healing models.

the difference function between the linear and the generalized nonlinear super healing models, and it is written as follows:

$$f_1(R) = \frac{\varphi(1-R)}{1-\varphi R} - \varphi(1-R) \tag{5.68}$$

After simplification of equation (5.68) one obtains the following expression:

$$f_1(R) = \frac{\varphi^2 R(1-R)}{1-\varphi R} \tag{5.69}$$

In order to find the maximum value of the difference function one calculates the first derivative of equation (5.69) with respect to R. One sets the derivative equal to zero as follows:

$$\varphi R^2 - 2R + 1 = 0 \tag{5.70}$$

Solving the quadratic equation (5.70), two roots are obtained following the form $(1 \pm \sqrt{(1-\varphi)})/\varphi$. It is clearly seen that the solution R with the sign " $-$ " is not appropriate because it gives a value of super healing parameter less than 1 which represents the healing concept. Thus, the root taken into consideration takes the following expression

$$R = h_s(n+1) = \frac{1+\sqrt{1-\varphi}}{\varphi} \tag{5.71}$$

It is seen from equation (5.71) that the value of the super healing variable depends on the value of the damage variable. Figure 5.7 shows the variation of the super healing variable as function of damage variable φ. It is clearly seen from the figure that the super healing variable is greater than 1. For the damage variable in the interval $\varphi \in [0,1]$, the values of the super healing parameter R drops from infinity to a finite value of $R = 1$.

According to Figure 5.7, one sees that at damage variable $\varphi = 0.05$ the value of super healing parameter $h_s(n+1)$ is equal to 40. It should be noted that the value of super healing parameter $h_s(n+1)$ can be a case of multiple super healing mechanisms with different numbers of healing parameter (n) and values of super healing parameter (h_s) (e.g. $h_s = 2$ and $n = 19$). Substituting the value $R = 40$ into the difference equation $f_1(R)$ of equation (5.69), one obtains

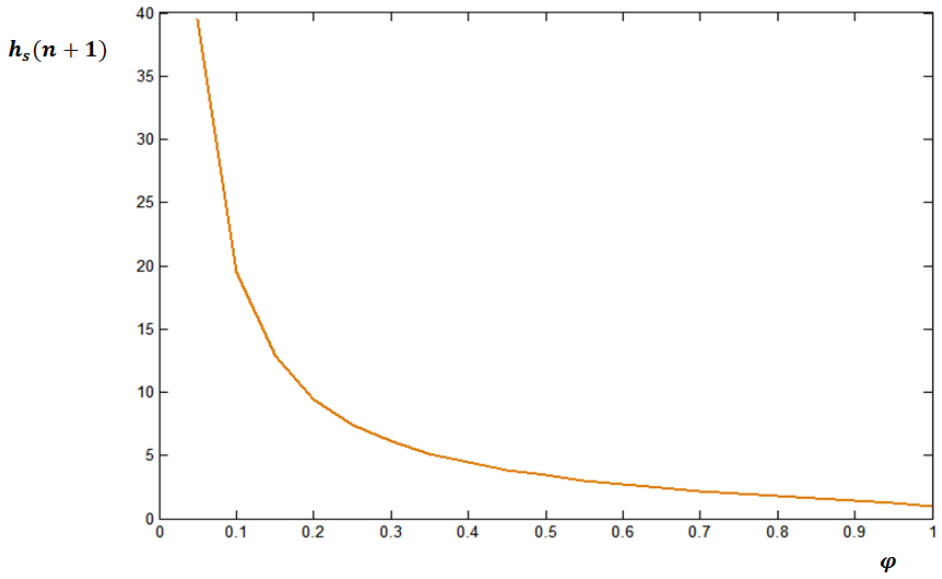

Figure 5.7: Variation of the super healing parameter as function of damage variable according to equation (5.71).

$$f_1(40) = \frac{-1560\varphi^2}{1-40\varphi} \tag{5.72}$$

If one supposes that the maximum value of equation (5.72) occurs at $\varphi = 0.05$ which results in $f_1(40) = 3.9$, consequently, the maximum difference between the linear and generalized nonlinear super healing is 3.9.

Now one examines the difference between the linear and quadratic super healing models. Therefore, one denotes $f_2(R)$ as the difference function which is written as follows:

$$f_2(R) = \varphi(1-R+\varphi R\varphi R^2) - \varphi(1-R) \tag{5.73}$$

After simplification of equation (5.73), one obtains

$$f_2(R) = \varphi^2 R(1-R) \tag{5.74}$$

Applying the first derivative of equation (5.74) with respect to R and setting it

equal to zero, one obtains

$$\varphi^2(1-2R) = 0 \tag{5.75}$$

It is clearly seen that the solution of equation (5.75) is $R = 0.5$ which is less than 1. It is observed that the solution represents the healing concept in which the healing variable R takes the value from 0 to 1. One can say that in this case the parameter R represents the solution which defines the healing variable. Therefore, the solution obtained from equation (5.75) is discarded in the case of super healing theory.

Next one calculates the difference between the generalized and quadratic super healing models. One denotes $f_3(R)$ as the difference function which is written as follows:

$$f_3(R) = \frac{\varphi(1-R)}{1-\varphi R} - \varphi(1-R+\varphi R\varphi R^2 \tag{5.76}$$

Simplifying the expression of equation (5.76) one obtains the following form

$$f_3(R) = \frac{\varphi^3 R^2(1-R)}{1-\varphi R} \tag{5.77}$$

In order to find the maximum value of the difference function $f_3(R)$, one applies the first derivative of equation (5.77) with respect to R and sets it equal to zero. After simplification, the following expression of quadratic function is obtained

$$\varphi R^2 - (3+\varphi)R + 2 = 0 \tag{5.78}$$

After solving equation (5.78), one obtains the following root

$$R = \frac{3+\varphi \pm \sqrt{\varphi^2 - 10\varphi + 9}}{4\varphi} \tag{5.79}$$

It is seen from the root expression in equation (5.79) that the value of the super healing parameter R depends on the value of the damage variable φ. The solution R with the " $-$ " sign is discarded because it gives values less than 1 as Figure 5.8 shows. This figure shows that the root of equation (5.79) with " $-$ " sign represents the healing concept ($h_s \in [0,1]$ and $n = 0$) because the maximum value of the

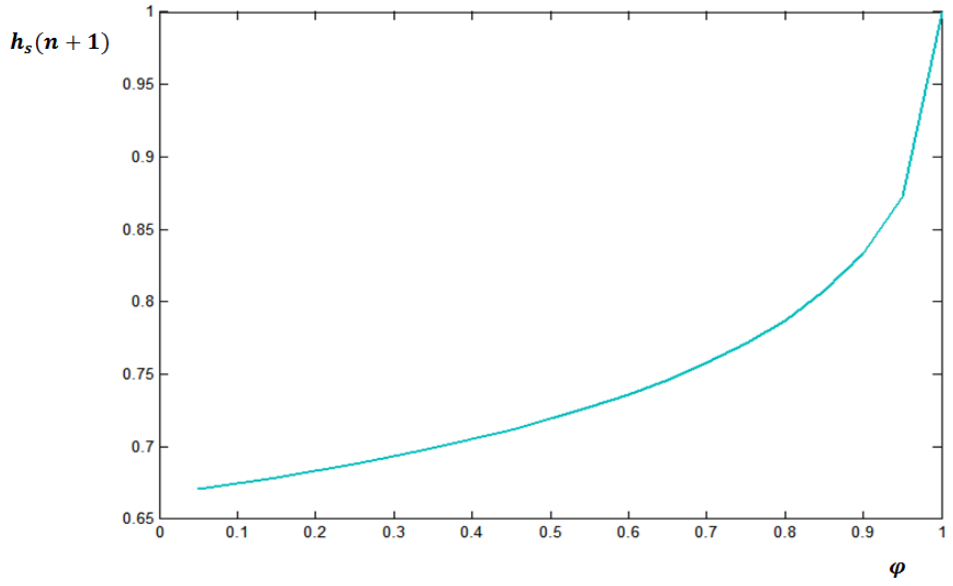

Figure 5.8: Variation of the super healing parameter as function of damage variable according to equation (5.79) with "-" sign

parameter $h_s\,(n+1)$. Thus, this case seems not appropriate for nonlinear super healing.

The second solution with "+" seems to give values of R greater than 1. Therefore, the following expression in taken under consideration:

$$R = \frac{3+\varphi+\sqrt{\varphi^2-10\varphi+9}}{4\varphi} \tag{5.80}$$

The plot of the expression of equation (5.80) is given in Figure 5.9. It is clearly seen from Figure 5.9 that the super healing parameter $h_s\,(n+1)$ is greater than 1. For the damage variable on the interval $\varphi \in [0,1]$, the values of the super healing parameter R drops from infinity to a finite value of $R=1$. It is seen from Figure 5.9 that at damage variable $\varphi = 0.05$ the value of super healing parameter $h_s\,(n+1)$ is equal to 30. This value can be a case of multiple super healing mechanism with different numbers and values of super healing parameter (e.g. $h_s = 2$ and $n = 14$). Substituting the value $R = 30$ into the difference equation $f_3\,(R)$ of equation (5.76), one obtains

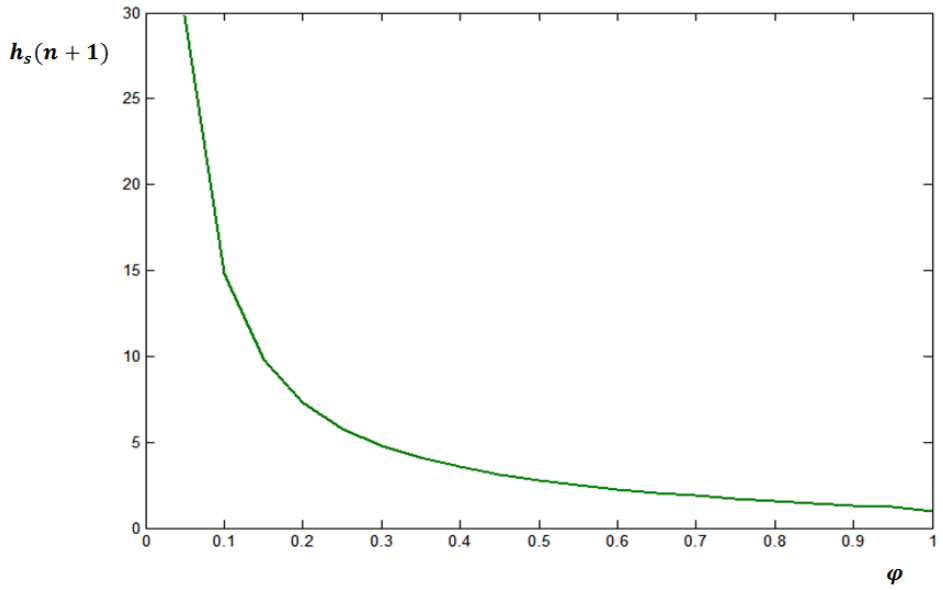

Figure 5.9: Variation of the super healing parameter as function of damage variable according to equation (5.80).

$$f_3(30) = \frac{-26100\varphi^3}{1-30\varphi} \tag{5.81}$$

If one supposes that the maximum value of equation (5.81) occurs at $\varphi = 0.05$ which gives $f_3(30) = 6.52$. Thus, the maximum difference between the linear and generalized nonlinear super healing is 6.52. Comparing Figure 5.7 with Figure 5.9, it is seen that both figures describe similar evolution of the super healing variable as function of damage variable. However, at damage variable $\varphi = 0.05$ the super healing variable in Figures 5.7 and 5.9 are 40 and 30, respectively. Therefore, one observes that the maximum super healing variables given by the difference function between linear and generalized nonlinear super healing models is greater than the maximum super healing variable given by the difference function between generalized nonlinear and quadratic super healing models.

5.12 Efficiency of super healing models

In this section one examines the efficiency of the three super healing models and shows which model is the most appropriate to describe the super healing mechanism. It was found in the previous section that at damage variable $\varphi = 0.05$ the super healing variables obtained for the difference functions $f_1(R)$ and $f_3(R)$ are 40 and 30, respectively. Then, one can observes that the maximum super healing variables obtained with the difference function $f_1(R)$ is greater than the maximum super healing variables obtained with the difference function $f_3(R)$. It should be noted that the difference function between the quadratic and linear super healing models ($f_2(R)$) is discarded because it gives values of super healing parameter less than 1, which is appropriate for the self-healing concept.

It was also found that at $\varphi = 0.05$ the difference function between the quadratic and generalized nonlinear super healing models ($f_3(R)$) and the difference between the linear and generalized nonlinear super healing models ($f_1(R)$) are 6.52 and 3.9 ($f_3(R) > f_1(R)$), respectively. This means that the difference function between linear and generalized nonlinear super healing models overestimates the super healing parameter.

Next one examines the difference functions $f_1(R)$ and $f_3(R)$ for the damage values φ from 0 to 1. The super healing variables obtained from the difference functions $f_1(R)$ and $f_3(R)$ which are presented in Figures 5.7 and 5.9 will be used. Therefore, one extracts the super healing variables from Figure 5.7 where $h_s(n+1) \in [0, 40]$ and substitutes these variables into equation (5.69), and extracts the super healing variables from Figure 5.9 where $h_s(n+1) \in [0, 30]$ and substitutes theses variables into equation (5.78). The variation of the difference functions as function of damage variable is shown in Figure 5.10.

It is seen from Figure 5.10 that at the maximum value of the damage variable $\varphi = 0.95$, the values of the difference functions $f_1(R)$ and $f_3(R)$ are 1.49 and 1.76, respectively. While when the damage variable $\varphi = 0.05$, the values of difference functions $f_1(R)$ and $f_3(R)$ are maximum and take the values 3.9 and 6.52, respectively.

It is also observed that as the damage variables increase the difference between the difference functions decreases. This difference is larger when the damage vari-

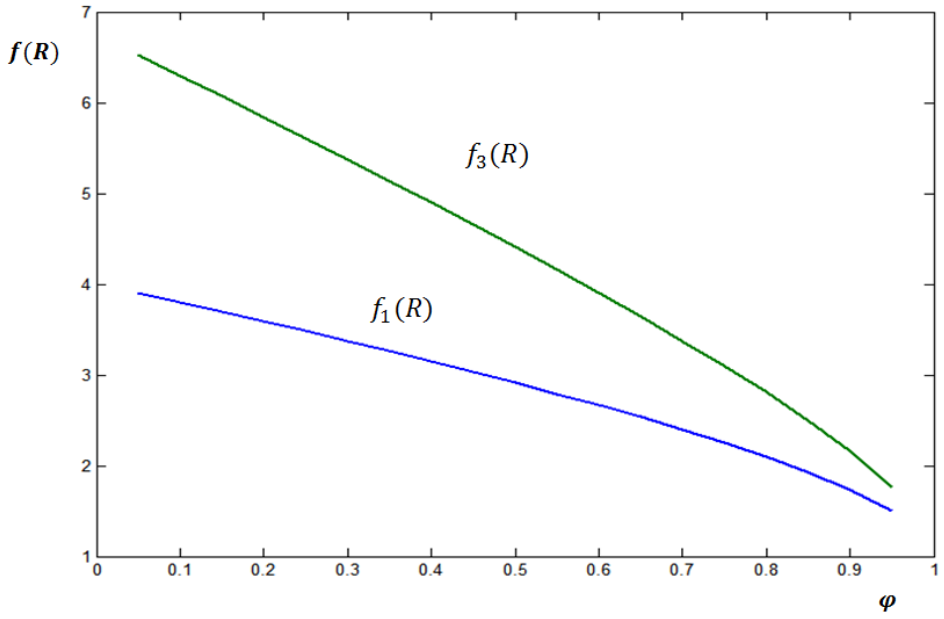

Figure 5.10: Variation of the difference functions $f_1(R)$ and $f_3(R)$ as function of damage.

ables equal to 0.05; where the super healing variables for $f_1(R)$ and $f_3(R)$ are 40 and 30, respectively. At this point the difference function between generalized nonlinear and quadratic super healing models is diverging from the difference function between generalized nonlinear and linear super healing models. One can say that the difference function between generalized nonlinear and linear super healing models seems more reasonable since it gives a small difference. This confirms that the generalized nonlinear super healing model is more appropriate to describe the nonlinear super healing. It is not the intention of the present section to characterize the material used for nonlinear super healing theory but only to point the way of the concept and the possible realization of the proposed theory.

From equation (5.69), one can extract the expression $\left(\varphi^3 R(1-R)\right)/(1-\varphi R)$ and substitute it into equation (5.76) of the difference function $f_3(R)$. Thus, one obtains the relationship between the difference functions $f_1(R)$ and $f_3(R)$ as follows:

$$f_3(R) = \varphi R f_1(R) \tag{5.82}$$

As it is written above in the section " Quadratic super healing " that the term $h_s(n+1)\varphi$ ($R\varphi$) represents the super healed damaged part. Therefore, one calls $R\varphi$ in equation (5.82) the super-healable damage parameter. In order to describe the variation of the super healing parameter R , the latter is extracted from equation (5.82) which gives the following expression:

$$R = \frac{f_3(R)}{\varphi f_1(R)} \tag{5.83}$$

Figure 5.11 shows the variation of the super healing parameter R as a function of the difference function between generalized nonlinear and linear super healing models. It is seen from the figure that as the difference function $f_1(R)$ increases the super healing variable decreases.

5.13 Undamageable materials

In this section, we combines the proposed refined theory of super healing with the theory of undamageable materials and writes the characteristics of the proposed refined theory of super healing. This framework of continuum damage mechanics

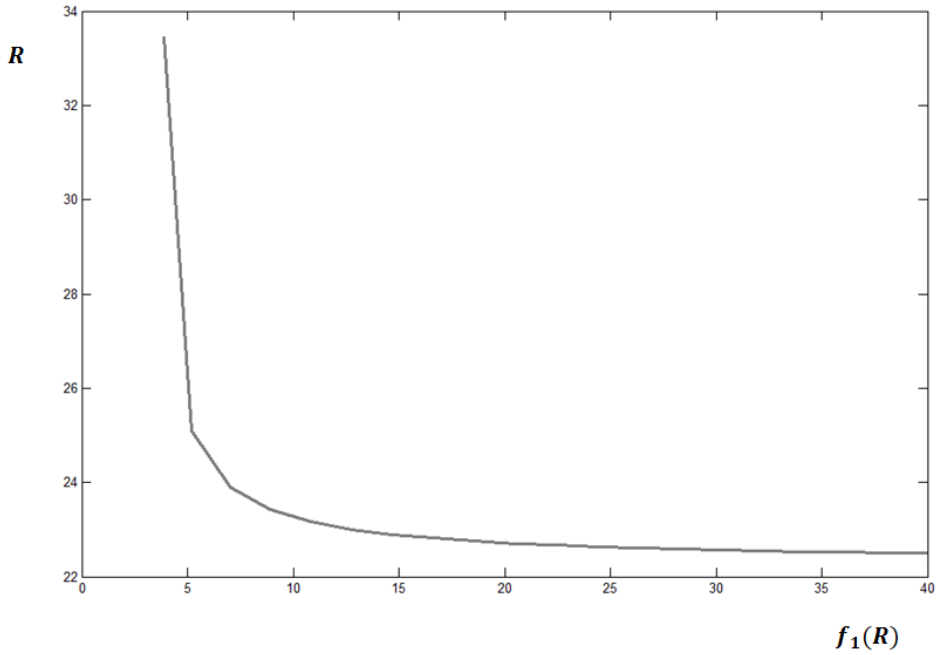

Figure 5.11: Variation of super healing parameter as function of difference function between generalized nonlinear and linear super healing models.

assumes that the material may undergo deformation while a zero state of damage is maintained [163]. According to the theory of undamageable materials and the proposed refined theory of super healing materials as presented in this study, the following expression of the combination of both theories is proposed:

$$\overline{\sigma} = \frac{\sigma}{1 + [h_s (n+1) - 1] \varphi^{1/k}} \tag{5.84}$$

where k is an integer that takes integer values from 1 to infinity. It is proposed that the parameter $1/k$ takes the following expression:

$$\frac{1}{k} = h_s (n+1) + 1 \tag{5.85}$$

It should be noted that equations (5.84) and (5.85) are proposed in order to satisfy the theory of undamageable materials and the proposed refined theory of super healing materials. Both theories lead to a material that is totally strengthened and that undergoes zero damage during the deformation process. The parameter $\varphi^{1/k}$ in equation (5.84) is called here the combined super-healed/zero damage variable. Substituting equation (5.85) into equation (5.84), one obtains the equation of the combined super-healing/undamageable theories:

$$\overline{\sigma} = \frac{\sigma}{1 + [h_s (n+1) - 1] \varphi^{(h_s(n+1)+1)}} \tag{5.86}$$

Before describing the features of equation (5.86), it should be noted that according to continuum damage-healing mechanics and the theory of super healing materials, the history of the variation of the state of the material passes through three phases which are shown in Table 5.2.

Now one shows that the proposed equation (5.86) reflects the three phases of the variation of the state of the material shown in Table 5.2. If one supposes that the material is fully damaged ($\varphi = 1$) without healing ($h_s = 0$), then one finds that the effective stress explodes and approaches infinity. On the other hand, if the material is fully healed ($h_s = 1$ and $n = 0$), equivalence between the effective stress and the nominal stress will be obtained. In the case of super healing materials ($h_s \geq 1$ and $n \geq 0$), one obtains two cases. These two cases are explained below with an example. Let us assume for example in the case of the multiple super healing mechanism that

Table 5.2: History of variation of the material state.

	Material state	Damage φ	Healing h	Super healing h_s	Effective stress
Phase 1	fully damaged material	1	0	0	$\overline{\sigma} \to \infty$
Phase 2	fully healed material	0	1	0	$\overline{\sigma} = \sigma$
Phase 3	super healed material	0	1	> 1	$\overline{\sigma} < \sigma$

$h_s = 1$ and $n = 5$. Applying equation (5.85), one obtains:

$$\overline{\sigma} = \frac{\sigma}{1 + 5\varphi^7} \tag{5.87}$$

It is observed from equation (5.87) that if the damaged material is represented by the maximum damage variable $\varphi = 1$, one obtains the exact solution of equation (5.1) in the case of the refined theory of super healing materials. This proves that the combined super-healing/undamageable material theories are equivalent in this case. On the other hand, if the damaged material is represented by the maximum damage variable $\varphi < 1$, one finds that the super-healed/zero damage variable φ^7 is minimized by the introduction of the parameter $1/k$. Therefore, if $1/k$ approaches infinity, the equivalence between the effective stress and the nominal stress ($\overline{\sigma} = \sigma$) will be obtained. It is also observed that if the parameter k approaches infinity, one obtains the exact solution of equation (5.1) and this solution is irrespective of the damage variable ($\varphi \leq 1$).

Based on the refined theory of super healing materials and its nonlinear formulation, the following characteristics of the proposed theory are extracted:

- Physically, the maximum damage variable φ does not always reach the value of 1 (e.g. 0.9). This is because material degradation depends on many parameters (e.g. loading type and rate, boundary conditions, material characteristics, . . ., etc). In this case, when super healing is imposed and the material is fully healed, the healing variable can take a value greater than the maximum damage variable. One can say that the refined theory of super healing is irrespective of the state of the damaged material.

- The proposed equation (5.1) can be used for two cases of super healing mechanisms:
  - Case 1: when the super healing is imposed with only one single value of the super healing variable h_s. In this case one sets $n = 0$ and h_s can take a single large value (e.g. 4, 5, 6, 7... and so on).
  - Case 2: when super healing is imposed with a resultant of super healing that represent multiple super healing variables operating at the same time. In this case, the parameter n is the number of super healing variables, and h_s takes the value of the multiple super healing variables.
- From equation (5.1), it can be seen that the effective stress approaches zero in three cases:
  - Case 1: when the value of super healing variable h_s approaches infinity.
  - Case 2: when the number of super healing variables n approaches infinity.
  - Case 3: when both h_s and n approach infinity.
- According to the combined super-healing/undamageable material theory defined in equation (5.86), when $\varphi < 1$ and $1/k$ approaches infinity one notes that the proposed theory is equivalent to the theory of undamageable materials.
- The super healing variable h_s is not restricted to only integer values. However, it can also take non-integer values.
- According to the nonlinear super healing theory, the generalized nonlinear super healing model is the most appropriate to describe the nonlinear super healing.
- The generalized nonlinear super healing model can be used in the cases of plane stress and plane strain.
- The linear, generalized nonlinear and quadratic super healing can all be used to describe the healing concept. In this case one sets $n = 0$ and $h_s\,(n+1) \in [0, 1]$.

5.14 Conclusion

Contribution to the design of new theory of strengthening of materials has been presented in the present chapter based on a new theory of super healing materials. In this concept, the healing process is continued beyond what is necessary to recover the original stiffness of the material. It is assumed that the same material used for self-healing can be used for super healing. The concept of the proposed theory of super healing has been presented for both cases of isotropic and anisotropic materials. Two examples were solved to elucidate the mechanism of the proposed theory of super healing. The first consists of the special cases of plane stress and plane strain. In these examples, it was shown that the anisotropic definition of the refined theory reduces to the proposed isotropic definition of the theory. In the second example, a one-dimensional damage-healing model has been applied in which the behavior of the refined super healing material was described. Difference between nonlinear and linear super healing theories was revealed and the efficiency of the different nonlinear super healing models was studied. It was found that the generalized nonlinear super healing model is the most appropriate to describe the super healing concept.

Chapter 6

Investigation of the super healing theory in continuum damage and healing mechanics

6.1 Introduction

In this chapter, the super healing theory is extended and defined based on the elastic stiffness variation. It concerns the degradation, recovery and strengthening of the elastic stiffness in the case of damage, healing and super healing materials, respectively. Comparison of the healing and super healing efficiencies between the hypotheses of the elastic strain and elastic energy equivalence is carried out.

6.2 Hypothesis of elastic strain equivalence

In this section, we compute the relations of the elastic modulus in the damaged (E_φ), healed (E_h), and super healed (E_{sh}) configurations with the effective configuration. In the case of the hypothesis of elastic strain equivalence, the strains in the damaged, healed, super healed and effective configurations are equal:

$$\varepsilon = \overline{\varepsilon} \tag{6.1}$$

$$\frac{\sigma}{E} = \frac{\overline{\sigma}}{\overline{E}} \tag{6.2}$$

where E is the elastic modulus that can represent the damaged, healed, and super healing configurations. The elastic modulus E is replaced with the damaged elastic modulus E_{φ}, and the effective stress is substituted from equation (3.2) into equation (6.2). This results in the following relation of the damaged elastic modulus and the effective elastic modulus:

$$E_{\varphi} = \overline{E}\,(1 - \varphi) \tag{6.3}$$

It is clear from equation (6.3) that the damaged elastic modulus becomes zero in the case of fully damaged material ($\varphi = 1$), and it equals to the effective modulus if no damage occurs ($\varphi = 0$). From equation (6.3), the damage variable can be written as follows:

$$\varphi = \frac{\overline{E} - E_{\varphi}}{E} \tag{6.4}$$

It can be observed from equation (6.4) that the damage variable φ becomes zero when the material is undamaged ($E_{\varphi} = \overline{E}$), and takes the maximum value $\varphi = 1$ when the material is totally damaged ($E_{\varphi} = 0$).

The elastic modulus E is replaced with the healed elastic modulus E_h , and the effective stress is substituted from equation (3.5) into equation (6.2). This results in the following relation of the healed elastic modulus and effective elastic modulus:

$$E_h = \overline{E}\,[1 - \varphi\,(1 - h)] \tag{6.5}$$

From equation (6.5), it can be observed that the healed elastic modulus equals to the effective elastic modulus if the material is fully healed ($h = 1$), and becomes equal to the damaged elastic stiffness in equation (6.3) if there is no healing ($h = 0$) . From equation (6.5), the healing variable can be written as follows:

$$h = 1 - \frac{\overline{E} - E_h}{\varphi E} \tag{6.6}$$

From equation (6.6), it can be seen that the healing variable takes its maximum

value $h = 1$ when the material is fully healed ($E_h = \overline{E}$), and it becomes zero when the material is unhealed ($E_h = 0$). It is observed that the healing variable defined in equation (6.6) represents the effect of the uncoupled self-healing mechanism [83, 164]. In this case, the material is loaded until it becomes damaged, and exposed to the healing during the rest period, and reloaded afterwards. In the uncoupled self-healing mechanism the damage and healing evolve separately.

Next, R is denotes the super healing parameter where $R = h_s\,(n+1)$, and the elastic modulus E is replaced with the super healed elastic modulus E_{sh} in equation (6.2). Substituting the effective stress from equation (5.1) into equation (6.2) results in the following relation of the super healed elastic modulus and effective elastic modulus:

$$E_{sh} = \overline{E}\,[1 + (R-1)\,\varphi] \tag{6.7}$$

It is clear from equation (6.7) that the super healed elastic modulus E_{sh} is greater than the effective elastic modulus $\overline{E}$ in the case of $R > 1$, while it becomes equal to the healed elastic modulus if the super healing variable is replaced with the healing variable ($R = h$). On the other hand, it becomes equal to the damaged elastic modulus if there is neither self-healing nor super healing effects ($R = h = 0$). From equation (6.7), the super healing variable can be written as follows:

$$R = \frac{E_{sh} - \overline{E}}{\varphi E} + 1 \tag{6.8}$$

It is assumed that the same material used for self-healing is used for super healing. When the super healing variable R takes a value greater than 1 the material is supposed to be super healed ($E_{sh} > \overline{E}$). On the other hand, equation (6.8) reduces to equation (6.6) when the material is exposed to only healing ($R = h$ & $E_{sh} = E_h$). The healing variable R in equation (6.8) represents both single and multiple super healing mechanisms. In the former case, one sets $n = 0$ and in the later case the parameter n should be greater or equal to one ($n \geq 1$).

6.3 Hypothesis of elastic energy equivalence

Applying the hypothesis of elastic energy equivalence, we will also compute the relations of the elastic modulus in the damaged (E_φ), healed (E_h), and super healed (E_{sh}) configurations with the effective configuration. In this case, the energies in the damaged, healed, super healed and effective configurations are equivalent:

$$\frac{1}{2E}\sigma^2 = \frac{1}{2\overline{E}}\overline{\sigma}^2 \tag{6.9}$$

Again, it should be noted that E can represent the elastic modulus of the damaged, healed, and super healing configurations. The elastic modulus E is replaced with the damaged, healed, and super healed elastic moduli and substituted, respectively, from equations (3.2), (3.5), and (5.1) into equation (6.9). The following relations of the damaged, healed and super healed elastic moduli are respectively obtained:

$$E_\varphi = \overline{E}\,(1-\varphi)^2 \tag{6.10}$$

$$E_h = \overline{E}\,[1-\varphi\,(1-h)]^2 \tag{6.11}$$

$$E_{sh} = \overline{E}\,[1+(R-1)\,\varphi]^2 \tag{6.12}$$

It should be noted that the upper and lower bounds of equations (6.10), (6.11), and (6.12) equal to the upper and lower bounds of equations (6.3), (6.5), and (6.7), respectively. It should be also noted that equation (6.12) of the super healing can represent the equation (6.11) of the self-healing when the material is subjected only to healing, and it can also represent equation (6.10) of the damage when the material is damaged and subjected neither to healing nor to super healing. When there is no damage and no healing ($\varphi = h = 0$) the super healed elastic modulus becomes equal to the initial elastic modulus ($E_{sh} = E_0$), and when the material is fully healed ($R = h = 1$), the super healed elastic modulus becomes equal to the effective elastic modulus ($E_{sh} = \overline{E}$). In addition, when the material is supper healed ($R > 1$), one obtains $E_{sh} > \overline{E}$. It should be noted that these upper and lower bounds

Table 6.1: Elastic modulus in the damaged, healed, and super healed material states using the hypotheses of elastic strain equivalence and elastic energy equivalence.

	Elastic strain equivalence		**Elastic energy equivalence**	
Phase	Elastic modulus	Variable	Elastic modulus	Variable
Damage	$E_\varphi = \bar{E}\,(1-\varphi)$	$\varphi = \frac{\bar{E}-E_d}{\bar{E}}$	$E_\varphi = \bar{E}\,(1-\varphi)^2$	$\varphi = 1-\sqrt{\frac{E_\varphi}{\bar{E}}}$
Healing	$E_h = \bar{E}\,[1-\varphi\,(1-h)]$	$h = 1-\frac{\bar{E}-E_h}{\varphi\bar{E}}$	$E_h = \bar{E}\,[1-\varphi\,(1-h)]^2$	$h = 1-\frac{\sqrt{\bar{E}}-\sqrt{E_h}}{\varphi\sqrt{\bar{E}}}$
Super healing	$E_{sh} = \bar{E}\,[1+(R-1)\,\varphi]$	$R = \frac{E_{sh}-\bar{E}}{\varphi\bar{E}}+1$	$E_{sh} = \bar{E}\,[1+(R-1)\,\varphi]^2$	$R = \frac{\sqrt{E_h}-\sqrt{\bar{E}}}{\varphi\sqrt{\bar{E}}}+1$

are consistent with the fundamental continuum damage-healing and super healing frameworks [22, 84, 142, 164].

Consequently, from equations (6.10), (6.11), and (6.12) the expressions of the damage, healing and super healing variables can be expressed respectively as follows:

$$\varphi = 1-\sqrt{\frac{E_\varphi}{\overline{E}}} \tag{6.13}$$

$$h = 1-\frac{\sqrt{\overline{E}}-\sqrt{E_h}}{\varphi\sqrt{\overline{E}}} \tag{6.14}$$

$$R = \frac{\sqrt{E_h}-\sqrt{E}}{\varphi\sqrt{\overline{E}}}+1 \tag{6.15}$$

The same assumption considered for equation (6.6) of the self-healing variable using the hypothesis of elastic strain equivalence is considered for equation (6.14) using the hypothesis of elastic energy equivalence. Equations (6.11) and (6.14) then represent, respectively, the healed elastic modulus and the healing variable in the uncoupled self-healing theory in which the healing variable evolves separately than the damage variable. Table 6.1 shows the summary of the elastic moduli and the damage, healing and super healing variables in both hypotheses of elastic strain equivalence and elastic energy equivalence.

Figure 6.1 shows the variation of the ratio of the damaged elastic stiffness over the effective elastic stiffness ($E_\varphi/\overline{E}$) in the case of the hypotheses of elastic strain

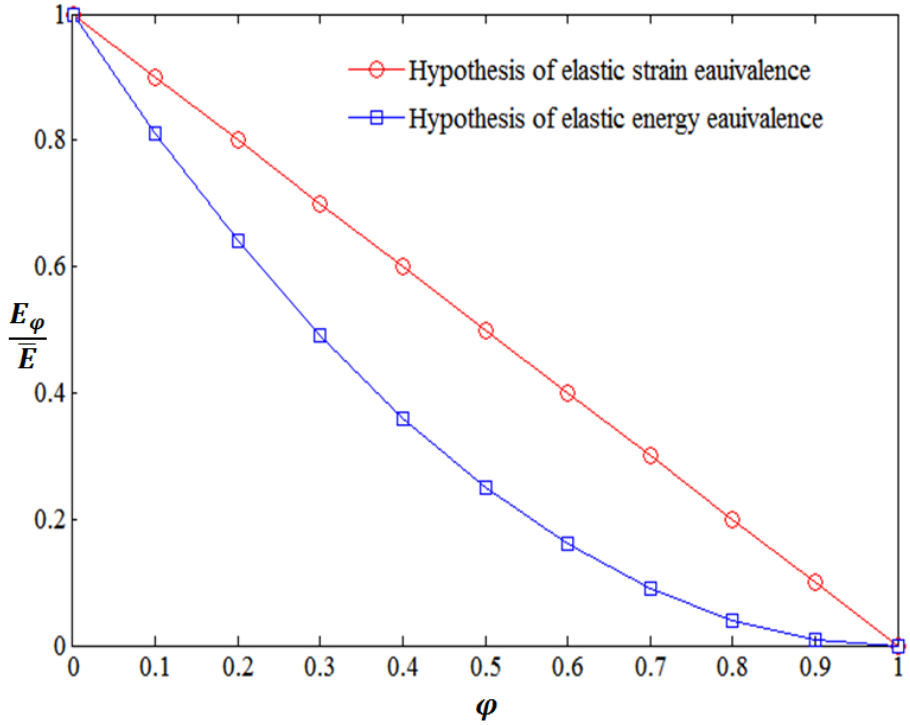

Figure 6.1: Degradation of the damaged elastic modulus as function of damage variable in both hypotheses of elastic strain equivalence and elastic energy equivalence.

equivalence and elastic energy equivalence. It is clear from Figure 6.1 that the damaged elastic stiffness equals to the effective elastic stiffness in both hypotheses when there is no damage ($\varphi = 0$), and it becomes zero when the material is totally damaged ($\varphi = 1$). It is also observed that the hypothesis of the elastic energy equivalence underestimates the elastic stiffness degradation in the interval $0 < \varphi < 1$ compared to the hypothesis of the elastic strain equivalence.

Figure 6.2 shows the variation of the ratio of the healed elastic modulus over the effective elastic modulus and the ratio of the super healed elastic modulus over the effective elastic modulus as a function of the healing and super healing variables. It should be noted that the variable R represents the healing effect in the interval [0, 1], while it represents the super healing variable in the interval [1, 4]. In the super healing domain, the plot of the curve represents the case of multiple super healing in which we take as an example $h_s = 1$ and $n = 3$, which leads to the maximum

super healing variable $R = 4$. From Figure 6.2, it can be observed in the healing domain that when there is no healing ($R = 0$) the healed elastic stiffness becomes zero in the case of the totally damaged material ($\varphi = 1$) and becomes equal to the damaged elastic stiffness in the case of the partially damaged material [$\varphi < 1$ & $E_{\varphi} = (1 - \varphi)\,\overline{E}$]. On the other hand, when there is complete healing the healed elastic stiffness becomes equal to the effective elastic stiffness. It is also shown that the hypothesis of the elastic energy equivalence underestimates the healing efficiency in the interval $0 < R < 1$ compared to the hypothesis of the elastic strain equivalence. These results of the healing efficiency corresponding to the hypotheses of equivalence are consistent with the results obtained in [118]. In the super healing domain, it is shown that the ratio $E_{sh}/\overline{E}$ increases with the increase of the super healing variable which reflects the strengthening of the elastic stiffness, and it is clearly observed that the hypothesis of the elastic energy equivalence overestimates the super healing efficiency compared with the hypothesis of the elastic strain equivalence.

6.4 Hypothesis of elastic strain equivalence applied to GNSH

In this section, a comparison of the elastic modulus strengthening in the GNSH theory between the hypotheses of elastic strain equivalence and elastic energy equivalence is performed. The elastic modulus E is replaced with the super healed elastic modulus E_{shns}, and the effective stress of the GNSH theory is substituted from equation (5.37) into equation (6.2) with replacing $h_s(n + 1)$ with R. This results in the following relation of the super healing elastic modulus and effective elastic modulus:

$$E_{shns} = \frac{\overline{E}\,(1 - \varphi)}{1 - R\varphi} \tag{6.16}$$

where E_{shns} is the generalized nonlinear super healed elastic modulus of the hypothesis of elastic strain equivalence. From equation (6.16), the super healing parameter can be written as follows:

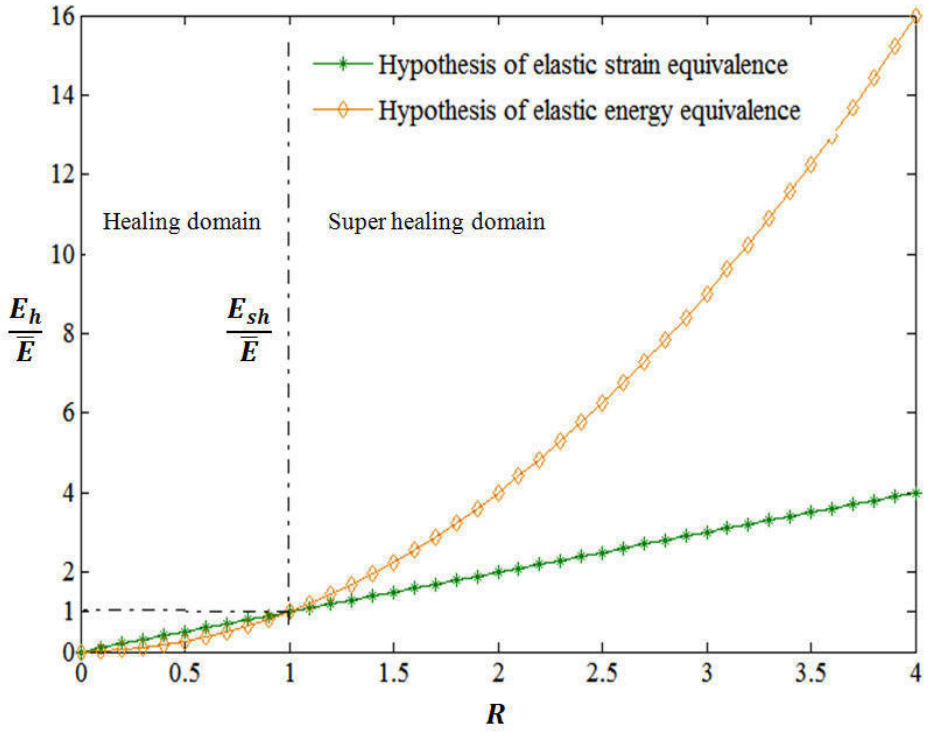

Figure 6.2: Healed and super healing elastic stiffness recovery and strengthening as a function of healing and super healing variables.

$$R = \frac{E_{shns} - \overline{E}\,(1-\varphi)}{\varphi E_{shns}} \tag{6.17}$$

According to the nonlinear super healing theory, it is assumed that only a part of the damaged area is subjected to super healing. Therefore, it is assumed that the damage variable in equation (6.16) is limited to the interval [0, 4]. From equation (6.16), it can be seen that the super healed elastic modulus becomes equal to equation (6.3) of the damaged elastic modulus when the material is damaged and unhealed ($R = h = 0$), while it becomes equal to the effective elastic modulus when the material is totally healed ($R = h = 1$). On the other hand, when the material is subjected to the super healing, it can be observed from the denominator of equation (6.16) that the super healing variable R cannot take any variable as for the linear super healing theory. Therefore, different limits of the super healing variables will be investigated in order to predict the limitation of the generalized nonlinear super healing theory based on the elastic stiffness strengthening. Figure 6.3 shows the evolution of the ratio $E_{shns}/\overline{E}$ with the interval limit of the super healing variable $R \in [0, 2]$ and with different damage variables ranging from 0.1 to 0.4. It should be noted that the parameter R represents the healing variable in the interval $R \in [0, 1]$, and it reflects the single super healing mechanism since its maximum value is limited to 2. It is clear from Figure 6.3 that the material is fully healed $\left(E_h = \overline{E}\right)$ when the super healing parameter R takes the value of 1. In the super healing domain, it is clear that the super healed elastic modulus is strengthened $\left(E_{shns} > \overline{E}\right)$, and the super healing efficiency increases when the damage variable increases, and the highest super healing efficiency is shown in the case of the damage variable $\varphi = 0.4$. This can be explained by the fact that damage provokes the healing and super healing in the material. The behavior of the single super healing mechanism can be found in the case of autonomous self-healing mechanism based on microcapsules (or hollow fibres). This is due to the fact that with each microcapsule only one single crack can be healed. When damage increases and reaches a certain critical value, the microcracks occur and break the microcapsules. Following that, the healing agent releases from the microcapsules, fills the microcracks, reacts with the catalyst and forms a solid material. Therefore, in order to obtain a high amount of broken microcapsules and high release of healing agent, and consequently, high healing and

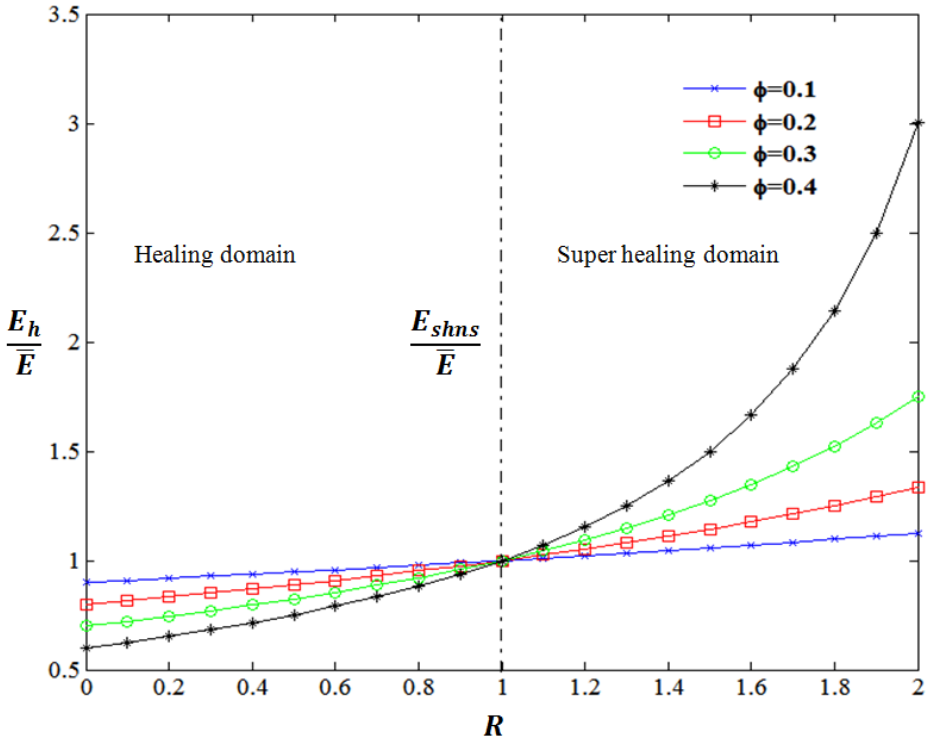

Figure 6.3: Healed and super healed elastic stiffness recovery and strengthening of GNSH using the hypothesis of elastic strain equivalence

super healing efficiency, certain amount of microcracks and damage are needed.

In order to evaluate the limit of the super healing parameter, we plot in Figure 6.4 the evolution of the super healed elastic modulus with the super healing limit value of 4 with different damage variables ranging from 0.1 to 0.4. It can be seen from Figure 6.4 that the super healed elastic stiffness strengthening is reasonable when the damage variable takes the values 0.1 and 0.2, while the ratio $E_{shns}/\overline{E}$ becomes negative with $\varphi = 0.3$ and $\varphi = 0.4$, which is unphysical behavior. In addition, the super healing efficiency can be reached with the maximum value of the super healing variable $R = 2$, while partially super healing efficiency is reached with the super healing parameters $R = 3$ and $R = 4$. It is concluded from Figure 6.4 that the super healing variable can only take a large value when the damaged area in the material is very small compared to the intact area. This can be explained by the fact that the generalized nonlinear super healing theory can only be efficient in the

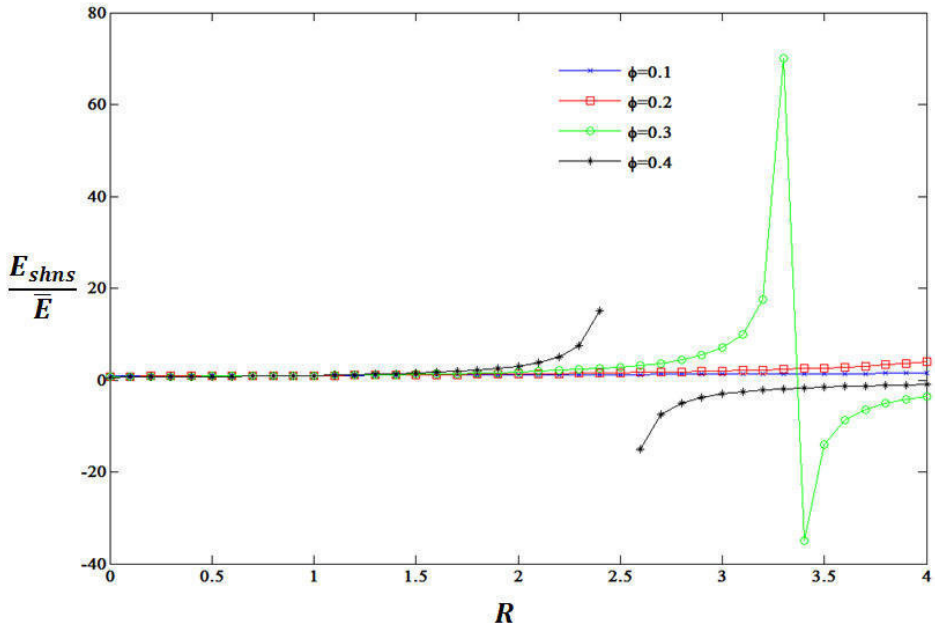

Figure 6.4: Super healed elastic stiffness strengthening of GNSH with the limit value of the super healing parameter $R = 4$ using the hypothesis of elastic strain equivalence.

case of the single super healing mechanism which is represented by the super healing variable $R = 2$ $(n = 1)$. On the other hand, the linear super healing theory can be applied in the case of single and multiple super healing mechanisms (see above Figure 6.2).

6.5 Hypothesis of elastic energy equivalence applied to GNSH

The super healed elastic stiffness strengthening is now generated using the hypothesis of elastic energy equivalence. The elastic modulus E is replaced with the super healed elastic modulus E_{shne}, and the effective stress of the GNSH theory is substituted from equation (5.37) into equation (6.9). This results in the following relation of the super healing elastic modulus and effective elastic modulus:

$$E_{shne} = \frac{\overline{E}\,(1-\varphi)^2}{(1-R\varphi)^2} \tag{6.18}$$

where E_{shne} is the generalized nonlinear super healed elastic modulus of the hypothesis of elastic energy equivalence. The super healing variable is this case can be written as follows:

$$R = \frac{\sqrt{E_{shne}} - \sqrt{\overline{E}}\,(1-\varphi)}{\varphi\sqrt{E_{shne}}} \tag{6.19}$$

From equation (6.18) of the super healed elastic modulus obtained using the hypothesis of elastic energy equivalent it can be observed that the upper and lower bounds of damage and healing mechanisms are satisfied. When the material is fully damaged ($R = 0$), the super healed elastic modulus reduces to $E_{shne} = E_{\varphi} = \overline{E}\,(1-\varphi)^2$, while when it is fully healed ($R = h = 1$ & $\varphi = 0$) the super healed elastic modulus reduces to $E_{shne} = E_h = \overline{E}$. Since it was concluded from Figures 6.3 and 6.4 that the generalized nonlinear super healing theory can only be efficient in the case of single super healing mechanism ($R = 2$), the comparison of the super healing efficiency between the hypotheses of elastic strain equivalence and elastic energy equivalence will be limited to the super healing variable ranging from 0 to 2. Figure 6.5 illustrates the ratio $E_{shne}/\overline{E}$ as function of the super healing variable R. It is clear from Figure 6.5 that the super healing efficiency increases with the increase of the damage variable. Comparing Figure 6.5 with Figure 6.3, it is observed that the hypothesis of elastic energy equivalence overestimates the super healing efficiency, which is consistent with the results of the linear super healing efficiency illustrated in Figure 6.2. Again, the results obtained using the hypothesis of elastic energy equivalence fit the results obtained in [118].

6.6 Hypothesis of elastic strain equivalence applied to QSH

Using equation (5.37) of the hypothesis of elastic strain equivalence, the elastic modulus E is replaced with the super healed elastic modulus E_{shqs}, and the effective stress of the QSH theory is substituted from equation (5.39) into equation (5.37)

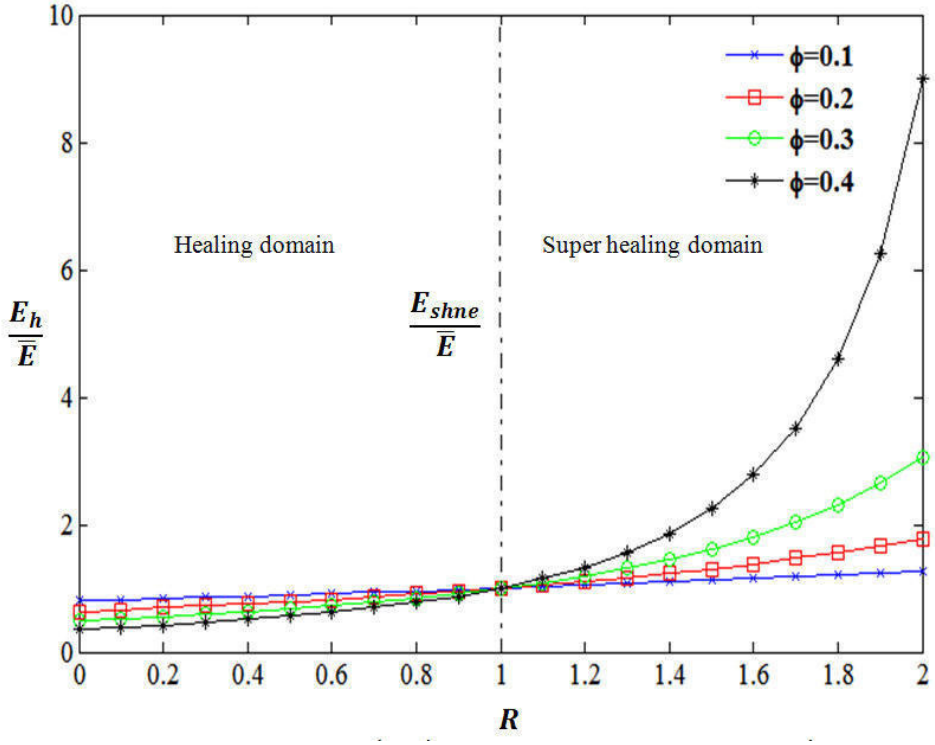

Figure 6.5: Healed and super healed elastic stiffness recovery and strengthening of GNSH using the hypothesis of elastic energy equivalence.

with replacing $h_s(n+1)$ with R. This results in the following relation of the super healed elastic modulus and effective elastic modulus:

$$E_{shqs} = \overline{E}(1 - \varphi + R\varphi - R\varphi^2 + R^2\varphi^2) \tag{6.20}$$

where E_{shqs} is the quadratic super healed elastic modulus of the hypothesis of elastic strain equivalence. From equation (6.20) and after simplification the expression of the super healing variable R as the solution of the second order equationis obtained as follows:

$$R = \frac{\varphi - 1 + \sqrt{\varphi^2 + 2\varphi + \frac{4E_{shqs}}{E} - 3}}{2\varphi} \tag{6.21}$$

It is clearly observed from equation (6.20) that when the material is unhealed ($R = h = 0$), the quadratic super healed elastic modulus becomes equal to the damaged elastic modulus [$E_{shqs} = E_\varphi = \overline{E}\,(1 - \varphi)$], while when the material is fully healed ($R = 1$), the quadratic super healed elastic modulus becomes equal to the effective elastic modulus ($E_{shqs} = \overline{E}$). Figure 6.6 shows the evolution of the ratio $E_h/\overline{E}$ and $E_{shqs}/\overline{E}$ as a function of the super healing parameter ranging from 0 to 2. As in the GNSH theory, it is shown in the QSH theory that the super healing efficiency increases with the increase of the damage variable. On the other hand, comparing Figure 6.6 with Figure 6.3 it can be seen that the GNSH theory overestimates the performance of the super healing efficiency in the case of the hypothesis of elastic strain equivalence. This conclusion fits the results obtained in Chapter 5.

6.7 Hypothesis of elastic energy equivalence applied to QSH

In this section, the quadratic super healing behavior is investigated using the hypothesis of the elastic energy equivalence. The elastic modulus E in equation (6.9) is replaced with the quadratic super healed elastic modulus E_{shqe}, and the effective stress of the QSH theory substituted from equation (5.39) into equation (6.9). This results in the following relation of the super healed elastic modulus and effective

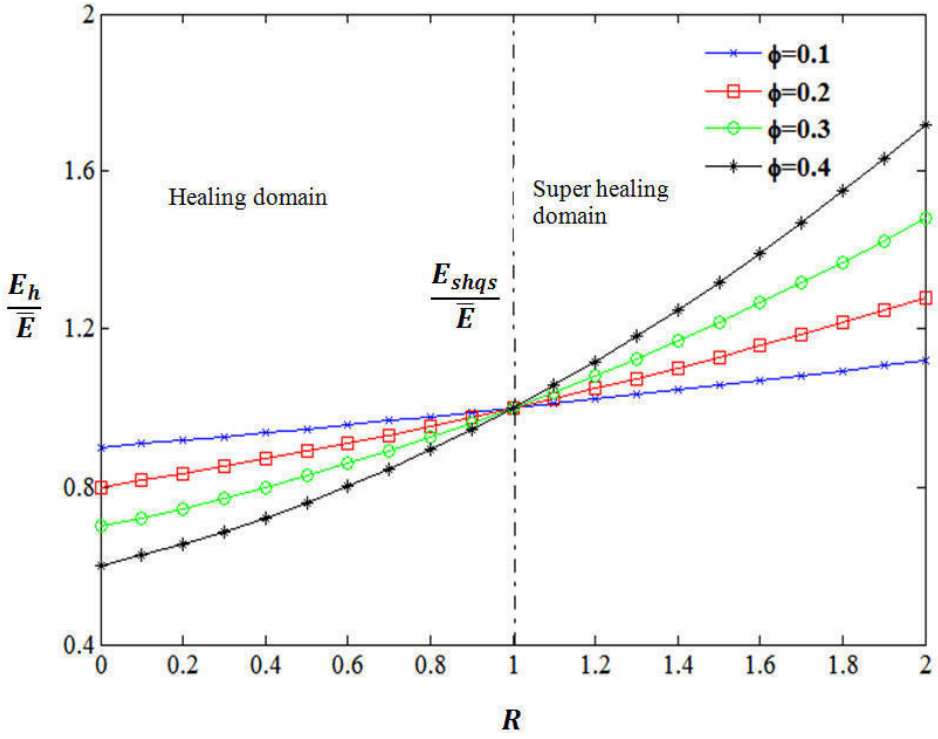

Figure 6.6: Healed and super healed elastic stiffness recovery and strengthening of QSH using the hypothesis of elastic strain equivalence.

elastic modulus:

$$E_{shqe} = \overline{E}(1 - \varphi + R\varphi - R\varphi^2 + R^2\varphi^2)^2 \tag{6.22}$$

where E_{shqe} is the quadratic super healed elastic modulus of the hypothesis of elastic energy equivalence. From equation (6.22) and after simplification the expression of the super healing variable R as the solution of the second order equation is obtained as follows:

$$R = \frac{\varphi - 1 + \sqrt{2\varphi + \varphi^2 + 4\sqrt{\frac{E_{shqs}}{E}} - 3}}{2\varphi} \tag{6.23}$$

Equation (6.22) satisfies the upper and lower bounds of the damage and self-healing. If the material is fully healed, the elastic modulus E_{shqe} reduces to $\overline{E}$, and if the material is damaged the elastic modulus E_{shqe} reduces to the damaged elastic modulus $[E_{shqe} = \overline{E}\,(1-\varphi)^2]$ in the case of the hypothesis of the elastic energy equivalence. The upper and lower bounds of the super healing are shown in Figure 6.7 in which the super healing parameter varies from 0 to 2. It is can observed from Figure 6.7 that the super healing efficiency increases with the increase of the damage variable. Comparing the quadratic super healing behavior between the elastic energy equivalence in Figure 6.7 and the elastic strain equivalence in Figure 6.6, it can be seen that the super healing efficiency is overestimated with the application of the hypothesis of the elastic energy equivalence. Moreover, comparing Figure 6.7 of the QSH theory with Figure 6.5 of the GNSH theory using the hypothesis of elastic energy equivalence, it is seen that the GNSH overestimates the super healing efficiency. It should be again noted that this conclusion of the GNSH efficiency is consistent with the results obtained in Chapter 5.

6.8 Conclusion

New investigation of the linear and nonlinear super healing theories has been presented in the present chapter. The behavior of the linear, generalized nonlinear, and quadratic super healing were analyzed based on the elastic stiffness recovery and strengthening. Comparison of the linear healing and super healing efficiencies

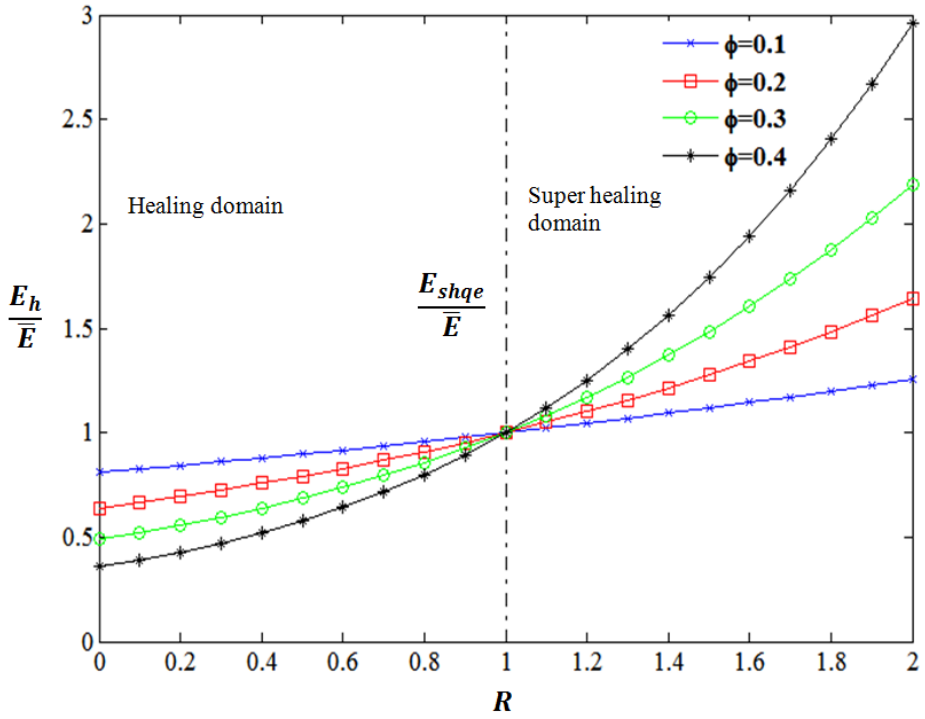

Figure 6.7: Healed and super healed elastic stiffness recovery and strengthening of QSH with the super healing parameter interval $R \in [0, 2]$ using the hypothesis of elastic energy equivalence.

based on the hypotheses of the elastic strain equivalence and elastic energy equivalence were carried out. The results revealed that the hypothesis of elastic energy equivalence overestimates the super healed elastic stiffness strengthening of both generalized nonlinear and quadratic super healing theories. In addition, the generalized nonlinear super healing theory gives high strengthening of the super healed elastic stiffness compared with the quadratic super healing theory in both transformation hypotheses.

Chapter 7

Ballistic behavior of plain and reinforced concrete slabs under high velocity impact

7.1 Introduction

This chapter presents the numerical simulation of ballistic penetration and high velocity impact behavior of plain and reinforced concrete slabs. We focus on the comparison of the performance of plain and reinforced concrete slabs of unconfined compressive strength 41 MPa under ballistic impact. The concrete slab has dimensions of 675 mm x 675 mm x 200 mm, and is meshed with 8-node hexahedron solid elements in the impact and outer zones. The ogive-nosed projectile is considered as rigid element that has a mass of 0.386 kg and a length of 152 mm. The applied velocities vary between 540 and 731 m/s. 6 mm of steel reinforcement bars are used in the reinforced concrete slabs. The constitutive material modeling of the concrete and steel reinforcement bars is performed using the Johnson-Holmquist-2 damage and the Johnson-Cook plasticity material models, respectively. The analysis is conducted using the commercial finite element package Abaqus/Explicit. Damage diameters and residual velocities obtained by the numerical model are compared with the experimental results and effect of steel reinforcement and projectile diameter are studied.

7.2 Material models

The concrete material is simulated using the Johnson-Holmquist damage model (JH-2). The JH-2 is the second version of the Johnson-Holmquist (JH-1) ceramic model [165], that is able to simulate the impact behavior of brittle materials such as dilatation, pressure-strength dependence, strain-rate effect resulted by damage [165]. According to the JH-2 model, the yield strength degrades with damage accumulation whereas in the JH-1 model the yield strength degrades when critical damage is reached. The strength is defined in terms of the equivalent stress as follows:

$$\sigma^* = \sigma_i^* - D\left(\sigma_i^* - \sigma_f^*\right) \tag{7.1}$$

where σ_i^* is the normalized intact equivalent stress, D is the damage variable, and σ_f^* is the normalized fractured equivalent stress. It is important to point out that the intact and fully damaged materials are represented by the damage values D=0 and D=1, respectively. The normalization of the term in equation (7.1) to the equivalent stress at the Hugoniot Elastic Limit (HEL) can also be used to define the equations of the strength, which will correspond to the one-dimensional shock wave that exceeds the elastic limit as defines in equation (7.2), and the normalized equation as presents equation (7.3) :

$$\sigma_{HEL} = \frac{3}{2}\left(HEL - P_{HEL}\right) \tag{7.2}$$

$$\sigma^* = \frac{\sigma}{\sigma_{HEL}} \tag{7.3}$$

where P_{HEL} is the pressure at the Hugoniot Elastic Limit. According to the JH-2 model, the equation of the strength in the case of undamaged and fully damaged material states is assumed to be, respectively, written as function of pressure and strain rate as follows:

$$\sigma_i^* = A\left(P^* + T^*\right)^N \left(1 + Cln\varepsilon^*\right) \leq \sigma_i^{max} \tag{7.4}$$

$$\sigma_f^* = B\left(P^*\right)^M \left(1 + Cln\varepsilon^*\right) \leq \sigma_f^{max} \tag{7.5}$$

where A, B, C, M and N are the material parameters. σ_i^{max} and σ_f^{max} are the strengths limits. The normalized pressure is defined as

$$P^* = \frac{P}{P_{HEL}} \tag{7.6}$$

where P is the actual pressure. The normalized maximum tensile hydrostatic pressure is also written as

$$T^* = \frac{T}{T_{HEL}} \tag{7.7}$$

where T is the maximum tensile pressure supported by the material and T_{HEL} is the tensile pressure at the Hugoniot Elastic Limit. The strain rate is defined as $\dot{\varepsilon}^{pl} = \dot{\varepsilon}^{pl}/\dot{\varepsilon}_0$ and $\dot{\varepsilon}^{pl}$ is the equivalent plastic strain rate. Damage accumulation is used in JH-2 model similarly to the Johnson-Cook model in addition to the assumption that damage increases along with the plastic strain as follows:

$$D = \sum \frac{\Delta \overline{\epsilon}^{pl}}{\overline{\epsilon}_f^{pl}\left(P\right)} \tag{7.8}$$

$$\overline{\epsilon}^{pl} = D_1 \left(P^* + T^*\right)^{D_2} ; \overline{\epsilon}_{f,min}^{pl} \leq \overline{\epsilon}^{pl} \leq \overline{\epsilon}_{f,max}^{pl} \tag{7.9}$$

It is important to point out that $\Delta \overline{\epsilon}^{pl}$ is the increment of the equivalent plastic strain, and $\overline{\epsilon}_f^{pl}\left(P\right)$ is the equivalent plastic strain at failure. D_1 and D_2 are material constants. In order to limit the minimum and maximum values of the fracture strain, the parameters $\overline{\epsilon}_{f,min}^{pl}$ and $\overline{\epsilon}_{f,max}^{pl}$ are introduced. The pressure-volume relationship of the brittle materials is defined as

$$P = \begin{cases} K_1\mu + K_2\mu^2 + K_3\mu^3 & if \mu \geq 0 \, (compression) \\ K_1\mu & if \mu < 0 \, (tension) \end{cases} \tag{7.10}$$

where K_1, K_2, K_3 are material constants, and $\mu = \rho/\rho_0 - 1$ with ρ and ρ_0 representing the current and reference densities, respectively. An additional pressure increment ΔP in the case of material failure, which is expressed as

$$P = K_1\mu + K_2\mu^2 + K_3\mu^3 + \Delta P \tag{7.11}$$

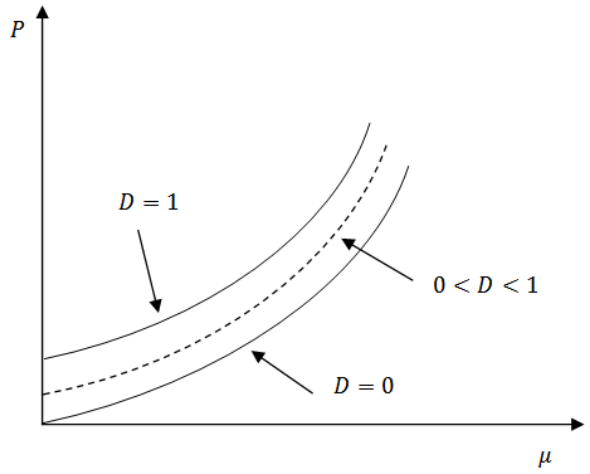

Figure 7.1: Pressure-volumetric strain relationship of the JH-2 model.

The pressure increment is determined based on the energy consideration. Due to the decrease in strength the deviatoric elastic energy ΔU decreases in the case of damaged material. Figure 7.1 shows the relationship pressure-volumetric strain according to the JH-2 model.

The decrease of the elastic energy is converted into the potential energy by the increase of the pressure increment ΔP, such that

$$\Delta P_{t+\Delta t} = -K_1 \mu_{t+\Delta t} + \sqrt{\left(K_1 \mu_{t+\Delta t} + \Delta P_t\right)^2 + 2\beta K_1 \Delta U} \tag{7.12}$$

where β is the fraction of the elastic energy increase converted to potential energy ($0 \leq \beta \leq 1$).

In the present work, the parameters of the JH-2 model based on HEL are calculated, while the parameters based on equation of state, strength and damage are taken from the literature. The Hugoniot elastic limit HEL for brittle materials is calculated using the following equation [166]:

$$HEL = \frac{1-\upsilon}{(1-\upsilon)^2} f_c \tag{7.13}$$

where υ is the Poisson's ratio and f_c is the compressive strength. Afterward, the pressure at HEL is calculated using the following expression:

Table 7.1: Material parameters of the concrete material.

ρ (kg/m^3)	G (GPa)	υ	A	B	n	C
2440	14.86	0.15	0.3	2	0,75	0.007
m	$\dot{\varepsilon}_0$	S_{max}	T (GPa)	$\bar{\varepsilon}^{pl}_{f,min}$	$\bar{\varepsilon}^{pl}_{f,max}$	P_{HEL} (MPa)
0.61	1	7	0.004	0.001	1	33.43
D_1	D_2	K_1 (GPa)	K_2 (GPa)	K_3 (GPa)	HEL (MPa)	f_c
0.04	1	17.12	-171	208	71.12	41

$$P_{HEL} = HEL\left(1 - \frac{4G}{3k + 4G}\right) \tag{7.14}$$

where G and K are the shear and bulk moduli, respectively. The parameters related to the strength, damage, and equation of state are taken from [165, 167]. Table 7.1 illustrates the material parameters of the JH-2 model for unconfined compressive strength concrete 41 MPa.

The steel reinforcement are simulated in the present work using the Johnson-Cook plasticity model (J-C) that is capable to simulate the strain hardening, softening, plastic flow, yielding of metals [168]. According to the Johnson-Cook model the Von Mises stress is expressed as a function of the equivalent strain $\bar{\varepsilon}^{pl}$, equivalent plastic strain rate $\dot{\varepsilon}^{pl}$, and temperature T as follows:

$$\overline{\sigma} = \left(A + B\left(\bar{\varepsilon}^{pl}\right)^n\right)\left[1 + Cln\left(\dot{\varepsilon}^{pl}/\dot{\varepsilon}^{pl}_0\right)\right](1 - T^{*m}) \tag{7.15}$$

where A, B, C and M are constants; $\dot{\varepsilon}^{pl}/\dot{\varepsilon}^{pl}_0$ and T^* are the normalized equivalent plastic strain rate and the temperature, respectively. The temperature T^* is expressed as follows:

$$T^* = (T - T_r)\,/\,(T_{melt} - T_r) \tag{7.16}$$

where T is the current temperature, T_{melt} is the melting temperature and T_r is the

Table 7.2: Material parameters of the steel reinforcement [11].

ρ (kg/m^3)	υ	A	B	n	m	Melting temperature (Kelvin)
$2x10^{11}$	0.33	490	807	0.73	0.94	1800
Transition temperature (Kelvin)	d_1	d_2	d_3	d_4	d_5	Strain rate (S^{-1})
293	0.0705	1.732	-0.54	-0.015	0	0.0005

room temperature. The expression of the fracture according to the Johnson-Cook model is defined in terms of the equivalent failure strain as follows:

$$\bar{\varepsilon}_D^{pl} = \left[d_1 + d_2 ex\left(-d_3\eta\right)\right]\left[1 + d_4 ln\left(\dot{\varepsilon}_0^{pl}/\varepsilon_0^{pl}\right)\right]\left(1 + d_5 T^*\right) \tag{7.17}$$

where $\eta = -p/\bar{\sigma}$ is the stress triaxiality, p is the pressure and d_1, d_2, d_3, d_4, d_5 are constants. According to the J-C model, the damage is assumed to accur when the damage variable D reaches its limit value of 1.0. The Johnson-Cook material parameters for steel reinforcement used in the present work are presented in Table 7.2 [11].

7.3 Numerical simulation of RC targets

The Johnson-Holmquist-2 and Johnson-Cook material models are applied on the penetration experiment of reinforced concrete by Wu et al. [169] and incorporated into the commercial finite element package Abaqus/Explicit. The numerical models consists of the study of the impact behavior of reinforced concrete slabs of dimensions 675 mm x 675 mm x 200 mm simulated as three dimensional deformable solid penetrated with an ogive-nosed steel projectile of 152 mm of length, 25.3 mm of diameter, and 3.00 of the caliber-radius-head (CRH) ratio (Figure 7.2). The pro-

jectile is simulated as rigid element with 0.386 kg of mass assigned at a reference point with striking velocities ranging from 540 to 731 m/s. The steel reinforcements are simulated as truss elements of diameter 6 mm and embedded into the concrete solid body. The embedded truss elements to the concrete makes the nodes of the steel bars kinematically constrained to the nodes of the concrete solid body. The distribution of the steel reinforcement bars is illustrated in Figure 7.3. General contact surface with nodal erosion between the projectile and the RC concrete slab is considered. Using nodal erosion, the nodes of the element based surfaces are removed from the contact domain once the contact faces are eroded. All the edges of the concrete slab are fixed in all directions in terms of translation and rotation. In addition, the reference point of the hard projectile is fixed in all directions in terms of translation and rotation expect the translation in the impact direction. A circular partition of 20 mm was created at the impact location in order to refine the mesh. Three dimensional eight node reduced integration (C3D8R) element was adopted for all the regions with 1 mm x 1 mm x 1 mm of mesh at the impact location and 3.5 mm x 3.5 mm x 3.5 mm of mesh at the rest of the sample. A mesh convergence study of element sizes of 0.8 mm, 0.9 mm, 1 mm, 1.5 mm and 2 mm for the RC slab at the impact location subjected to the projectile penetration at the striking velocity of 641 m/s is performed. The residual velocity of the projectile with different mesh sizes is compared as shown in Figure 7.4. It is found that the residual velocity increases with the decrease of the element size. When the mesh size increases from 0.9 mm to 1 mm, the residual velocity decreases from 441.31 m/s to 439.36 m/s indicating a slight difference of 0.44 %. Thus, it is believed that using the mesh size of 1 mm provides reasonable results in the numerical simulation with less computational time. Two node three dimensional truss elements (T3D2) with mesh size of 2 mm were considered for the vertical, horizontal and transverse steel reinforcements, and four node three dimensional bilinear rigid quadrilateral (R3D4) meshes with size of 2 mm were considered for the projectile. Figure 7.5 illustrates the finite element meshing of the reinforced concrete slab. The mesh of the concrete slab was generated in the aim to obtain accurate results with less time consuming of the finite element analysis.

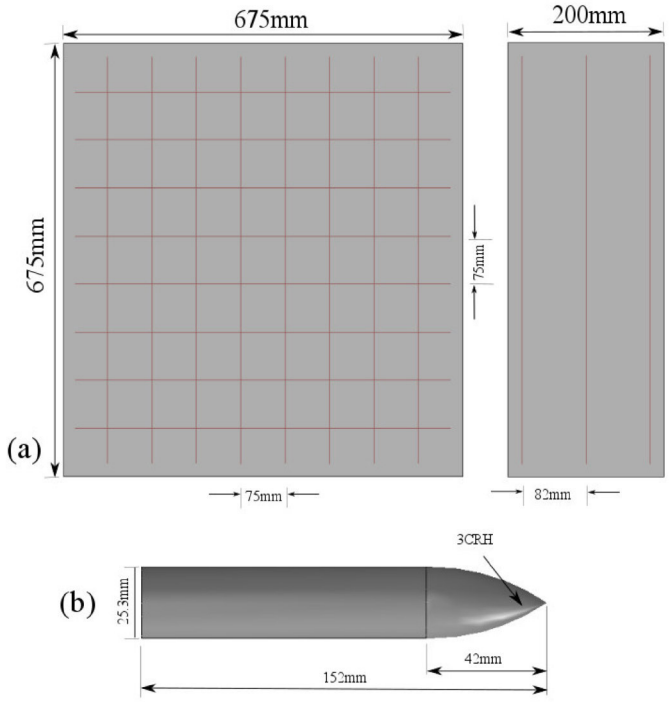

Figure 7.2: (a) Reinforced concrete slab and (b) projectile geometries.

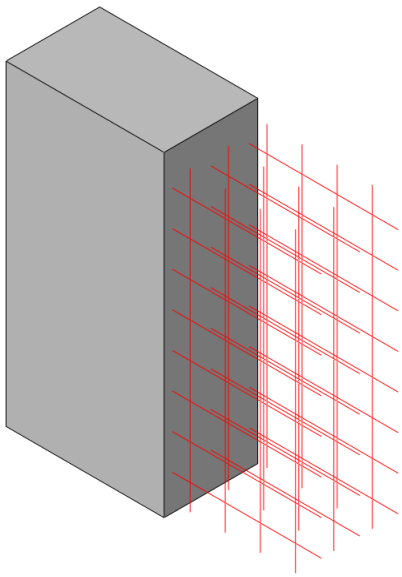

Figure 7.3: FE model of steel reinforcement configuration.

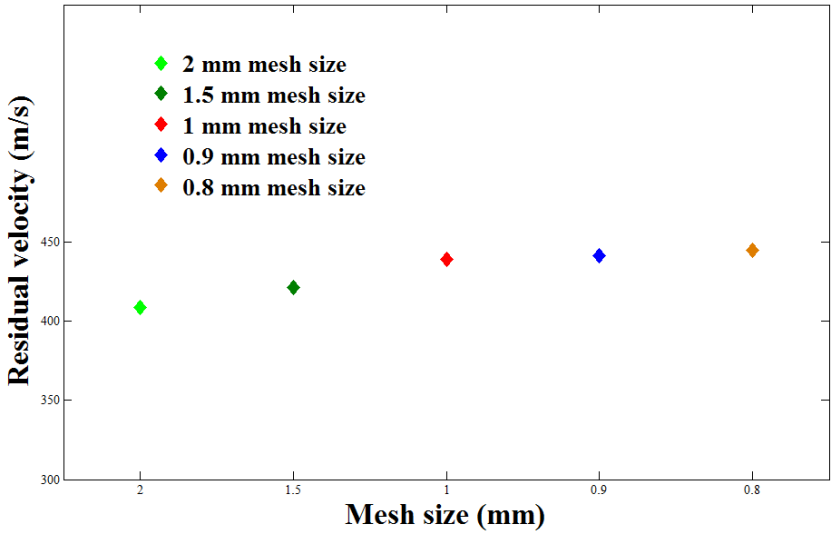

Figure 7.4: Mesh convergence study with various mesh sizes.

7.4 Model validation

The JH-2 model for concrete and Johnson-Cook model for steel reinforcement are incorporated into Abaqus/Explicit. The penetration experiment of reinforced concrete slabs by Wu et al. [169] was simulated. In this section, the comparison of the cratering and scabbing damages of the reinforced concrete slabs and the residual velocity of the projectile is performed. The dimensions of the diameters of front and back craters formed in the RC slabs due to the penetration of the hard projectile are calculated. The equivalent damage diameter D_m at the front and back of craters is calculated as $(D_m = (D_1 + D_2 + D_3 + D_4)/4)$ in which D_1, D_2, D_3 and D_4 are shown in Figure 7.6. Figure 7.7 shows the comparison of the numerical and experimental cratering and scabbing damages of the reinforced concrete slab subjected to the impact velocity 640 m/s. The equivalent diameters at the front face in the experimental and numerical studies are found to be 275 mm and 277 mm, respectively, while they are, respectively, 242.5 mm and 286 mm at the back face. Differences of 0.72% and 15% at the front and back faces are respectively obtained. In the whole, it can be observed that the damages at the front and back faces predicted numerically are in good agreement with the experimental results.

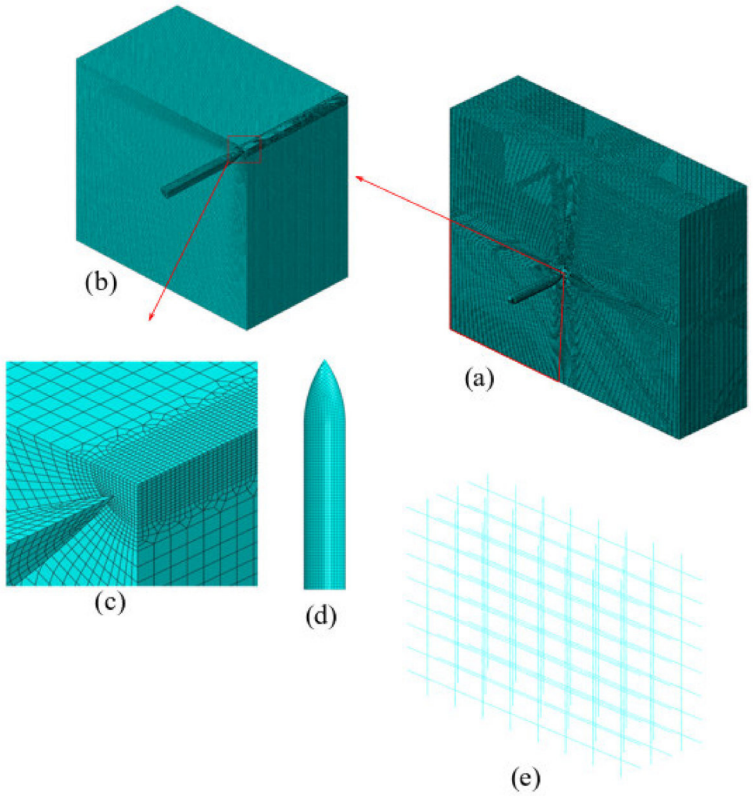

Figure 7.5: E meshing of (a) total geometry, (b) quarter of geometry, (c) impact location details, (d) projectile and (e) steel reinforcement.

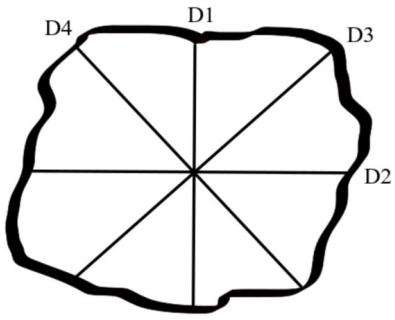

Figure 7.6: Calculation of equivalent diameter of front and back craters.

Figure 7.8 shows the predicted residual velocity compared with the experimental residual velocity corresponding to the impact velocities 540 m/s, 597 m/s, 641 m/s and 731 m/s. It can be seen that the numerical model reproduces well the residual velocity comparing to the experimental results.

7.5 Effect of steel reinforcement

In this section, the effect of steel reinforcement on the impact resistance and cratering damage is analyzed. The cratering damage and residual velocity of plain, reinforced, and additionally reinforced concrete slabs are compared under the striking velocities 540 m/s, 597 m/s, 641 m/s and 731 m/s. The equivalent damage diameter (d_m) is calculated at the front and back surfaces as the average diameter values (d_1, d_2, d_3 and d_4) as shown above in Figure 7.6. Different configurations of the longitudinal steel reinforcement are tested in addition to a sample with transverse steel reinforcements. The steel reinforcements are located at the front and back surfaces of the slabs. The diameter used for all the longitudinal and transverse steel reinforcements is 6 mm. Six concrete samples were simulated under different striking velocities. The first sample represents the plain concrete without steel reinforcement (PCS). The second, third, fourth and fifth samples represent the reinforced concrete samples with different configurations of longitudinal steel reinforcement which are illustrated, respectively, in Figures 7.2(a) (NRCS), 7.9(a) (RCS1), 7.9(b) (RCS2) and 7.9(c) (RCS3). The sixth sample contains transverse steel reinforcement bars

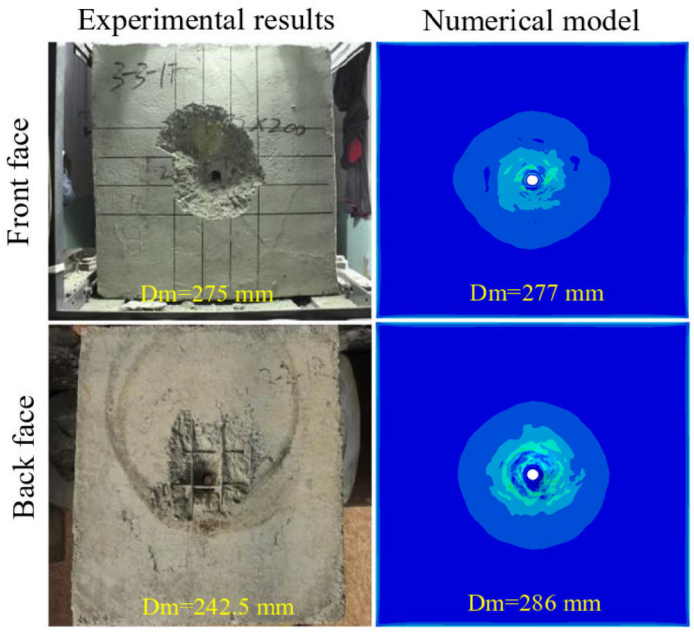

Figure 7.7: Experimental and numerical comparison of front and back damages at impact velocity of 641 m/s.

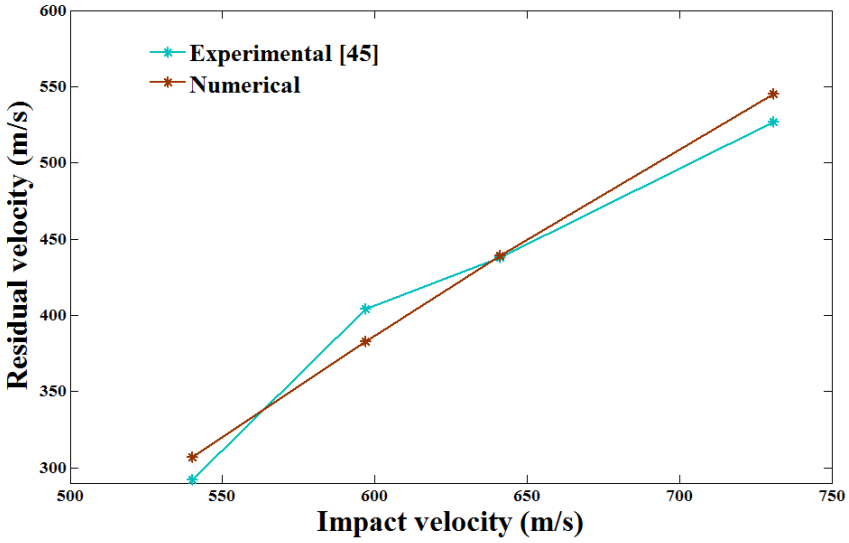

Figure 7.8: Comparison of numerical and experimental residual velocities.

in addition to the normal reinforced concrete sample of Figure 7.2(a) as shown in Figure 7.9(d) (SRCS). In the sample NRCS the spacing mesh of the steel bars is 75 mm, while in the rest of the samples the spacing mesh is 37.5 mm. The minimum mesh spacing was resepcted such that the projectile diamteer is less than the mesh spacing between the steel bars in the impact zone. It should be noted that the mechanical properties of concrete and steel reinforcement are the same presented above in Tables 7.1 and 7.2. The residual velocity, cratering and scabbing damages of each concrete sample are shown in Table 7.3 and Figure 7.10.

From Table 7.3, it is observed that there is negligible difference in the ballistic resistance between the samples CPS and NRCS. However, the ballistic resistance of the samples NRCS, RCS1, RCS2, RCS3 and SRCS are higher comparing to the ballistic resistance of the plain concrete sample PCS. The maximum difference of ballistic resistance of the normal reinforced concrete sample NRCS comparing to PCS is found to be 2.5%, while the maximum difference in the ballistic resistance of all the reinforced concrete samples comparing to PCS is found in the case od RCS2 with 5.18% corresponding to the striking velocity 540 m/s. On the other hand, the normal reinforced concrete sample exhibits the maximum difference in the ballistic resistance with the striking velocities 597 m/s, 641 m/s and 731 m/s comparing to the sample PCS. It is also observed that the transverse steel reinforcements affect slightly the ballistic resistance when added to the normal reinforced concrete sample. It is also seen that for all the concrete samples the ballistic resistance increases with the decrease of the impact velocity. From Table 7.3, it is also observed that the equivalent damage diameter in the front and back surfaces of the reinforced concrete samples is lower than the equivalent damage diameter of plain concrete sample. On the other hand, the equivalent damage diameter is found to decrease with the increase of the impact velocity. One can conclude that the ballistic resistance is mostly affected by the spacing mesh of steel reinforcement bars than the amount of steel reinforcement. Therefore, appropriate distribution of reinforcement is needed to reach a high ballistic resistance of steel reinforced concrete slabs. On the other hand, it can also be concluded that at high striking velocities the amount of steel reinforcement can also be efficient to improve the ballistic resistance of concrete slabs.

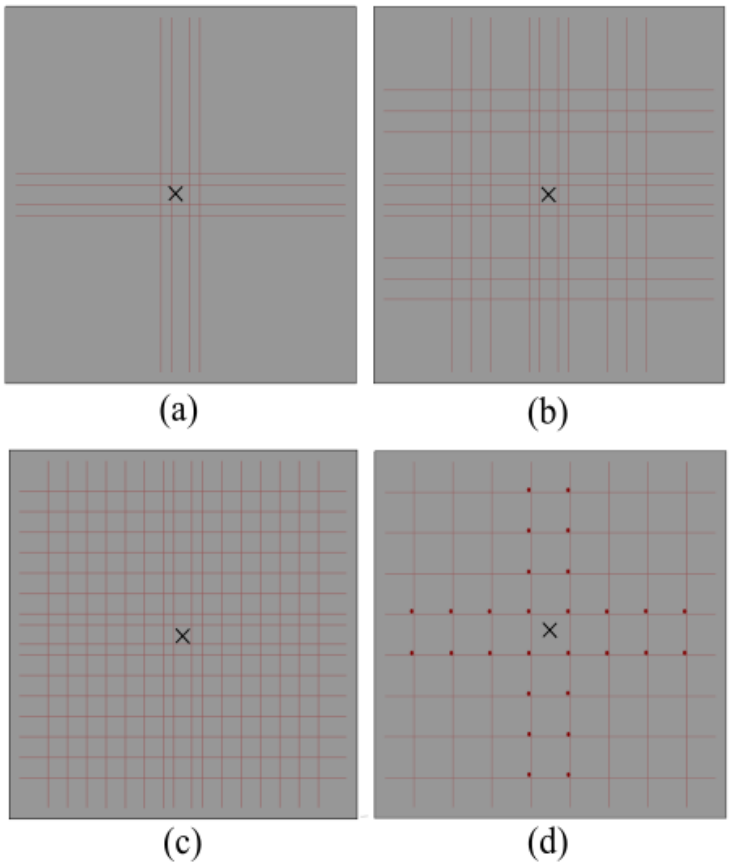

Figure 7.9: Configurations of longitudinal and transverse reinforcement steels.

Table 7.3: Residual velocity and equivalent damage diameter of plain, reinforced and additionally reinforced concrete samples.

Velocity		Front surface					Back surface				
V_0 (m/s)	V_r (m/s)	d_1 (mm)	d_2 (mm)	d_3 (mm)	d_4 (mm)	d_m (mm)	d_1 (mm)	d_2 (mm)	d_3 (mm)	d_4 (mm)	d_m (mm)
PCS											
540	308.71	287.57	298.16	280.07	285.40	287.8	321.96	337.23	327.81	332.16	329.79
597	382.49	305.18	304.32	280.54	284.23	293.57	314.06	313.22	309.31	320.73	314.33
641	439.15	301.66	312.22	295.64	299.03	302.14	323.87	318.45	324.51	313.63	320.12
731	547.86	302.56	302.59	308.85	315.59	307.4	343.16	334.49	334	327	334.66
NRCS											
540	307.24	284.8	281.4	235.5	238.2	259.98	318.4	306.97	278.93	278.75	295.76
597	383.10	292.82	296.36	238.63	232.94	265.18	305.17	289.29	285	300.43	294.97
641	439.36	299.95	301.71	246.89	244.04	273.15	298.14	295.76	276.25	270.19	285.09
731	545.90	304.32	302.54	225	238.35	267.55	293.7	287.57	274.82	289.95	286.51
RCS1											
540	293.5	246.34	248.85	232.96	231.15	239.83	284.04	305.34	287.13	280.05	289.14
597	375.21	262.97	262.92	239.89	221.9	246.92	288.37	302.64	298.19	308.24	299.36
641	430.36	277	269.96	267.97	265.35	270.07	295.51	290.21	300.43	302.85	297.25
731	537.94	277	280.53	277.10	286.72	280.34	320.4	305.18	302.85	297.48	306.48
RCS2											
540	293.5	246.34	245.31	233.6	224.62	237.46	284.96	301.66	284.95	294.79	291.59
597	375.21	2262.96	260.37	238.36	219.31	242.75	285.74	297.22	303.22	303.91	297.52
641	430.36	273.48	269.94	238.45	262.47	261.08	295.51	288.52	291.14	292.81	291.99
731	537.94	277	277	276.68	281.37	278.01	309.57	303.45	294.89	297.53	301.36
RCS3											
540	297.08	241.78	246.32	190.44	204.78	220.83	282.39	287.57	274.71	281.21	281.47
597	374.44	236.82	237.23	216.49	213.77	226.08	284.98	284.05	268.82	262.76	275.15
641	430.62	236.82	235.79	219.2	213.77	226.4	301.69	298.14	257.67	257.37	278.72
731	536.75	252.35	253.35	221.62	230.04	239.34	300.78	301.66	260.56	265.21	282.05
SRCS											
540	301.40	283.25	282.51	211.68	213.88	247.83	304.35	302.62	243.60	246.26	274.21
597	378.6	290.31	290.32	232.89	222.25	258.94	322.02	316.66	265.2	268.14	293.01
641	433.33	295.61	292.10	214.23	208.98	252.63	304.49	302.61	262.56	263.43	283.27
731	542.05	300	298.24	221.98	224.71	261.23	300	299.12	281.74	278.66	289.88

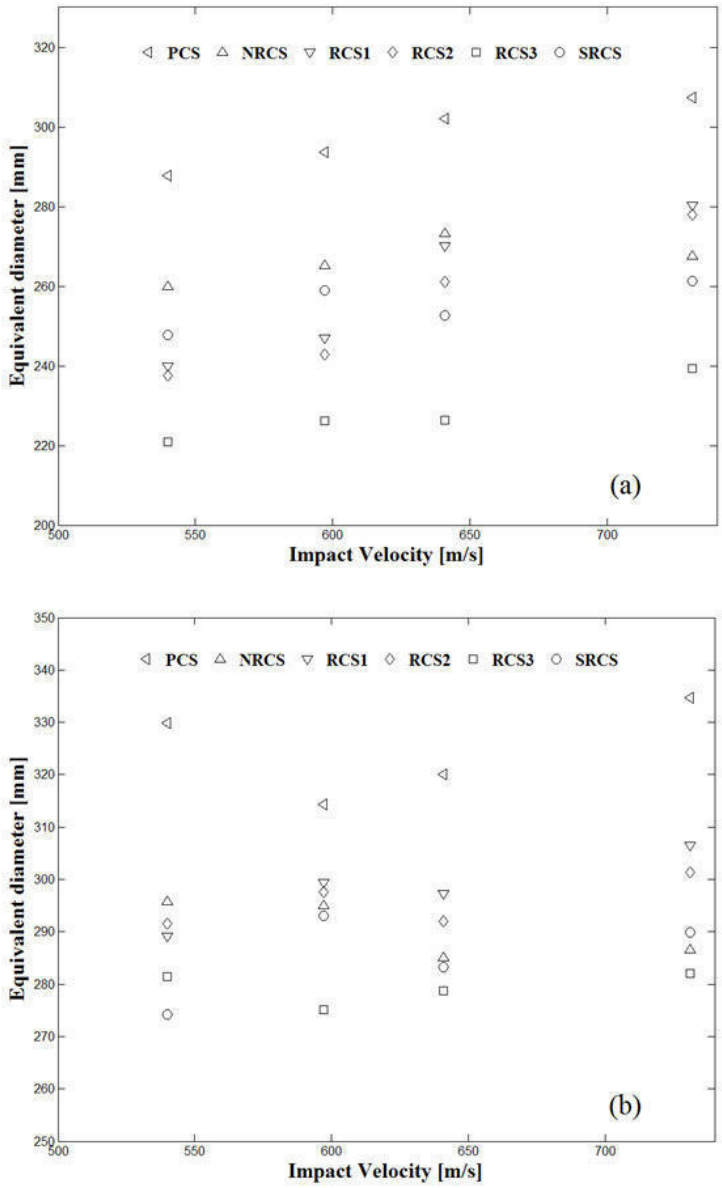

Figure 7.10: Residual velocity and equivalent damage diameter of plain, reinforced and additionally reinforced concrete samples: (a) front surface ; (b) back surface.

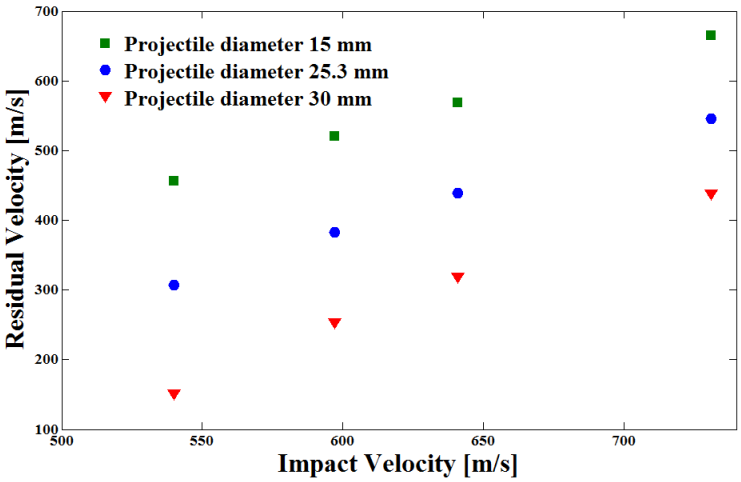

Figure 7.11: Ballistic resistance of reinforced concrete sample with different projectile diameters.

7.6 Effect of projectile diameter

The effect of the ogive-nosed projectile diameter on the ballistic resistance of the normal reinforced concrete sample NRCS is studied in this section. The projectile diameter was varied such that it takes the values 15, 25.3 and 30 mm as shown in Figure 7.11. To ensure that the projectile will strike the concrete sample through impact, the maximum projectile diameter is taken such that is less than the mesh spacing of the longitudinal steel bars at the impact location. The mechanical properties of concrete and steel reinforcement are similar to the ones used in the previous sections. Figure 7.11 shows the variation of the residual velocity with different diameters of the projectiles. It is clearly shown that the residual velocity increases with the increase of the initial velocity and with the increase in the projectile diameter. It is concluded that the ballistic resistance is improved with the increase of the projectile diameter and the energy absorbed by the reinforced concrete slab is higher with the biggest projectile diameter and decreases with the decrease of the projectile diameter.

7.7 Conclusion

The Johnson-Holmquist-2 damage model was implemented for concrete material to study the behavior of plain and reinforced concrete slab under impact loads. The steel bars were simulated using the Johnson-Cook plasticity model and the ogive-nosed projectile was modelled as rigid body with a mass assigned at a reference point. The implemented impact model was validated and the numerical results showed good agreement with the experimental ones. It was found that the added steel reinforcement to the concrete sample has signicant inuence on the ballistic resistance comparing to the plain concrete. On the other hand, it was found that the simple transverse reinforcement affects slightly the ballistic resistance of the concrete sample.

Chapter 8

Conclusions

8.1 Summary of achievements

This dissertation is dedicated to the development of analytical framework of self-healing and super healing materials. We aimed at describing the recovery and strengthening of material stiffness and strength. Continuum damage mechanics and continuum damage-healing mechanics were used to simulate both self-healing and super healing of damage in the materials. In this context, the thesis proposed a new damage-healing law that can be applied on both autonomous (coupled healing mechanism) and autogenous (uncoupled healing mechanism) self-healing in concrete.

Qualitative comparison of the numerical results with experimental investigations showed that the proposed damage-healing model is capable to predict the stiffness recovery and failure properties in both coupled and uncoupled self-healing mechanisms with different loading conditions. It was observed that in both coupled and uncoupled self-healing mechanisms the generalized nonlinear and quadratic healing models underestimate the healing efficiency comparing to the linear healing model. It was found that the linear self-healing model applied on uncoupled healing mechanism with 2000 s of rest period exhibits similar behavior as the quadratic self-healing model applied on uncoupled healing mechanism with 5000 s of rest period, which both give 17.14 % of the stiffness recovery. On the other hand, we found that the linear self-healing model applied on coupled self-healing mechanism resulted in full recovery of material stiffness using the value of material parameter $\gamma = 0.02$,

while only 75 % of stiffness recovery was obtained using the generalized nonlinear self-healing model.

In the same context of self-healing analysis, the results of the healing formulation based on elastic stiffness revealed that the healing variable calculated based on elastic stiffness is greater than the one calculated based on cross-section in the case of the hypothesis of elastic energy equivalence. In addition, the healing tensors obtained in isotropic elasticity, plane stress and plane strain cases fit the upper and lower limits of the healing variable in the case of scalar formulation.

In the context of super healing analysis, we presented theoretically a new concept of materials strengthening using a proposed super healing theory. It was assumed that the same repairing material used for self-healing is used for super healing. The plane stress example of super healing was found to be consistent with the isotropic definition of the super healing theory. In addition, it was found that the generalized nonlinear super healing model is the most appropriate to describe the super healing process. New super healing matrix in plane strain case was also proposed and demonstrated in comparison to the isotropic formulation. Investigation of super healing theory in terms of elastic stiffness was presented in this thesis. The results revealed that the hypothesis of elastic energy equivalence overestimates the super healed elastic stiffness of both the generalized nonlinear and quadratic super healing models. In addition, it was found that the generalized nonlinear super healing theory gives a high strengthening of the elastic stiffness comparing to the quadratic super healing theory in both hypotheses of elastic strain and elastic energy equivalence.

The results of the numerical modeling of plain and reinforced concrete slabs revealed that the added steel reinforcement to the concrete sample has significant influence on the ballistic resistance comparing to the plain concrete. On the other hand, it was found that the simple transverse reinforcement affects slightly the ballistic resistance of the concrete sample. It was also concluded that the ballistic resistance is mostly affected by the spacing mesh of the steel bars than the amount of the steel reinforcement in the concrete sample. However, at high striking velocity the amount of steel reinforcement can be efficient to improve the ballistic resistance of concrete slabs. The effect of projectile diameter was also studied in the present work in which it was found that the ballistic resistance and energy absorption of the reinforced concrete slab increase with the increase of the projectile diameter.

8.2 Outlook

The present work mainly investigated the analytical analysis of self-healing and super healing behaviors using sound mathematical and mechanical principles. Additionally, we also focused on numerical modeling of impact behavior of reinforced concrete slabs under ballistic impact. The following possible extensions of the present work can be considered:

- The softening behavior of brittle materials leads to mesh-dependence of their responses due to strain localization when local damage-healing models are used. This issue was thoroughly addressed in CDM using non-conventional damage models (e.g. gradient and nonlocal damage models), while non-conventional damage-healing models are not yet addressed. Therefore, future investigations of non-conventional damage-healing models are needed.

- The theoretical investigation of super healing materials introduced in the present work represents a crucial solution of material strengthening. We believe that this theory can be exploited to be applied in the area of the strengthening of materials and structural elements. It is hoped that further research will be carried out in the future to find, design and manufacture the appropriate material that can reflect physically the behavior of super healing materials. The present work of super healing theory has been limited to elasticity and to damage in tension. Future research may include inelastic materials and damage in compression and show any advantages the type of material plays in the super healing model.

- Implementation of the proposed models into computational software.

- Concrete behavior under impact loads is sensitive to stain rate effect. The numerical model developed in the present work can be extended to take into account the effect of strain rate on the behavior of reinforced concrete slabs.

References

[1] Nynke ter Heide and Erik Schlangen. Self-healing of early age cracks in concrete. In *First International Conference on Self Healing Materials*, pages 1–12, 2007. x, 9, 10

[2] Scott R White, Nancy R Sottos, Philippe H Geubelle, Jeffrey S Moore, M_R Kessler, SR Sriram, EN Brown, and S Viswanathan. Autonomic healing of polymer composites. *Nature*, 409(6822):794, 2001. x, 10, 11, 41, 50, 90

[3] RP Wool and KM Oconnor. A theory crack healing in polymers. *Journal of Applied Physics*, 52(10):5953–5963, 1981. x, 14, 16, 17, 25

[4] Hyun-Jong Lee and Y Richard Kim. Viscoelastic continuum damage model of asphalt concrete with healing. *Journal of Engineering Mechanics*, 124:1224–1232, 1998. x, 21, 22

[5] Rashid K Abu Al-Rub, Masoud K Darabi, Dallas N Little, and Eyad A Masad. A micro-damage healing model that improves prediction of fatigue life in asphalt mixes. *International Journal of Engineering Science*, 48(11):966–990, 2010. x, 3, 22, 23, 24

[6] Julia Mergheim and Paul Steinmann. Phenomenological modelling of self-healing polymers based on integrated healing agents. *Computational Mechanics*, 52(3):681–692, 2013. x, 24, 26

[7] George Z Voyiadjis, Amir Shojaei, Guoqiang Li, and Peter I Kattan. A theory of anisotropic healing and damage mechanics of materials. *Proc. R. Soc. A*, 468(2137):163–183, 2012. x, 26, 28, 66, 92, 95

[8] Romain Balieu, Nicole Kringos, Feng Chen, and Enrique Córdoba. Multiplicative viscoelastic-viscoplastic damage-healing model for asphalt-concrete materials. In *8th RILEM International Conference on Mechanisms of Cracking and Debonding in Pavements*, pages 235–240. Springer, 2016. x, 28, 29

[9] S Granger, A Loukili, G Pijaudier-Cabot, and G Chanvillard. Mechanical characterization of the self-healing effect of cracks in ultra high performance concrete (uhpc). In *Proceedings Third International Conference on Construction Materials, Performance, Innovations and Structural Implications, ConMat*, volume 5, pages 22–24, 2005. xi, 46, 47

[10] Antonis Kanellopoulos, Petros Giannaros, and Abir Al-Tabbaa. The effect of varying volume fraction of microcapsules on fresh, mechanical and self-healing properties of mortars. *Construction and Building Materials*, 122:577–593, 2016. xi, 53, 54

[11] T Børvik, OS Hopperstad, T Berstad, and M Langseth. Numerical simulation of plugging failure in ballistic penetration. *International Journal of Solids and Structures*, 38(34-35):6241–6264, 2001. xiv, 155

[12] Tae-Ho Ahn and Toshiharu Kishi. Crack self-healing behavior of cementitious composites incorporating various mineral admixtures. *Journal of Advanced Concrete Technology*, 8(2):171–186, 2010. 2

[13] Kim Van Tittelboom and Nele De Belie. Self-healing in cementitious materialsa review. *Materials*, 6(6):2182–2217, 2013. 2, 12

[14] Andrew W Herrmann. Asce 2013 report card for america's infrastructure. In *IABSE symposium report*, pages 9–10. International Association for Bridge and Structural Engineering, 2013. 2

[15] Yingzi Yang, Michael D Lepech, En-Hua Yang, and Victor C Li. Autogenous healing of engineered cementitious composites under wet–dry cycles. *Cement and Concrete Research*, 39(5):382–390, 2009. 2

[16] Bo Pang, Zonghui Zhou, Pengkun Hou, Peng Du, Lina Zhang, and Hongxin Xu. Autogenous and engineered healing mechanisms of carbonated steel slag

aggregate in concrete. *Construction and Building Materials*, 107:191–202, 2016. 2

[17] Eric N Brown, Scott R White, and Nancy R Sottos. Fatigue crack propagation in microcapsule-toughened epoxy. *Journal of materials science*, 41(19):6266–6273, 2006. 2, 47

[18] Souradeep Gupta, Sze Dai Pang, and Harn Wei Kua. Autonomous healing in concrete by bio-based healing agents–a review. *Construction and Building Materials*, 146:419–428, 2017. 2

[19] RA Schapery. On the mechanics of crack closing and bonding in linear viscoelastic media. *International Journal of Fracture*, 39(1-3):163–189, 1989. 3, 15, 17

[20] Dallas N Little and Amit Bhasin. Exploring mechanism of h ealing in asphalt mixtures and quantifying its impact. In *Self healing materials*, pages 205–218. Springer, 2007. 3, 17

[21] Amit Bhasin, Dallas N Little, Rammohan Bommavaram, and Kamilla Vasconcelos. A framework to quantify the effect of healing in bituminous materials using material properties. *Road Materials and Pavement Design*, 9(sup1): 219–242, 2008. 3, 17

[22] George Z Voyiadjis, Amir Shojaei, and Guoqiang Li. A thermodynamic consistent damage and healing model for self healing materials. *International Journal of Plasticity*, 27(7):1025–1044, 2011. 3, 13, 136

[23] Masoud K Darabi, Rashid K Abu Al-Rub, and Dallas N Little. A continuum damage mechanics framework for modeling micro-damage healing. *International Journal of Solids and Structures*, 49(3-4):492–513, 2012. 3, 23, 32, 33

[24] Nataliya Hearn. Self-sealing, autogenous healing and continued hydration: what is the difference? *Materials and structures*, 31(8):563, 1998. 8

[25] Abrams A. Autogenous healing of concrete. *Concrete*, pages 10–50, 1925. 8

[26] Gilkey H. J. Annual survey of the american chemistry. *National Academies*, V, p,453, 1930. 8

[27] Kenneth R Lauer et al. Autogenous healing of cement paste. In *Journal Proceedings*, volume 52, pages 1083–1098, 1956. 8

[28] Ravindra Kumar Dhir, Chander M Sangha, and John GL Munday. Strength and deformation properties of autogenously healed mortars. In *Journal Proceedings*, volume 70, pages 231–236, 1973. 9

[29] Kim Van Tittelboom, Didier Snoeck, Jianyun Wang, and Nele De Belie. Most recent advances in the field of self-healing cementitious materials. In *4th International conference on Self-Healing Materials (ICSHM 2013)*, pages 406–413. Ghent University. Magnel Laboratory for Concrete Research, 2013. 9

[30] Michael D Lepech and Victor C Li. Water permeability of engineered cementitious composites. *Cement and Concrete Composites*, 31(10):744–753, 2009. 9

[31] Carola Edvardsen. Water permeability and autogenous healing of cracks in concrete. *Materials Journal*, 96(4):448–454, 1999. 9, 10

[32] B Lubelli, TG Nijland, and RPJ Van Hees. Self-healing of lime based mortars: microscopy observations on case studies. *Heron, 56 (1/2)*, 2011. 9

[33] Adam Neville. Autogenous healinga concrete miracle? *Concrete international*, 24(11):76–82, 2002. 9

[34] Corina-Maria Aldea, Won-Joon Song, John S Popovics, and Surendra P Shah. Extent of healing of cracked normal strength concrete. *Journal of materials in civil engineering*, 12(1):92–96, 2000. 10

[35] Mo Li and Victor C Li. Cracking and healing of engineered cementitious composites under chloride environment. *ACI Materials Journal*, 108(3), 2011. 10

[36] Daisuke Homma, Hirozo Mihashi, and Tomoya Nishiwaki. Self-healing capability of fibre reinforced cementitious composites. *Journal of Advanced Concrete Technology*, 7(2):217–228, 2009. 10

[37] Didier Snoeck and Nele De Belie. Mechanical and self-healing properties of cementitious composites reinforced with flax and cottonised flax, and compared with polyvinyl alcohol fibres. *Biosystems Engineering*, 111(4):325–335, 2012. 10

[38] HXD Lee, HS Wong, and NR Buenfeld. Potential of superabsorbent polymer for self-sealing cracks in concrete. *Advances in Applied Ceramics*, 109(5):296–302, 2010. 10

[39] Pieter Dejonghe, Nele De Belie, Stijn Steuperaert, Didier Snoeck, and Peter Dubruel. The behaviour of suberabsorbing polymers as a sealing agent in concrete: absorption kinetics, degradation and water permeability. In *3rd International conference on Self-Healing Materials (ICSHM 2011)*, pages 123–124, 2011. 10

[40] Didier Snoeck, Stijn Steuperaert, Kim Van Tittelboom, Peter Dubruel, and Nele De Belie. Visualization of water penetration in cementitious materials with superabsorbent polymers by means of neutron radiography. *Cement and Concrete Research*, 42(8):1113–1121, 2012. 10

[41] D Janssen. Water encapsulation to initiate self-healing in cementitious materials. *Master's Thesis, Delft University, Delft*, 2011. 10

[42] SZ Qian, J Zhou, and E Schlangen. Influence of curing condition and precracking time on the self-healing behavior of engineered cementitious composites. *Cement and concrete composites*, 32(9):686–693, 2010. 10

[43] Pipat Termkhajornkit, Toyoharu Nawa, Yoichi Yamashiro, and Toshiki Saito. Self-healing ability of fly ash–cement systems. *Cement and Concrete composites*, 31(3):195–203, 2009. 10

[44] Seung Hyun Na, Yukio Hama, Madoka Taniguchi, Osamu Katsura, Takahiro Sagawa, and Mohamed Zakaria. Experimental investigation on reaction rate

and self-healing ability in fly ash blended cement mixtures. *Journal of Advanced Concrete Technology*, 10(7):240–253, 2012. 10

[45] RH Haddad and MA Bsoul. Self-healing of polypropylene fiber reinforced concrete: Pozzolan effect. *Civil Engineering Department, Jordan University of Science and Technology, Irbid, Jordan*, 1999. 10

[46] Abd_Elmoaty M Abd_Elmoaty. Self-healing of polymer modified concrete. *Alexandria Engineering Journal*, 50(2):171–178, 2011. 10

[47] T Katsuhata, Y Ohama, and K Demura. Investigation of microcracks self-repair function of polymer-modified mortars using epoxy resins without hardeners. In *Proceedings of 10th International Congress on Polymers in Concrete, Honolulu, HI, USA*, pages 23–25, 2001. 10

[48] Yoshihiko Ohama. Recent progress in concrete-polymer composites. *Advanced Cement Based Materials*, 5(2):31–40, 1997. 10

[49] Bojana Boh and Boštjan Šumiga. Microencapsulation technology and its applications in building construction materials tehnologija mikrokapsuliranja in njena uporaba v gradbenih materialih. *RMZ–Materials and Geoenvironment*, 55(3):329–344, 2008. 10

[50] Shuai Zhou, Hehua Zhu, and Zhiguo Yan. Materials, theories and experiments of microcapsule self-healing methoda review. In *Geo-Shanghai 2014*, 2014. 10

[51] Rachid Naciri. *A review of the encapsulation strategy in structural self-healing materials*. PhD thesis, Massachusetts Institute of Technology, 2014. 10

[52] JY Wang, H Soens, Willy Verstraete, and Nele De Belie. Self-healing concrete by use of microencapsulated bacterial spores. *Cement and Concrete Research*, 56:139–152, 2014. 11, 39, 90

[53] Jianyun Wang, Kim Van Tittelboom, Nele De Belie, and Willy Verstraete. Use of silica gel or polyurethane immobilized bacteria for self-healing concrete. *Construction and building materials*, 26(1):532–540, 2012. 11

[54] K Sisomphon, O Copuroglu, and A Fraaij. Application of encapsulated lightweight aggregate impregnated with sodium monofluorophosphate as a self-healing agent in blast furnace slag mortar. *Heron, 56 (1/2)*, 2011. 11

[55] Haoliang Huang and Guang Ye. Simulation of self-healing by further hydration in cementitious materials. *Cement and Concrete Composites*, 34(4):460–467, 2012. 11

[56] Haoliang Huang and Guang Ye. The effects of capsules on self-healing efficiency in cementitious materials. In *Second International Conference on Microstructural-Related Durability of Cementitious Composites*, pages 11–13, 2012. 11

[57] Kim Van Tittelboom, Nele De Belie, Denis Van Loo, and Patric Jacobs. Self-healing efficiency of cementitious materials containing tubular capsules filled with healing agent. *Cement and Concrete Composites*, 33(4):497–505, 2011. 11, 67

[58] Eric N Brown, Scott R White, and Nancy R Sottos. Retardation and repair of fatigue cracks in a microcapsule toughened epoxy composite–part i: Manual infiltration. *Composites Science and Technology*, 65(15-16):2466–2473, 2005. 11

[59] Eric N Brown, Scott R White, and Nancy R Sottos. Retardation and repair of fatigue cracks in a microcapsule toughened epoxy compositepart ii: In situ self-healing. *Composites Science and Technology*, 65(15-16):2474–2480, 2005. 11

[60] Carolyn Dry. Matrix cracking repair and filling using active and passive modes for smart timed release of chemicals from fibers into cement matrices. *Smart Materials and Structures*, 3(2):118, 1994. 11

[61] CM Dry and MJT Corsaw. A time-release technique for corrosion prevention. *Cement and Concrete Research*, 28(8):1133–1140, 1998. 11

[62] JY Wang, Didier Snoeck, Sandra Van Vlierberghe, Willy Verstraete, and Nele De Belie. Application of hydrogel encapsulated carbonate precipitating bac-

teria for approaching a realistic self-healing in concrete. *Construction and building materials*, 68:110–119, 2014. 11, 12

[63] Yu N Rabotnov. Creep problems in structural members. *Journal of Applied Mathematics and Mechanics*, 1969. 12

[64] J Lemaitre and JL Chaboche. A non-linear model of creep-fatigue damage cumulation and interaction(for hot metallic structures). *Mechanics of visco-elastic media and bodies*, page 1975, 1975. 12

[65] DR Hayhurst. Creep rupture under multi-axial states of stress. *Journal of the Mechanics and Physics of Solids*, 20(6):381–382, 1972. 12

[66] F Ao Leckie and DR Hayhurst. Constitutive equations for creep rupture. *Acta Metallurgica*, 25(9):1059–1070, 1977. 12

[67] JL Chaboche. Continuum damage mechanics: present state and future trends. *Nuclear Engineering and Design*, 105(1):19–33, 1987. 12

[68] J Lin, FPE Dunne, and DR Hayhurst. Aspects of testpiece design responsible for errors in cyclic plasticity experiments. *International Journal of Damage Mechanics*, 8(2):109–137, 1999. 12

[69] N Murakami, S.; Ohno. Creep damage analysis in thin-walled tubes. *Inelastic Behavior of Pressure Vessel and Piping Components*, pages 55–69, 1978. 12

[70] Jean-Louis Chaboche. Continuous damage mechanicsa tool to describe phenomena before crack initiation. *Nuclear Engineering and Design*, 64(2):233–247, 1981. 12

[71] Jean-Louis Chaboche. *Une loi différentielle d'endommagement de fatigue avec cumulation non linéaire.* Office Nationale d'Etudes et de Recherches Aérospatiales, 1974. 12

[72] Juan C Simo and JW Ju. Strain-and stress-based continuum damage modelsi. formulation. *International journal of solids and structures*, 23(7):821–840, 1987. 12

[73] JC Simo and JW Ju. Strain-and stress-based continuum damage modelsii. computational aspects. *International journal of solids and structures*, 23(7): 841–869, 1987. 12

[74] G Cordier and K Dang Van. Strain hardening effects and damage in plastic fatigue. In *Physical Non-Linearities in Structural Analysis*, pages 52–55. Springer, 1981. 12

[75] SR Bodner. A procedure for including damage in constitutive equations for elastic-viscoplastic work-hardening materials. In *Physical Non-linearities in Structural Analysis*, pages 21–28. Springer, 1981. 12

[76] Lasar Kachanov. *Introduction to continuum damage mechanics*, volume 10. Springer Science & Business Media, 2013. 12

[77] J Lemaitre and Jean-Louis Chaboche. Aspect phénoménologique de la rupture par endommagement. *J Méc Appl*, 2(3), 1978. 12

[78] J Lemaitre and J Dufailly. Modelization and identification of endommagement plasticity of material. In *Proceedings of the 3rd French Congress of Mechanics, Grenoble, France*, pages 17–21, 1977. 12

[79] George Z Voyiadjis. Degradation of elastic modulus in elastoplastic coupling with finite strains. *International Journal of Plasticity*, 4(4):335–353, 1988. 12

[80] George Z Voyiadjis and Peter I Kattan. Decomposition of elastic stiffness degradation in continuum damage mechanics. *Journal of Engineering Materials and Technology*, 139(2):021005, 2017. 12

[81] George Z Voyiadjis and Peter I Kattan. Damage mechanics with fabric tensors. *Mechanics of Advanced Materials and Structures*, 13(4):285–301, 2006. 12

[82] Peter I Kattan and George Z Voyiadjis. Decomposition of damage tensor in continuum damage mechanics. *Journal of engineering mechanics*, 127(9): 940–944, 2001. 12, 27

[83] Ever J Barbero, Fabrizio Greco, and Paolo Lonetti. Continuum damage-healing mechanics with application to self-healing composites. *International Journal of Damage Mechanics*, 14(1):51–81, 2005. 13, 134

[84] George Z Voyiadjis, Amir Shojaei, Guoqiang Li, and Peter Kattan. Continuum damage-healing mechanics with introduction to new healing variables. *International Journal of Damage Mechanics*, 21(3):391–414, 2012. 13, 32, 34, 38, 136

[85] George Z Voyiadjis, Amir Shojaei, Guoqiang Li, and Peter I Kattan. A theory of anisotropic healing and damage mechanics of materials. *Proceedings of the Royal Society A: Mathematical, Physical and Engineering Sciences*, 468(2137): 163–183, 2011. 13, 67

[86] George Z Voyiadjis and Peter I Kattan. Healing and super healing in continuum damage mechanics. *International Journal of Damage Mechanics*, 23(2): 245–260, 2014. 13, 32, 33, 87

[87] George Z Voyiadjis and Peter I Kattan. Investigation of the damage variable basic issues in continuum damage and healing mechanics. *Mechanics Research Communications*, 68:89–94, 2015. 13

[88] George Z Voyiadjis and Peter I Kattan. Mechanics of damage, healing, damageability, and integrity of materials: A conceptual framework. *International Journal of Damage Mechanics*, 26(1):50–103, 2017. 13, 54, 55, 57

[89] George Z Voyiadjis and Peter I Kattan. Decomposition of healing tensor: In continuum damage and healing mechanics. *International Journal of Damage Mechanics*, 27(7):1020–1057, 2018. 13, 27

[90] KS Chan, SR Bodner, AF Fossum, and DE Munson. Constitutive representation of damage development and healing in wipp salt. Technical report, Sandia National Labs., 1994. 18, 19

[91] KS Chan, SR Bodner, and DE Munson. Recovery and healing of damage in wipp salt. *International Journal of Damage Mechanics*, 7(2):143–166, 1998. 19, 20

[92] Shuke Miao, Ming L Wang, and Howard L Schreyer. Constitutive models for healing of materials with application to compaction of crushed rock salt. *Journal of Engineering Mechanics*, 121(10):1122–1129, 1995. 19

[93] H Xu, C Arson, FM Chester, et al. Stiffness and deformation of salt rock subject to anisotropic damage and temperature-dependent healing. In *46th US Rock Mechanics/Geomechanics Symposium*. American Rock Mechanics Association, 2012. 20, 29

[94] Chloé Arson, Hao Xu, and Fred M Chester. On the definition of damage in time-dependent healing models for salt rock. *Gotechnique Letters*, 2012. 20

[95] Cheng Zhu and Chloé Arson. Theoretical bases of thermomechanical damage and dmt-healing model for rock. In *Geo-Congress 2014: Geo-characterization and Modeling for Sustainability*, pages 2785–2794, 2014. 20

[96] C Zhu and Chloé Arson. Using microstructure descriptors to model thermomechanical damage and healing in salt rock. In *Conference: 48th US Rock Mechanics / Geomechanics Symposium*. Georgia Institute of Technology, 2014. 20

[97] Cheng Zhu and Chloé Arson. A model of damage and healing coupling halite thermo-mechanical behavior to microstructure evolution. *Geotechnical and Geological Engineering*, 33(2):389–410, 2015. 20, 29

[98] Cheng Zhu and Chloé Arson. Fabric-enriched modeling of anisotropic healing induced by diffusion in granular salt. In *Conference: 49th US Rock Mechanics / Geomechanics Symposium*. Georgia Institute of Technology, 2015. 20

[99] Jie Xu, Jiawang Qu, Yufeng Gao, and Ning Xu. Study on the elastoplastic damage-healing coupled constitutive model of mudstone. *Mathematical Problems in Engineering*, 2017, 2017. 20

[100] JW Ju and KY Yuan. New strain-energy-based coupled elastoplastic two-parameter damage and healing models for earth-moving processes. *International Journal of Damage Mechanics*, 21(7):989–1019, 2012. 21

[101] JW Ju, KY Yuan, and AW Kuo. Novel strain energy based coupled elastoplastic damage and healing models for geomaterials–part i: formulations. *International Journal of Damage Mechanics*, 21(4):525–549, 2012. 21

[102] JW Ju, KY Yuan, and AW Kuo. Novel strain energy based coupled elastoplastic damage and healing models for geomaterials–part i: formulations. *International Journal of Damage Mechanics*, 21(4):525–549, 2012. 21

[103] KY Yuan and JW Ju. New strain energy–based coupled elastoplastic damage-healing formulations accounting for effect of matric suction during earth-moving processes. *Journal of Engineering Mechanics*, 139(2):188–199, 2012. 21

[104] A. Hampel. Description of damage reduction and healing with the cdm constitutive model for the thermo-mechanical behavior of rock salt. *Mechanical Behavior of Salt VIII*, pages 1–10, 201. 21

[105] S Hong, KY Yuan, and JW Ju. New strain energy-based thermo-elastoviscoplastic isotropic damage–self-healing model for bituminous compositespart i: Formulations. *International Journal of Damage Mechanics*, 26(5): 651–671, 2017. 21

[106] S Hong, KY Yuan, and JW Ju. New strain energy-based thermo-elastoviscoplastic isotropic damage–self-healing model for bituminous compositespart ii: Computational aspects. *International Journal of Damage Mechanics*, 26(5):672–696, 2017. 21

[107] S Hong, KY Yuan, and JW Ju. Initial strain energy-based thermo-elastoviscoplastic two-parameter damage–self-healing models for bituminous compositespart i: Formulations. *International Journal of Damage Mechanics*, 25(8):1082–1102, 2016. 21

[108] S Hong, KY Yuan, and JW Ju. Initial strain energy-based thermo-elastoviscoplastic two-parameter damage self-healing model for bituminous compositespart ii: Computational aspects. *International Journal of Damage Mechanics*, 25(8):1103–1129, 2016. 21

[109] Hyun-Jong Lee and Y Richard Kim. Viscoelastic constitutive model for asphalt concrete under cyclic loading. *Journal of engineering mechanics*, 124(1): 32–40, 1998. 21

[110] Richard A Schapery. Correspondence principles and a generalizedj integral for large deformation and fracture analysis of viscoelastic media. *International journal of fracture*, 25(3):195–223, 1984. 21, 38

[111] SH Carpenter and S Shen. A dissipated energy approach to study hma healing 36 in fatigue. *Transportation Research Record: Journal of the Transportation 37 Research Board*, page 38, 2007. 22

[112] Booil Kim and Reynaldo Roque. Evaluation of healing property of asphalt mixtures. *Transportation Research Record: Journal of the Transportation Research Board*, 1970:84–91, 2006. 22

[113] Stephen Prager and Matthew Tirrell. The healing process at polymer–polymer interfaces. *The journal of chemical physics*, 75(10):5194–5198, 1981. 22

[114] Shihui Shen and Samuel Carpenter. Application of the dissipated energy concept in fatigue endurance limit testing. *Transportation Research Record: Journal of the Transportation Research Board*, 1929:165–173, 2005. 22

[115] Shihui Shen, Gordon D Airey, Samuel H Carpenter, and Hai Huang. A dissipated energy approach to fatigue evaluation. *Road materials and pavement design*, 7(1):47–69, 2006. 22

[116] Alessandro Menozzi, Alvaro Garcia, Manfred N Partl, Gabriele Tebaldi, and Philipp Schuetz. Induction healing of fatigue damage in asphalt test samples. *Construction and Building Materials*, 74:162–168, 2015. 22

[117] Martin Riara, Ping Tang, Liantong Mo, Barugahare Javilla, Meng Chen, and Shaopeng Wu. Systematic evaluation of fracture-based healing indexes of asphalt mixtures. *Journal of Materials in Civil Engineering*, 30(10):04018264, 2018. 22

[118] Masoud K Darabi, Rashid K Abu Al-Rub, Eyad A Masad, and Dallas N Little. Constitutive modeling of fatigue damage response of asphalt concrete materials with consideration of micro-damage healing. *International Journal of Solids and Structures*, 50(19):2901–2913, 2013. 23, 24, 92, 138, 143

[119] Ammar A Alsheghri and Rashid K Abu Al-Rub. Thermodynamic-based cohesive zone healing model for self-healing materials. *Mechanics Research Communications*, 70:102–113, 2015. 23, 24

[120] Ammar A Alsheghri and Rashid K Abu Al-Rub. Finite element implementation and application of a cohesive zone damage-healing model for self-healing materials. *Engineering Fracture Mechanics*, 163:1–22, 2016. 23, 24

[121] George Z Voyiadjis, Amir Shojaei, and Guoqiang Li. A generalized coupled viscoplastic–viscodamage–viscohealing theory for glassy polymers. *International Journal of Plasticity*, 28(1):21–45, 2012. 24, 28

[122] Masoud K Darabi, Rashid K Abu Al-Rub, Eyad A Masad, Chien-Wei Huang, and Dallas N Little. A thermo-viscoelastic–viscoplastic–viscodamage constitutive model for asphaltic materials. *International Journal of Solids and Structures*, 48(1):191–207, 2011. 24

[123] Amir Shojaei, Guoqiang Li, and George Z Voyiadjis. Cyclic viscoplastic-viscodamage analysis of shape memory polymers fibers with application to self-healing smart materials. *Journal of Applied Mechanics*, 80(1):011014, 2013. 24

[124] B Underwood and Waleed Zeiada. Characterization of microdamage healing in asphalt concrete with a smeared continuum damage approach. *Transportation research record: journal of the transportation research board*, 2447:126–135, 2014. 24

[125] P Karki, R Li, and A Bhasin. Quantifying overall damage and healing behaviour of asphalt materials using continuum damage approach. *International Journal of Pavement Engineering*, 16(4):350–362, 2015. 24

[126] Julia Mergheim, Gunnar Possart, and Paul Steinmann. Modelling and computation of curing and damage of thermosets. *Computational Materials Science*, 53(1):359–367, 2012. 25

[127] Kazuaki Sanada, Yuta Mizuno, and Yasuhide Shindo. Damage progression and notched strength recovery of fiber-reinforced polymers encompassing self-healing of interfacial debonding. *Journal of Composite Materials*, 49(14):1765–1776, 2015. 25

[128] Abdalla Ahmed, Kazuaki Sanada, Mohamed Fanni, and Ahmed Abd El-Moneim. A practical methodology for modeling and verification of self-healing microcapsules-based composites elasticity. *Composite Structures*, 184:1092–1098, 2018. 25

[129] Luthfi M Mauludin, Xiaoying Zhuang, and Timon Rabczuk. Computational modeling of fracture in encapsulation-based self-healing concrete using cohesive elements. *Composite Structures*, 196:63–75, 2018. 25

[130] Luthfi Muhammad Mauludin and Chahmi Oucif. Interaction between matrix crack and circular capsule under uniaxial tension in encapsulation-based self-healing concrete. *Underground Space*, 3(3):181–189, 2018. 25

[131] Luthfi Muhammad Mauludin and Chahmi Oucif. The effects of interfacial strength on fractured microcapsule. *Frontiers of Structural and Civil Engineering*, pages 1–11, 2018. 25

[132] S Murakami. Mechanical modeling of material damage. *Journal of Applied Mechanics*, 55(2):280–286, 1988. 26

[133] GZ Voyiadjis and T Park. Anisotropic damage effect tensors for the symmetrization of the effective stress tensor. *Journal of Applied Mechanics*, 64(1): 106–110, 1997. 27

[134] George Z Voyiadjis and Peter I Kattan. Decomposition of elastic stiffness degradation in continuum damage mechanics. *Journal of Engineering Materials and Technology*, 139(2):021005, 2017. 27, 29

[135] George Z Voyiadjis and Peter I Kattan. On the decomposition of the damage variable in continuum damage mechanics. *Acta Mechanica*, 228(7):2499–2517, 2017. 27

[136] George Z Voyiadjis and Peter I Kattan. A comparative study of damage variables in continuum damage mechanics. *International Journal of Damage Mechanics*, 18(4):315–340, 2009. 28, 29, 74

[137] George Z Voyiadjis, Mohammed A Yousef, and Peter I Kattan. New tensors for anisotropic damage in continuum damage mechanics. *Journal of Engineering Materials and Technology*, 134(2):021015, 2012. 28

[138] Xikui Li, Zenghui Wang, Songge Zhang, and Qinglin Duan. Multiscale modeling and characterization of coupled damage-healing-plasticity for granular materials in concurrent computational homogenization approach. *Computer Methods in Applied Mechanics and Engineering*, 342:354–383, 2018. 29

[139] Xikui Li, Youyao Du, Qinglin Duan, and J Woody Ju. Thermodynamic framework for damage-healing-plasticity of granular materials and net damage variable. *International Journal of Damage Mechanics*, 25(2):153–177, 2016. 29

[140] George Z Voyiadjis and Peter I Kattan. Mechanics of damage processes in series and in parallel: a conceptual framework. *Acta Mechanica*, 223(9):1863–1878, 2012. 29

[141] L.M Kachanov. On the creep fracture time. *Izv Akad*, 8:26–31, 1958. 31, 34

[142] George Voyiadjis. *Advances in damage mechanics: metals and metal matrix composites*. Elsevier, 2012. 31, 34, 38, 93, 94, 136

[143] Timon Rabczuk, J Akkermann, and J Eibl. A numerical model for reinforced concrete structures. *International Journal of Solids and Structures*, 42(5-6): 1327–1354, 2005. 31, 34

[144] Chahmi Oucif, George Z Voyiadjis, and Timon Rabczuk. Modeling of damage-healing and nonlinear self-healing concrete behavior: Application to coupled and uncoupled self-healing mechanisms. *Theoretical and Applied Fracture Mechanics*, 96:216–230, 2018. 31

[145] Sébastien Granger, Ahmed Loukili, Gilles Pijaudier-Cabot, and Gilles Chanvillard. Experimental characterization of the self-healing of cracks in an ultra high performance cementitious material: Mechanical tests and acoustic emission analysis. *Cement and Concrete Research*, 37(4):519–527, 2007. 39, 67

[146] Xianfeng Wang, Feng Xing, Ming Zhang, Ningxu Han, and Zhiwei Qian. Experimental study on cementitious composites embedded with organic microcapsules. *Materials*, 6(9):4064–4081, 2013. 39

[147] C Joseph, Anthony Duncan Jefferson, B Isaacs, Robert John Lark, and Diane Ruth Gardner. Experimental investigation of adhesive-based self-healing of cementitious materials. *Magazine of Concrete Research*, 62(11):831–843, 2010. 41, 50

[148] Russell J Varley, David A Craze, Adrian P Mouritz, and Chun H Wang. Thermoplastic healing in epoxy networks: exploring performance and mechanism of alternative healing agents. *Macromolecular materials and engineering*, 298 (11):1232–1242, 2013. 46

[149] AR Jones, CA Watkins, Scott R White, and Nancy R Sottos. Self-healing thermoplastic-toughened epoxy. *Polymer*, 74:254–261, 2015. 46

[150] G Scheltjens, MM Diaz, J Brancart, G Van Assche, and B Van Mele. A self-healing polymer network based on reversible covalent bonding. *Reactive and Functional Polymers*, 73(2):413–420, 2013. 46

[151] Stephen J Kalista, John R Pflug, and Russell J Varley. Effect of ionic content on ballistic self-healing in emaa copolymers and ionomers. *Polymer Chemistry*, 4(18):4910–4926, 2013. 46

[152] Guoqiang Li and Damon Nettles. Thermomechanical characterization of a shape memory polymer based self-repairing syntactic foam. *Polymer*, 51(3): 755–762, 2010. 46

[153] Mariano M Escobar, Sebastián Vago, and Analía Vázquez. Self-healing mortars based on hollow glass tubes and epoxy–amine systems. *Composites Part B: Engineering*, 55:203–207, 2013. 50

[154] Sang-Ryoung Kim, Bezawit A Getachew, and Jae-Hong Kim. Toward microvascular network-embedded self-healing membranes. *Journal of Membrane Science*, 531:94–102, 2017. 50

[155] Andrew R Hamilton, Nancy R Sottos, and Scott R White. Self-healing of internal damage in synthetic vascular materials. *Advanced Materials*, 22(45): 5159–5163, 2010. 50

[156] George Z Voyiadjis, Ziad N Taqieddin, and Peter I Kattan. Theoretical formulation of a coupled elasticplastic anisotropic damage model for concrete using the strain energy equivalence concept. *International Journal of Damage Mechanics*, 18(7):603–638, 2009. 55

[157] Eric N Brown, Nancy R Sottos, and Scott R White. Fracture testing of a self-healing polymer composite. *Experimental mechanics*, 42(4):372–379, 2002. 67

[158] Eric N Brown, Scott R White, and Nancy R Sottos. Microcapsule induced toughening in a self-healing polymer composite. *Journal of Materials Science*, 39(5):1703–1710, 2004. 67

[159] Biqin Dong, Guohao Fang, Yanshuai Wang, Yuqing Liu, Shuxian Hong, Jianchao Zhang, Shangmin Lin, and Feng Xing. Performance recovery concerning the permeability of concrete by means of a microcapsule based self-healing system. *Cement and Concrete Composites*, 78:84–96, 2017. 90

[160] Jungyoul Choi. Comparative study of effective stresses of concrete beams strengthened using carbon-fibre-reinforced polymer and external prestressing tendons. *Structure and Infrastructure Engineering*, 10(6):753–766, 2014. 91

[161] George Z Voyiadjis and Peter I Kattan. A plasticity-damage theory for large deformation of solidsi. theoretical formulation. *International Journal of Engineering Science*, 30(9):1089–1108, 1992. 95

[162] Peter I Kattan and George Z Voyiadjis. A plasticity-damage theory for large deformation of solidsii. applications to finite simple shear. *International Journal of Engineering Science*, 31(1):183–199, 1993. 98

[163] George Z Voyiadjis and Peter I Kattan. Introduction to the mechanics and design of undamageable materials. *International Journal of Damage Mechanics*, 22(3):323–335, 2013. 128

[164] Chahmi Oucif, George Z Voyiadjis, Peter I Kattan, and Timon Rabczuk. Nonlinear superhealing and contribution to the design of a new strengthening theory. *Journal of Engineering Mechanics*, 144(7):04018055, 2018. 134, 136

[165] GR Johnson and TJ Holmquist. A computational constitutive model for brittle materials subjected to large strains, high strain rates and high pressures. *Shock Wave and High-Strain-Rate Phenomena in Materials*, pages 1075–1081, 1992. 151, 154

[166] Zvi Rosenberg. On the relation between the hugoniot elastic limit and the yield strength of brittle materials. *Journal of applied physics*, 74(1):752–753, 1993. 153

[167] Xiangzhen Kong, Qin Fang, Hao Wu, and Yong Peng. Numerical predictions of cratering and scabbing in concrete slabs subjected to projectile impact using a modified version of hjc material model. *International Journal of Impact Engineering*, 95:61–71, 2016. 154

[168] Gordon R Johnson and William H Cook. Fracture characteristics of three metals subjected to various strains, strain rates, temperatures and pressures. *Engineering fracture mechanics*, 21(1):31–48, 1985. 154

[169] H. Wu, Q. Fang, Y. Peng, Z.M. Gong, and X.Z. Kong. Hard projectile perforation on the monolithic and segmented rc panels with a rear steel liner. *International Journal of Impact Engineering*, 76:232 – 250, 2015. ISSN 0734-743X. doi: https://doi.org/10.1016/j.ijimpeng.2014.10.010. URL http://www.sciencedirect.com/science/article/pii/S0734743X14002516. 155, 158

Ehrenwörtlich Erklärung

Ich erkläre hiermit ehrenwörtlich, dass ich die vorliegende Arbeit ohne unzulässige Hilfe Dritter und ohne Benutzung anderer als der angegebenen Hilfsmittel angefertigt habe. Die aus anderen Quellen direkt oder indirekt übernommenen Daten und Konzepte sind unter Angabe der Quelle gekennzeichnet.

Weitere Personen waren an der inhaltlich-materiellen Erstellung der vorliegenden Arbeit nicht beteiligt. Insbesondere habe ich hierfür nicht die entgeltliche Hilfe von Vermittlungs- bzw. Beratungsdiensten (Pro-motionsberater oder anderer Personen) in Anspruch genommen. Niemand hat von mir unmittelbar oder mittelbar geldwerte Leistungen für Arbeiten erhalten, die im Zusammenhang mit dem Inhalt der vorgeleg-ten Dissertation stehen.

Die Arbeit wurde bisher weder im In- noch im Ausland in gleicher oder ähnlicher Form einer anderen Prü-fungsbehörde vorgelegt.

Ich versichere ehrenwörtlich, dass ich nach bestem Wissen die reine Wahrheit gesagt und nichts ver-schwiegen habe.

Chahmi Oucif
Weimar, Juli 2019

Curriculum Vitae

Chahmi Oucif
Institute of Structural Mechanics
Bauhaus-University Weimar
Marienstrasse 13D, 99423 Weimar, Germany
Email: chahmi.oucif@uni-weimar.de

Education

- PhD student: Institute of Structural Mechanics, Bauhaus-University Weimar, Germany, 2014-2019.
- Master of Civil Engineering: University of Science and Technology Mohamed Boudiaf Oran, Algeria, 2009-2011.
- Bachelor of Civil Engineering: University of Science and Technology Mohamed Boudiaf Oran, Algeria, 2006-2009.

Publications

1. Oucif C., Voyiadjis G. Z., Kattan P. I., Rabczuk T. Nonlinear Super Healing and Contribution to the Design of New Strengthening Theory. Journal of Engineering Mechanics, 144(7), 1-17, 2018.
2. Oucif C., Voyiadjis G. Z., Rabczuk T. Modeling of damage-healing and nonlinear self-healing concrete behaviour: Application to coupled and uncoupled self-healing mechanisms. Theoretical and Applied Fracture Mechanics, 96, 216-230, 2018.
3. Oucif C., Voyiadjis G. Z., Kattan P. I., Rabczuk T. Investigation of the super healing theory in continuum damage and healing mechanics. International Journal of Damage Mechanics, 1-22, 2018.
4. Oucif C., Mauludin L.M. Continuum Damage-Healing and Super Healing Mechanics in Brittle Materials: A State-of-the-Art Review. Applied Sciences, 8(12), 2350, 2018.
5. Voyiadjis G. Z. Oucif C., Kattan P. I., Rabczuk T. Damage and healing mechanics in plane stress, plane strain, and isotropic elasticity. International Journal of Damage Mechanics, 1-25, 2020.
6. Oucif C., Mauludin L. M. Numerical modeling of high velocity impact applied on reinforced concrete panel. Underground Space, 4(1), 1-9, 2019.
7. Oucif, C., Mauludin, L. M., & Abed, F. (2020). Ballistic behavior of plain and reinforced concrete slabs under high velocity impact. Frontiers of Structural and Civil Engineering, 14(2), 299-310.

8. Mauludin L. M., Oucif C. Interaction between matrix crack and circular capsule under uniaxial tension. Underground Space, 3(3), 181-189, 2018.
9. Mauludin L. M., Oucif C. The effects of interfacial strength on fractured microcapsules. Frontier of Structural and Civil Engineering, 13(2). 353-363, 2019.
10. Mauludin L. M., Oucif C. Modeling of Self-Healing Concrete: A Review. Journal of Applied and Computational Mechanics, 4(3), 536-539, 2019.